# HIRDLS

**TC-LOC-322A**

## HIGH RESOLUTION DYNAMICS LIMB SOUNDER

Originators: Nelson Pedreiro and Alain Carrier Date: 1998 November 23

Subject/Title: **Line-of-Sight Sensitivity Analysis**

Description/Summary/Contents:

Keywords: LOS knowledge, Sensitivities, Dynamic Model, Retrieval Algorithm

Purpose of this Document: (20 char max.) This document summarizes the analysis of the errors in the knowledge of the line-of-sight

| Reviewed/Approved by: | | | |
|---|---|---|---|
| Date (yy-mm-dd): | | | |

**Palo Alto Advanced Technology Center**
**CAGE Code 65113**
**Lockheed Martin Missiles & Space**
**3251 Hanover Street**
**Palo Alto, CA 94304-1191**
**United States of America**

EOS

# TABLE OF CONTENTS

# LIST OF TABLES

# LIST OF FIGURES

# 1 INTRODUCTION

Knowledge of the direction of the line-of-sight (LOS) with respect to inertial space depends on the knowledge of the relative position and orientation of the components of the instrument on the optical bench, as well as the orientation of the optical bench in inertial space. This document focuses on the LOS knowledge errors caused by errors in knowledge of the relative position and orientation of the components of the instrument on the optical bench.

Determination of relative position and orientation of the main components of the instrument requires knowledge of the geometrical and mechanical configuration of the system which depend on the alignment of components and on the characteristics and calibration of the sensors used to determine the configuration of the system. Therefore, determining the errors in the knowledge of LOS due to errors in the various parameters which are used to determine the configuration of the system is necessary to generate specifications for assembly, alignment, calibration and characteristics of components (*e.g.* sensors).

Analysis has been conducted to determine the errors in the LOS due to errors in the knowledge of the system configuration. The methods used in the analysis and the results obtained are presented in this document.

# 2 NOMENCLATURE

| | |
|---|---|
| $A$ | Line-of-sight inertial azimuth angle |
| $E$ | Line-of-sight inertial elevation angle |
| $a$ | Azimuth shaft angle |
| $e$ | Elevation shaft angle |
| $\delta$ | error in quantity |
| $\Delta$ | change in quantity |
| $\delta\Delta A$ | Error in the knowledge of the change in LOS inertial azimuth angle |
| $\delta\Delta E$ | Error in the knowledge of the change in LOS inertial elevation angle |
| N | Inertial reference frame |
| B | Reference frame fixed to the base plate |
| O | Reference frame fixed to the optical bench |
| R | Reference frame fixed to the azimuth gimbal |
| S | Reference frame fixed to the scanner elevation assembly |
| $x_m$ | mean value of variable $x$ |
| $\Delta E$, $\theta$ | angular separation of any two samples within a single elevation scan |

# 3 MEASURE OF PERFORMANCE

For the analysis described in this document the quantities used to measure performance are related to the knowledge of the line-of-sight in inertial space and the knowledge of the change of the line-of-sight in inertial space and are computed using the Alternate Global Mode Scan Pattern[1]. Specifically, the following metrics are used as a measure of performance:

- Maximum error in the absolute value of the LOS azimuth angle, $\delta A$[2], for 0<t<66 sec
- Maximum error in the absolute value of the LOS elevation angle, $\delta E$, for 0<t<66 sec
- Maximum error in the change of the LOS mean azimuth angle, $\delta\Delta A_m$ , for 0<t<66 sec
- Maximum error in the change of the LOS elevation angle, $\delta\Delta E$, for 0<t<66 sec

[1] HIRDLS Science Modes and Scanning Commands Sequence Document, TC-NCA-062A July 8, 1996. Table 6.2.1, p. 20.
[2] Only science portions of the scan are considered when computing maximum LOS errors, $\delta A$ and $\delta E$.

- Maximum error in the absolute value of the LOS azimuth angle, $\delta A$, for 0<t<10 sec, and azimuth shaft angle, $a$, for which it occurs
- Maximum error in the change of the LOS elevation angle, $\delta \Delta E$, for 0<t<10 sec, and angular separation, $\theta$, and azimuth shaft angle, $a$, for which it occurs

# 4 METHOD OF ANALYSIS

The approach taken here is to start from a baseline system configuration and vary parameters of the system from their baseline values to determine their effect on the various metrics used to measure performance. In order to implement this approach it is necessary to define a baseline system configuration and to develop a mathematical model of the system which represents the system behavior, encompasses the effects of all the parameters to be investigated, and provides a measure of system performance.

**Note:** The term sensitivity is defined as the ratio of the quantity used to measure performance over the associated variation in a given parameter characterizing the system from its baseline value. Once the sensitivities to the various parameters, which affect the performance, are determined they can be used to generate specifications which ensure that the resulting system conforms to the requirements. This document contains the data required to determine the sensitivities, *i.e.* the values of the metrics for variations in the parameters characterizing the system. The use of the sensitivities to compute system specifications is beyond the scope of this document and is not included here.

## 4.1 BASELINE SYSTEM CONFIGURATION

For the purposes of this analysis, it is sufficient to define a baseline system configuration in which the position and orientation of all system components are known perfectly. This implies perfect knowledge of placement and alignment of components with respect to the optical bench and perfect knowledge of the true quantities measured by sensors and encoders. For convenience, unless otherwise specified the baseline configuration is chosen such that the azimuth axis of rotation is parallel to the TRCF[1] z-axis, elevation axis of rotation parallel to the TRCF y-axis for the scan mirror in its datum position, normal to the mirror surface parallel to the TRCF x-axis for the scan mirror in its datum position. Wobble sensors sensitive axis parallel to the TRCF z-axis.

## 4.2 MATHEMATICAL MODEL

A dynamic model of the HIRDLS instrument has been created using AUTOLEV to generate the equations of motion, which were then interfaced with Matrixx/System Build where the closed-loop control logic was implemented. This model incorporates a line-of-sight inertial retrieval algorithm which can be executed independently of the simulation of the dynamic system provided that the inputs for the retrieval algorithm are available. The effect of several parameters on the knowledge of the line-of-sight can be obtained using the retrieval algorithm with inputs obtained from the simulation of the dynamic system for the baseline configuration. This avoids running the simulation of the system dynamics repeatedly for the various parameters to be investigated. This approach was taken whenever possible as it is simpler and avoids the time intensive simulation. The main characteristics of the dynamic model and retrieval algorithm are:

**Dynamic Model:**

[1] Telescope Reference Coordinate Frame (TRCF) defined in the Instrument Technical Specifications (ITS - SP-HIR-013-P - April 1997).

- Multiple rigid body dynamics. Separate rigid bodies are used to represent the baseplate, the optical bench, the azimuth gimbal, and the scanner
- Isolation system consists of 3 or 4 mounts (3 were used for this analysis) with compliance in six-axis and arbitrary mounting locations, and stiffness and damping characteristics
- On-orbit environmental disturbances[1] specified in terms of spacecraft angular and linear accelerations which are applied to the baseplate
- Arbitrary location and direction can be specified for the azimuth and elevation axis of rotation
- Arbitrary direction can be specified for the projected optical axis
- Arbitrary direction can be specified for the mirror normal for the scanner in its datum position
- Includes azimuth axis wobble
- Gyro, chopper and cryocoller disturbance loads can be specified
- Wobble sensors location and direction of sensitive axis can be arbitrarily specified
- Accelerometer location and direction of sensitive axis can be arbitrarily specified
- PID control for elevation and azimuth shaft angles[2]
- Incorporates a line-of-sight inertial retrieval algorithm

**Retrieval Algorithm:**

- Uses as inputs: (1) optical bench attitude in inertial space, (2) azimuth and elevation shaft angles, and (3) signals from wobble sensors
- Arbitrary location and direction can be specified for the azimuth and elevation axis of rotation
- Arbitrary direction can be specified for the projected optical axis
- Arbitrary direction can be specified for the mirror normal for the scanner in its datum position
- Includes azimuth axis wobble
- Wobble sensors location and direction of sensitive axis can be arbitrarily specified

# 5 PARAMETERS AFFECTING PERFORMANCE

The effect of the following parameters on the various metrics used to measure performance have been determined:

1. Knowledge of the direction of the projected optical axis
2. Knowledge of the direction of the normal to the scan mirror surface for the scan mirror in its datum position
3. Knowledge of the direction of the azimuth gimbal axis
4. Knowledge of the direction of the scanner elevation axis
5. Knowledge of the direction of the wobble sensors sensitive axis
6. Knowledge of the position of the wobble sensors
7. Azimuth and elevation sensor bias
8. Azimuth and elevation sensor drift
9. Azimuth and elevation sensor scale factor
10. Radiance/los sensors non-simultaneous sampling
11. Errors due to noise and non-linearities

# 6 RESULTS

Results are presented in this section for all the parameters/effects listed in Section 5. In each case, the values of the various metrics used to measure performance are given for various

[1] ITS SP-HIR-013P, p.39.
[2] The bandwidth of the azimuth and elevation shaft angle feedback control loop is 60 Hz.

values of the parameters and where applicable plots of the errors in line-of-sight inertial azimuth and elevation angles versus time during the Alternate Global Mode Scan Pattern are presented for a given value of the parameter.

A discussion of the methods of analysis used and a description of how the effects of the parameters are included in the mathematical model and simulation are also presented.

## 6.1 KNOWLEDGE OF THE DIRECTION OF THE PROJECTED OPTICAL AXIS

In the simulations the projected optical axis is defined as a vector, **POA**, expressed in the reference frame, O, fixed to the optical bench.

$$\mathbf{POA} = \cos A_0 \cos E_0 \ \mathbf{O_1} - \sin A_0 \cos E_0 \ \mathbf{O_2} + \sin E_0 \ \mathbf{O_3} \tag{6.1.1}$$

where, $A_0$ is the boresight azimuth angle, and $E_0$ is the boresight elevation angle. Baseline values for $A_0$ and $E_0$ are 0 and 25.3 degrees respectivelly.

The errors in knowledge of the absolute LOS and change in LOS, for 0 < t < 66 sec and 0 < t < 10 sec, caused by errors in the knowledge of the direction of the projected optical axis are presented in Table 6.1.1.

<u>Note on the Projected Optical Axis (POA):</u>

The instantaneous line of sight, **ILOS**, is given by:

$$\mathbf{ILOS} = -\cos A \cos E \ \mathbf{O_1} - \sin A \cos E \ \mathbf{O_2} + \sin E \ \mathbf{O_3} \tag{6.1.2}$$

Where it is assumed that the TRCF frame, O, fixed in the optical bench is parallel to the inertial frame, N. $A$ and $E$ are the azimuth and elevation angles of the line-of-sight with respect to the inertial frame as defined in the instrument IRD.

The telescope projected optical axis relates to the ILOS as follows:

$$\mathbf{ILOS} = \mathbf{POA} - 2(\mathbf{POA} \bullet \mathbf{S}_1)\mathbf{S}_1 \tag{6.1.3}$$

Where $\mathbf{S_1}$ is the unit vector parallel to the normal to the scan mirror surface but oriented in the opposite direction. For the baseline system configuration $\mathbf{S_1}$ coincides with $\mathbf{O_1}$ , when the mirror is in its datum position.

From the two equations above we obtain the expression for the **POA** for the scan mirror at its datum position, the baseline system configuration, $\mathbf{S_1} \equiv \mathbf{O_1}$ , and for frames N and O coincident.

$$\mathbf{POA} = \cos A_0 \cos E_0 \ \mathbf{O_1} - \sin A_0 \cos E_0 \ \mathbf{O_2} + \sin E_0 \ \mathbf{O_3} \tag{6.1.4}$$

$A_0$ and $E_0$ define the **POA** when the scan mirror is in its datum position. For the baseline system $A_0$ = 0 and $E_0$ = 25.3 degrees.

Figures 6.1.1 and 6.1.2 show the errors in the direction of the line-of-sight in inertial space due to errors in the knowledge of the projected optical axis.

| Parameter | | | 0 < t < 66 sec | | 0 < t < 10 sec | | | | |
|---|---|---|---|---|---|---|---|---|---|
| | $\delta A$ (arcsec) | $\delta E$ (arcsec) | $\delta \Delta A_m$ (arcsec) | $\delta \Delta E$ (arcsec) | $\delta A$ (arcsec), $a$ (deg) | | $\delta \Delta E$ (arcsec), $\theta$ (arcsec), $a$ (deg) | | |
| $\delta E_0$ (arcsec) | | | | | | | | | |
| +10 | 1.558E−1 | 1.000E+1 | 2.488E−2 | 1.026E−3 | 1.558E−1 | −19.5 | 3.645E−5 | 140 | −19.5 |
| −10 | 1.558E−1 | 1.000E+1 | 2.488E−2 | 1.026E−3 | 1.558E−1 | −19.5 | 3.645E−5 | 140 | −19.5 |
| +100 | 1.558 | 1.000E+2 | 2.489E−1 | 1.026E−2 | 1.558 | −19.5 | 3.646E−4 | 140 | −19.5 |
| −100 | 1.557 | 1.000E+2 | 2.488E−1 | 1.025E−2 | 1.557 | −19.5 | 3.644E−4 | 140 | −19.5 |
| $\delta A_0$ (arcsec) | | | | | | | | | |
| +10 | 1.009E+1 | 1.295E−1 | 9.962 | 1.985E−1 | 1.009E+1 | −19.5 | 2.452E−3 | 140 | −19.5 |
| −10 | 1.009E+1 | 1.295E−1 | 9.962 | 1.985E−1 | 1.009E+1 | −19.5 | 2.452E−3 | 140 | −19.5 |
| +100 | 1.0094E+2 | 1.294 | 9.962E+1 | 1.984 | 1.0094E+2 | −19.5 | 2.450E−2 | 140 | −19.5 |
| −100 | 1.0094E+2 | 1.296 | 9.962E+1 | 1.986 | 1.0094E+2 | −19.5 | 2.454E−2 | 140 | −19.5 |

Table 6.1.1: Maximum errors in the knowledge of the absolute LOS and change in LOS caused by errors in knowledge of the direction of the projected optical axis.

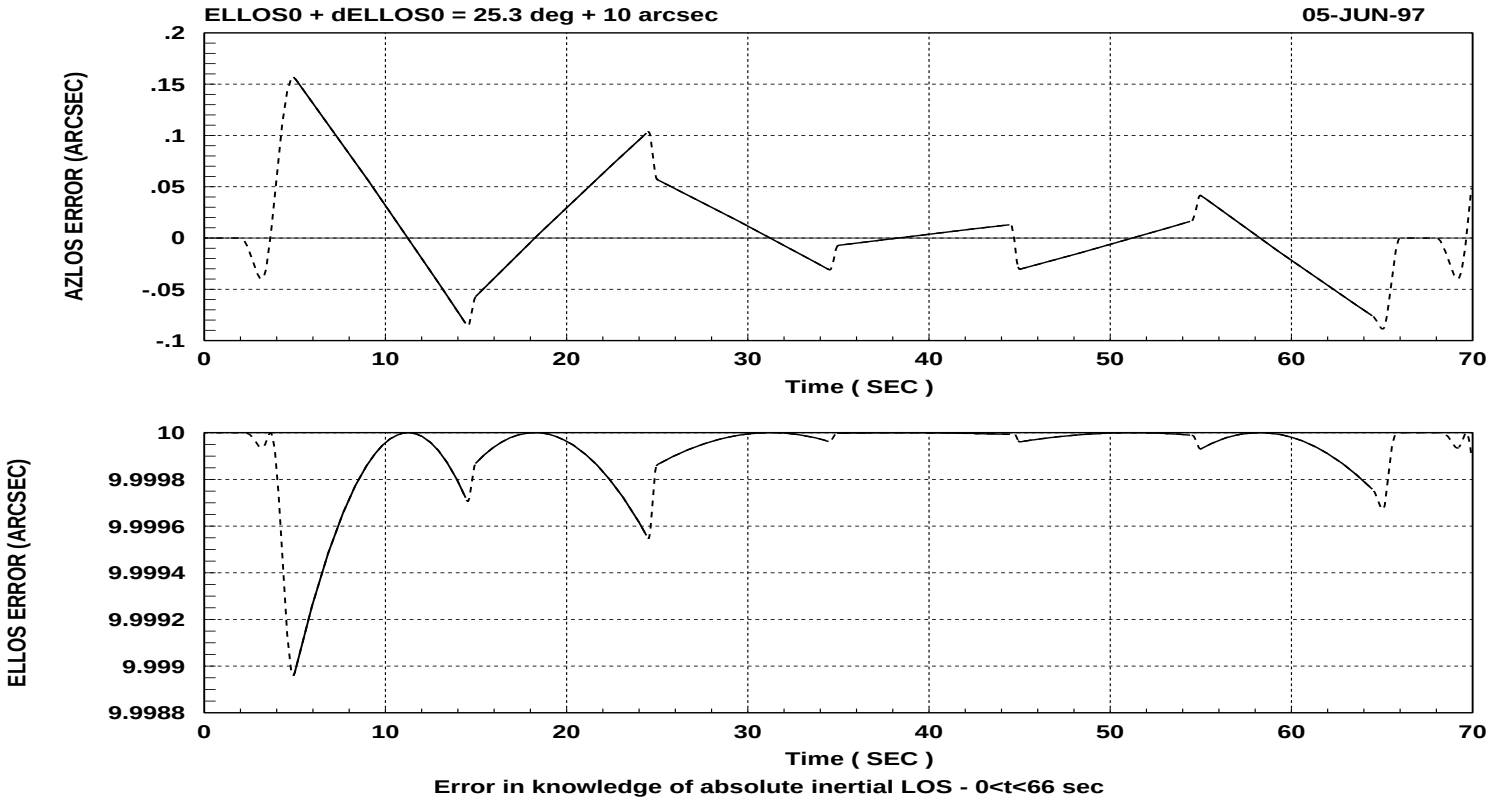


Figure 6.1.1: Errors in the knowledge of the inertial LOS caused by errors in knowledge of the direction of the projected optical axis (ELLOS0).

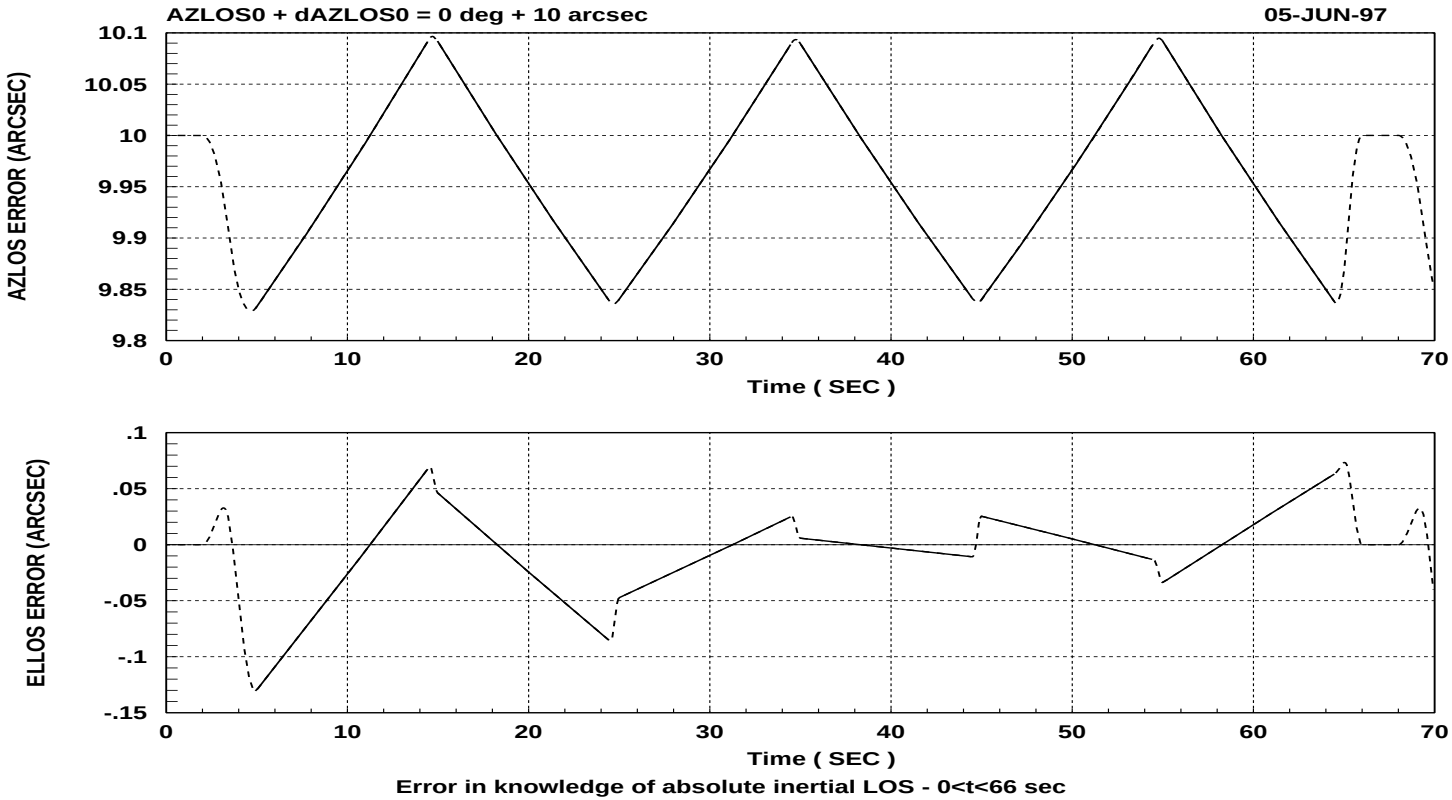


Figure 6.1.2: Errors in the knowledge of the inertial LOS caused by errors in knowledge of the direction of the projected optical axis (AZLOS0).

## 6.2 KNOWLEDGE OF THE DIRECTION OF THE NORMAL TO THE SCAN MIRROR SURFACE FOR THE SCAN MIRROR IN ITS DATUM POSITION

In the baseline system configuration when the scan mirror in its datum position the normal to the scanner mirror planar surface is parallel the TRCF X-axis. Errors in knowledge of the direction of the normal to the mirror surface result in errors in knowledge of the line-of-sight. The simulation program allows the introduction of misalignment of the normal to the mirror surface from its baseline direction. The misalignments are introduced through rotations $ROT_2$ and $ROT_3$ about the $\mathbf{O_2}$ and $\mathbf{O_3}$ axis respectively[1], from the system baseline configuration in which the normal to the mirror surface, **n**, is parallel to the $\mathbf{O_1}$ axis ($\mathbf{n} = -\mathbf{O_1}$). Note that only one rotation is considered at a time:

$$\mathbf{n} = -\cos(ROT_2)\mathbf{O_1} + \sin(ROT_2)\mathbf{O_3} \qquad \text{or} \qquad (6.2.1)$$

$$\mathbf{n} = -\cos(ROT_3)\mathbf{O_1} - \sin(ROT_3)\mathbf{O_2} \qquad (6.2.2)$$

The errors in knowledge of the absolute LOS and change in LOS for $0 < t < 66$ sec and $0 < t < 10$ sec caused by errors in knowledge of the direction of the mirror normal are listed in Table 6.2.1.

Figures 6.2.1 and 6.2.2 show the errors in the direction of the line-of-sight in inertial space due to errors in the knowledge of the direction of the normal to the mirror surface.

[1] Note that these misalignments as introduced are equivalent to adding bias errors to the elevation shaft angle and azimuth shaft angle respectively.

| Parameter | | | 0 < t < 66 sec | | 0 < t < 10 sec | | | | |
|---|---|---|---|---|---|---|---|---|---|
| | $\delta A$ (arcsec) | $\delta E$ (arcsec) | $\delta \Delta A_m$ (arcsec) | $\delta \Delta E$ (arcsec) | $\delta A$ (arcsec), $a$ (deg) | | $\delta \Delta E$ (arcsec), θ (arcsec), $a$ (deg) | | |
| $ROT_2$ (arcsec) | | | | | | | | | |
| +10 | 3.348 | 1.999E+1 | 2.165 | 1.161 | 3.348 | −19.5 | 8.175E−4 | 140 | −19.5 |
| −10 | 3.347 | 1.999E+1 | 2.165 | 1.161 | 3.347 | −19.5 | 8.173E−4 | 140 | −19.5 |
| +100 | 3.352E+1 | 1.999E+2 | 2.168E+1 | 1.162E+1 | 3.352E+1 | −19.5 | 8.188E−3 | 140 | −19.5 |
| −100 | 3.343E+1 | 1.999E+2 | 2.162E+1 | 1.161E+1 | 3.343E+1 | −19.5 | 8.161E−3 | 140 | −19.5 |
| $ROT_3$ (arcsec) | | | | | | | | | |
| +10 | 2.009E+1 | 1.295E−1 | 1.996E+1 | 1.985E−1 | 2.009E+1 | −19.5 | 2.452E−3 | 140 | −19.5 |
| −10 | 2.009E+1 | 1.295E−1 | 1.996E+1 | 1.985E−1 | 2.009E+1 | −19.5 | 2.453E−3 | 140 | −19.5 |
| +100 | 2.0095E+2 | 1.293 | 1.9963E+2 | 1.982 | 2.0095E+2 | −19.5 | 2.449E−2 | 140 | −19.5 |
| −100 | 2.0095E+2 | 1.297 | 1.9963E+2 | 1.988 | 2.0095E+2 | −19.5 | 2.456E−2 | 140 | −19.5 |

Table 6.2.1: Maximum errors in the knowledge of the absolute LOS and change in LOS caused by errors in knowledge of the direction of the normal to the scan mirror surface.

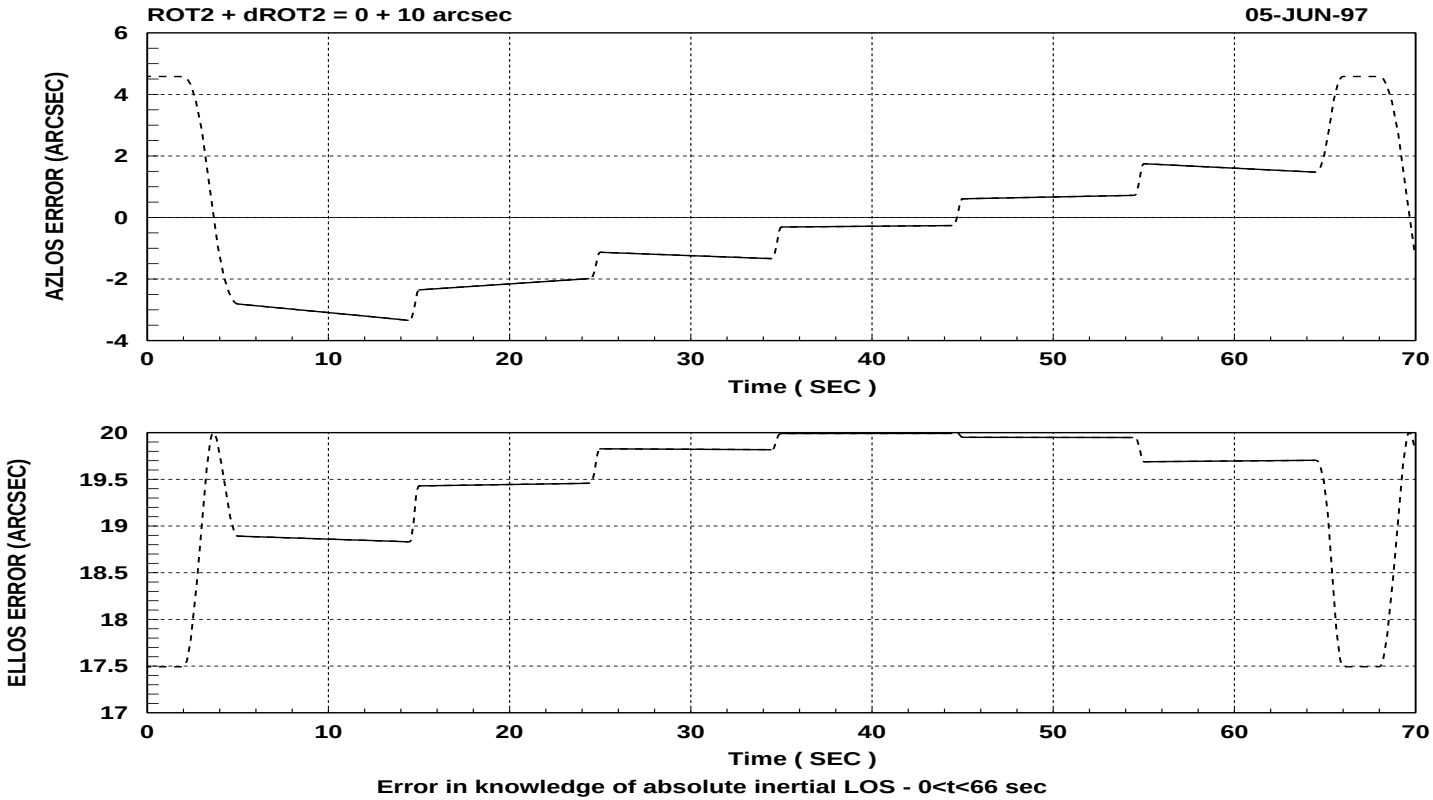


Figure 6.2.1: Errors in the knowledge of the inertial LOS caused by errors in knowledge of the direction of the normal to the scan mirror surface (ROT2).

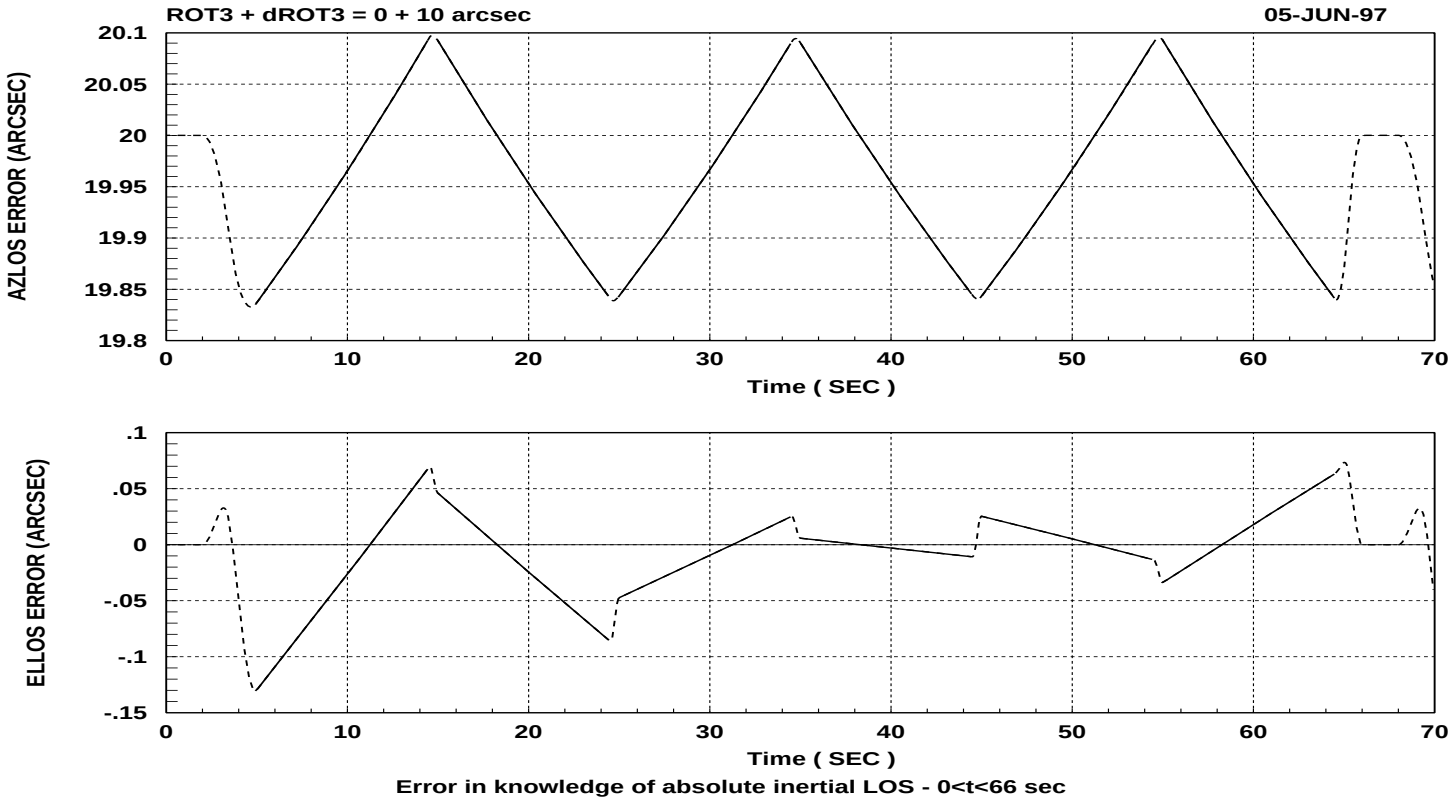


Figure 6.2.2: Errors in the knowledge of the inertial LOS caused by errors in knowledge of the direction of the normal to the scan mirror surface (ROT3).

## 6.3 KNOWLEDGE OF THE DIRECTION OF THE AZIMUTH GIMBAL AXIS

In the simulations the azimuth gimbal axis is defined as a vector, **AZA**, expressed in the reference frame, WOB2, which is an auxiliary frame obtained as follows: Starting from frame O fixed to the optical bench a simple rotation is performed about the $\mathbf{O_1}$ axis and results in an intermediate frame WOB1, a second rotation about axis $\mathbf{WOB1_2}$ results in frame WOB2. Frames WOB1 and WOB2 are used to model the wobble of the azimuth axis. In the case where the wobble is zero these frames coincide with frame O.

$$\mathbf{AZA} = AZA_1\ \mathbf{WOB2_1} + AZA_2\ \mathbf{WOB2_2} + AZA_3\ \mathbf{WOB2_3} \tag{6.3.1}$$

In the baseline system configuration the azimuth gimbal axis is parallel to the unit vector $\mathbf{WOB2_3}$ ( = $\mathbf{O_3}$) of the reference frame fixed to the optical bench. Errors in the knowledge of the **AZA** vector are introduced by considering rotations $\theta_{AZA1}$ and $\theta_{AZA2}$ about the $\mathbf{WOB2}_1$ and $\mathbf{WOB2}_2$ vectors respectively. Note that only one rotation is considered at a time:

$$\mathbf{AZA} = -\sin\theta_{AZA1}\ \mathbf{WOB2_2} + \cos\theta_{AZA1}\ \mathbf{WOB2_3} \qquad \text{or} \tag{6.3.2}$$

$$\mathbf{AZA} = \sin\theta_{AZA2}\ \mathbf{WOB2_1} + \cos\theta_{AZA2}\ \mathbf{WOB2_3} \tag{6.3.3}$$

The errors in knowledge of the absolute LOS and change in LOS, for 0 < t < 66 sec and 0 < t < 10 sec, caused by errors in the knowledge of the direction of the azimuth gimbal axis with respect to the optical bench are presented in Table 6.3.1.

Figures 6.3.1 and 6.3.2 show the errors in the direction of the line-of-sight in inertial space due to errors in the knowledge of the direction of the azimuth gimbal axis of rotation.

| Parameter | | | 0 < t < 66 sec | | 0 < t < 10 sec | | | | |
|---|---|---|---|---|---|---|---|---|---|
| | $\delta A$ (arcsec) | $\delta E$ (arcsec) | $\delta \Delta A_m$ (arcsec) | $\delta \Delta E$ (arcsec) | $\delta A$ (arcsec), $a$ (deg) | | $\delta \Delta E$ (arcsec), θ (arcsec), $a$ (deg) | | |
| $\theta_{AZA1}$ (arcsec) | | | | | | | | | |
| +10 | 1.129 | 6.308 | 5.063E−1 | 9.744 | 1.129 | −19.5 | 2.627E−4 | 140 | −19.5 |
| −10 | 1.130 | 6.308 | 5.065E−1 | 9.744 | 1.130 | −19.5 | 2.627E−4 | 140 | −19.5 |
| +100 | 1.129E+1 | 6.308E+1 | 5.055 | 9.744E+1 | 1.129E+1 | −19.5 | 2.627E−3 | 140 | −19.5 |
| −100 | 1.131E+1 | 6.308E+1 | 5.073 | 9.744E+1 | 1.131E+1 | −19.5 | 2.627E−3 | 140 | −19.5 |
| $\theta_{AZA2}$ (arcsec) | | | | | | | | | |
| +10 | 2.921E−1 | 1.085 | 8.165E−2 | 1.076 | 2.921E−1 | −19.5 | 7.660E−5 | 140 | −19.5 |
| −10 | 2.918E−1 | 1.085 | 8.142E−2 | 1.076 | 2.918E−1 | −19.5 | 7.659E−5 | 140 | −19.5 |
| +100 | 2.937 | 1.085E+1 | 8.270E−1 | 1.076E+1 | 2.937 | −19.5 | 7.663E−4 | 140 | −19.5 |
| −100 | 2.903 | 1.085E+1 | 8.037E−1 | 1.076E+1 | 2.903 | −19.5 | 7.656E−4 | 140 | −19.5 |

Table 6.3.1: Maximum errors in the knowledge of the absolute LOS and change in LOS caused by errors in knowledge of the direction of the azimuth gimbal axis.

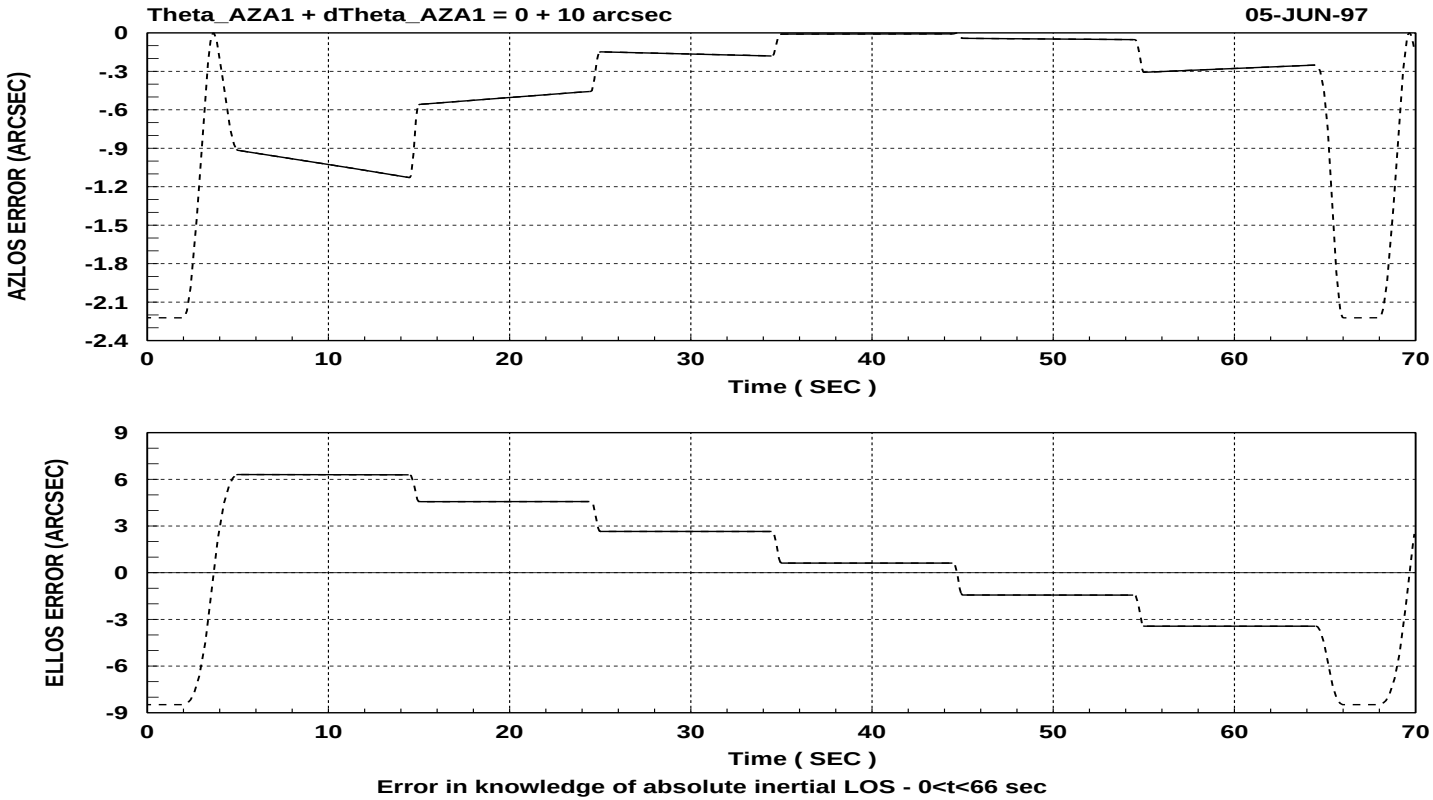


Figure 6.3.1: Errors in the knowledge of the inertial LOS caused by errors in knowledge of the direction of the azimuth gimbal axis of rotation ($\theta_{AZA1}$).

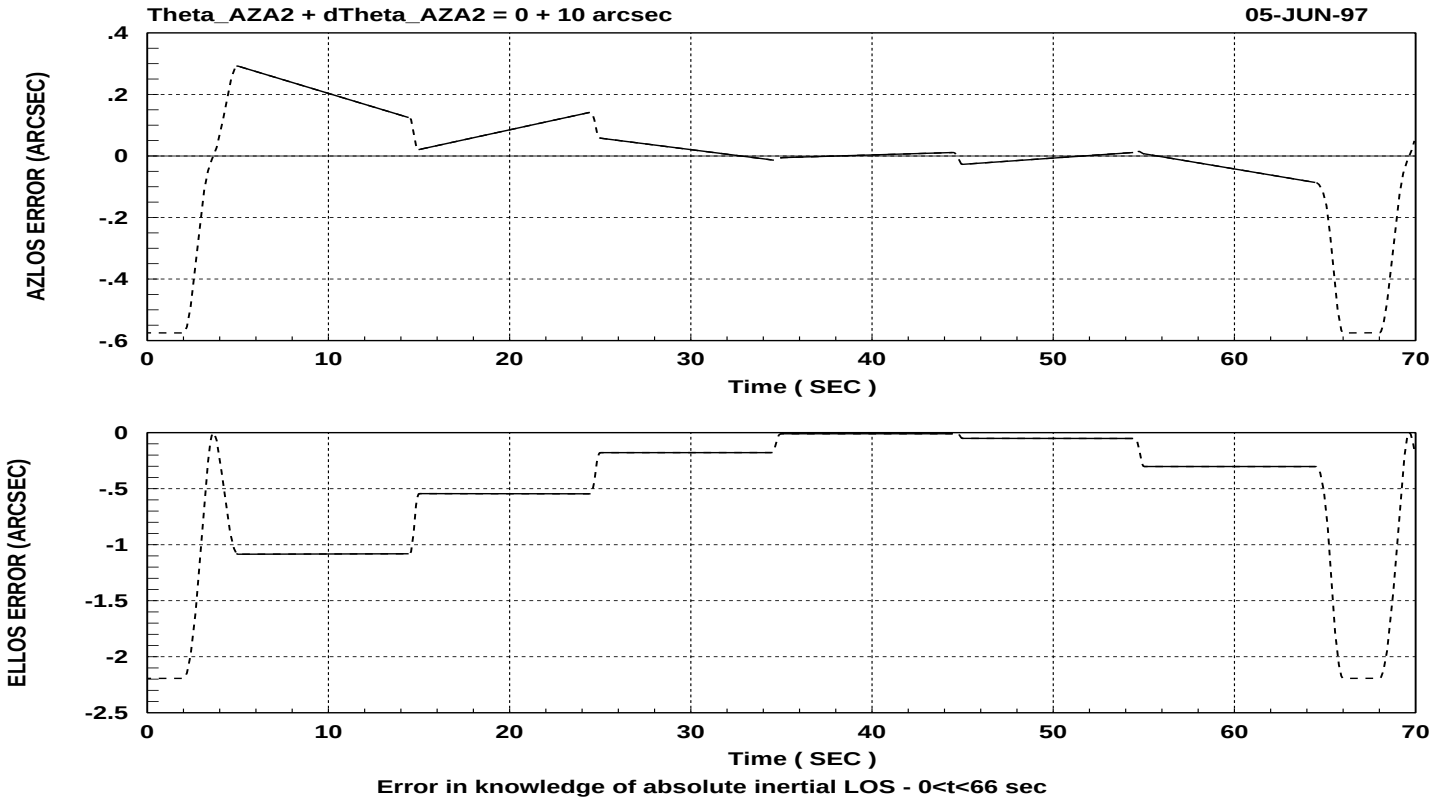


Figure 6.3.2: Errors in the knowledge of the inertial LOS caused by errors in knowledge of the direction of the azimuth gimbal axis of rotation ($\theta_{AZA2}$).

## 6.4 KNOWLEDGE OF THE DIRECTION OF THE SCANNER ELEVATION AXIS

In the simulations the scanner elevation axis is defined as a vector, **ELA**, expressed in the reference frame, R, fixed to the azimuth gimbal,

$$\mathbf{ELA} = ELA_1\ \mathbf{R_1} + ELA_2\ \mathbf{R_2} + ELA_3\ \mathbf{R_3} \tag{6.4.1}$$

Two different directions are used as baseline directions for the scanner elevation axes:

In the first configuration **ELA** is parallel to $\mathbf{R_2}$ , this is the direction of the elevation axis in the baseline system configuration as defined in Section 4.1. Errors in knowledge of the direction of the **ELA** vector are introduced by considering rotations $\theta_{ELA1}$ and $\theta_{ELA3}$ about the $\mathbf{R_1}$ or $\mathbf{R_3}$ vectors respectively. Note that only one rotation is considered at a time:

$$\mathbf{ELA} = \cos\theta_{ELA1}\ \mathbf{R_2} + \sin\theta_{ELA1}\ \mathbf{R_3} \qquad \text{or} \tag{6.4.2}$$

$$\mathbf{ELA} = -\sin\theta_{ELA3}\ \mathbf{R_1} + \cos\theta_{ELA3}\ \mathbf{R_2} \tag{6.4.3}$$

A second configuration is used as baseline in which **ELA** is obtained by rotating the Y-axis of the optical bench, $\mathbf{O_2}$ , by $\theta_{ELA3o}$ = 0.05 degrees about the Z-axis of the optical bench, $\mathbf{O_3}$. Errors in knowledge of the direction of the **ELA** vector are introduced by considering rotations, from this modified baseline direction, $\delta\theta_{ELA3o}$ and $\delta\theta_{ELA1}$ about $\mathbf{O_3}$ and the rotated X-axis respectively. Note that only one rotation is considered at a time:

$$\begin{aligned}\mathbf{ELA} = &-\cos\delta\theta_{ELA1}\sin(\theta_{ELA3o} + \delta\theta_{ELA3})\,\mathbf{R_1} \\ &+ \cos\delta\theta_{ELA1}\cos(\theta_{ELA3o} + \delta\theta_{ELA3})\,\mathbf{R_2} + \sin\delta\theta_{ELA1}\ \mathbf{R_3}\end{aligned} \tag{6.4.5}$$

The errors in knowledge of the absolute LOS and change in LOS for 0 < t < 66 sec and 0 < t < 10 sec caused by errors in the knowledge of the direction of the scanner elevation axis with respect to the optical bench are presented in Tables 6.4.1 and 6.4.2, for the two different baseline directions of the scanner elevation axis.

Figures 6.4.1 through 6.4.4 show the errors in the direction of the line-of-sight in inertial space due to errors in the knowledge of the direction of the scanner elevation axis of rotation.

| Parameter | | | 0 < t < 66 sec | | 0 < t < 10 sec | | | | |
|---|---|---|---|---|---|---|---|---|---|
| | $\delta A$ (arcsec) | $\delta E$ (arcsec) | $\delta \Delta A_m$ (arcsec) | $\delta \Delta E$ (arcsec) | $\delta A$ (arcsec), $a$ (deg) | | $\delta \Delta E$ (arcsec), θ (arcsec), $a$ (deg) | | |
| $\theta_{ELA1}$ (arcsec) | | | | | | | | | |
| +10 | 3.911E−1 | 2.563E−3 | 8.883E−2 | 3.723E−3 | 3.911E−1 | −19.5 | 9.166E−5 | 140 | −19.5 |
| −10 | 3.911E−1 | 2.545E−3 | 8.883E−2 | 3.723E−3 | 3.911E−1 | −19.5 | 9.133E−5 | 140 | −19.5 |
| +100 | 3.912 | 2.644E−2 | 8.883E−1 | 3.725E−2 | 3.912 | −19.5 | 9.315E−4 | 140 | −19.5 |
| −100 | 3.911 | 2.463E−2 | 8.883E−1 | 3.721E−2 | 3.911 | −19.5 | 8.984E−4 | 140 | −19.5 |
| $\theta_{ELA3}$ (arcsec) | | | | | | | | | |
| +10 | 3.858E−3 | 3.421E−5 | 8.630E−4 | 4.250E−5 | 3.858E−3 | −19.5 | 1.509E−6 | 140 | −19.5 |
| −10 | 3.855E−3 | 1.961E−5 | 8.626E−4 | 3.576E−5 | 3.855E−3 | −19.5 | 1.180E−6 | 140 | −19.5 |
| +100 | 3.870E−2 | 1.155E−3 | 8.650E−3 | 1.658E−3 | 3.870E−2 | −19.5 | 2.994E−5 | 140 | −19.5 |
| −100 | 3.843E−2 | 9.899E−3 | 8.607E−3 | 1.462E−3 | 3.843E−2 | −19.5 | 2.236E−5 | 140 | +10.05 |

Table 6.4.1: Maximum errors in the knowledge of the absolute LOS and change in LOS caused by errors in knowledge of the direction of the scanner elevation axis. For a nominal direction parallel to the Azimuth Gimbal Y-axis ($\mathbf{R}_2$).

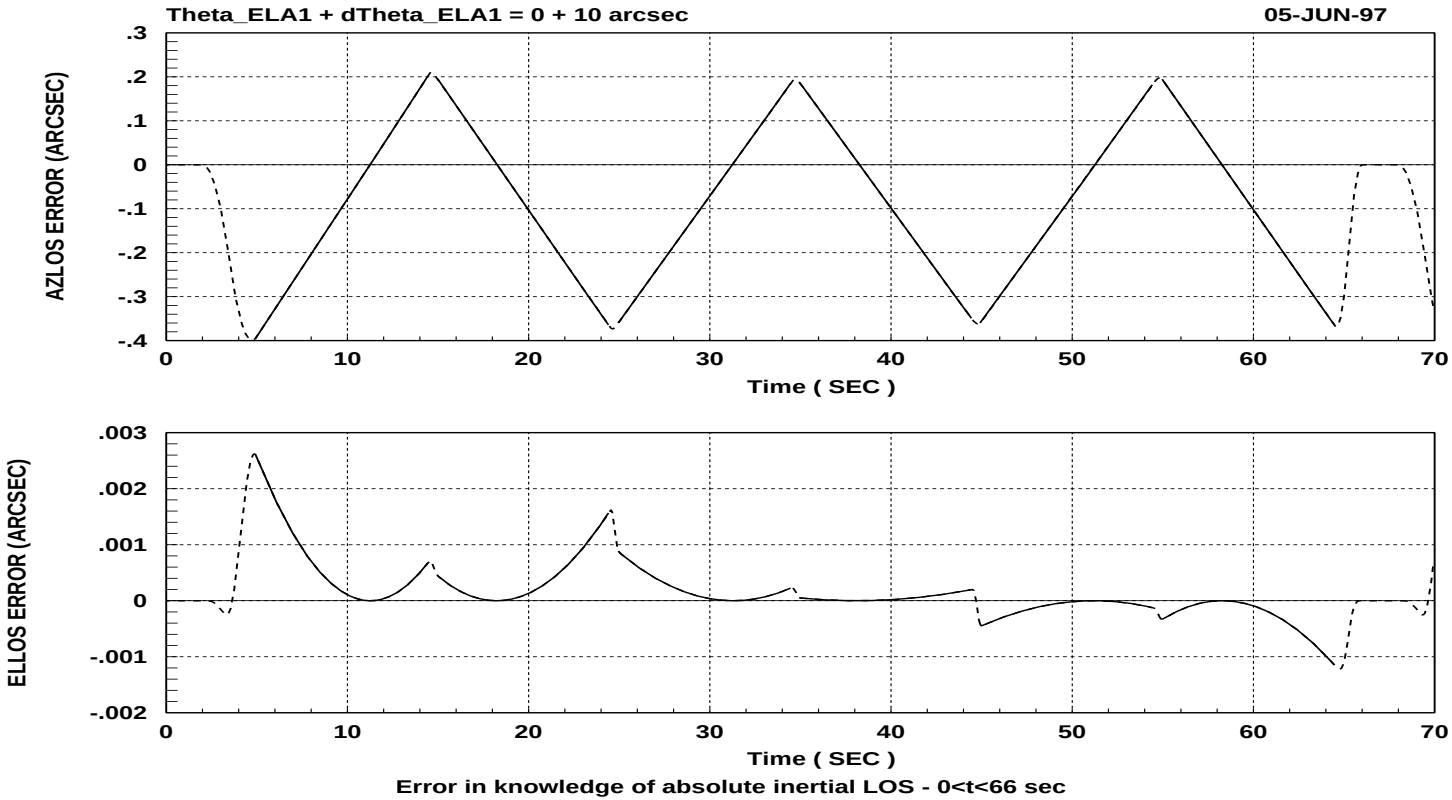


Figure 6.4.1: Errors in the knowledge of the inertial LOS caused by errors in knowledge of the direction of the scanner elevation axis ($\theta_{ELA1}$). For a nominal direction parallel to the Azimuth Gimbal Y-axis ($\mathbf{R}_2$).

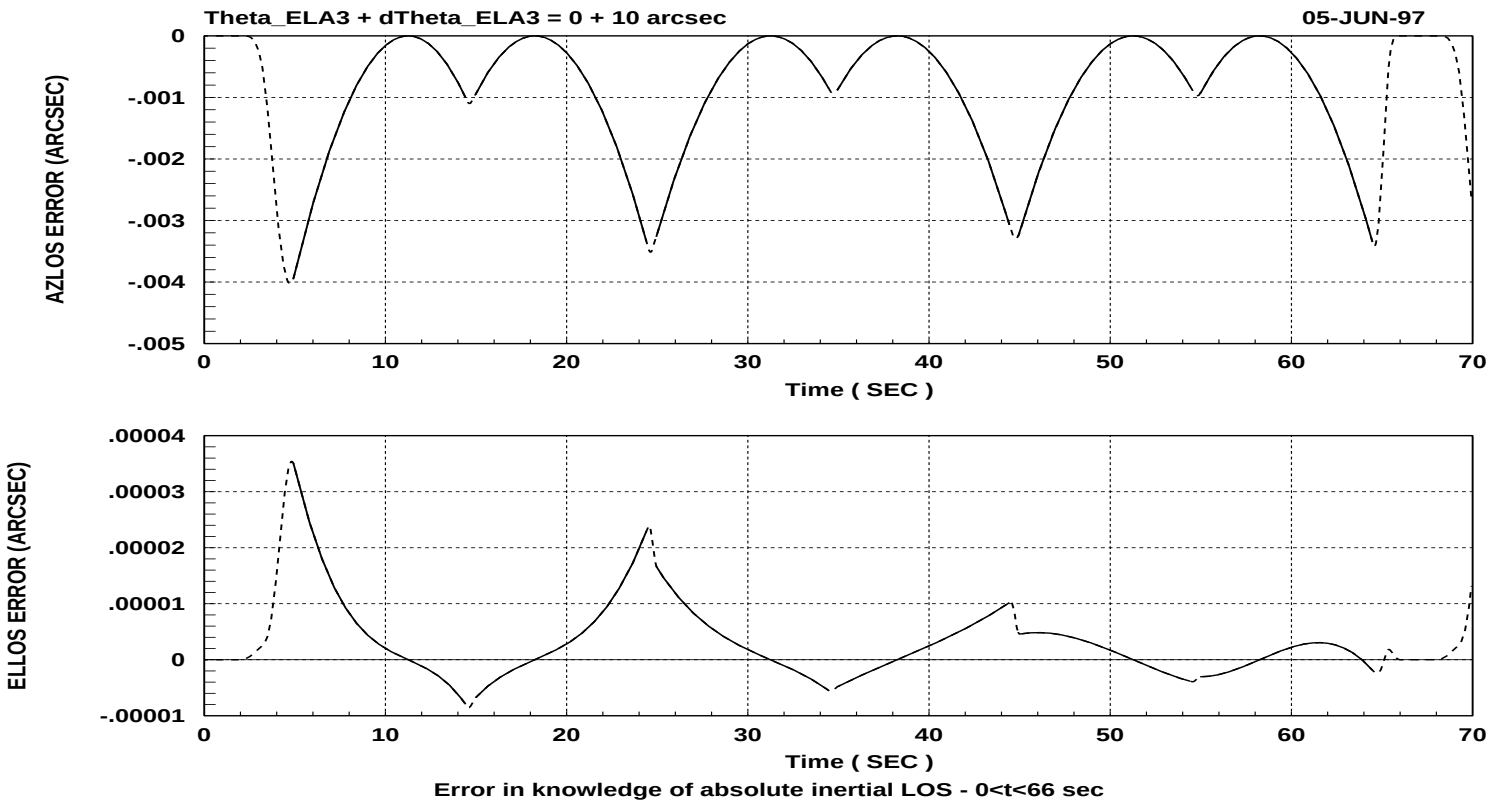


Figure 6.4.2: Errors in the knowledge of the inertial LOS caused by errors in knowledge of the direction of the scanner elevation axis ($\theta_{ELA3}$). For a nominal direction parallel to the Azimuth Gimbal Y-axis ($\mathbf{R}_2$).

| Parameter | | | 0 < t < 66 sec | | 0 < t < 10 sec | | | | |
|---|---|---|---|---|---|---|---|---|---|
| | $\delta A$ (arcsec) | $\delta E$ (arcsec) | $\delta \Delta A_m$ (arcsec) | $\delta \Delta E$ (arcsec) | $\delta A$ (arcsec), $a$ (deg) | | $\delta \Delta E$ (arcsec), θ (arcsec), $a$ (deg) | | |
| $\delta\theta_{ELA1}$ (arcsec) | | | | | | | | | |
| +10 | 3.911E−1 | 2.566E−3 | 8.883E−2 | 3.723E−3 | 3.911E−1 | −19.5 | 9.178E−5 | 140 | −19.5 |
| −10 | 3.911E−1 | 2.548E−3 | 8.883E−2 | 3.723E−3 | 3.911E−1 | −19.5 | 9.145E−5 | 140 | −19.5 |
| +100 | 3.912 | 2.647E−2 | 8.883E−1 | 3.725E−2 | 3.912 | −19.5 | 9.326E−4 | 140 | −19.5 |
| −100 | 3.911 | 2.466E−2 | 8.883E−1 | 3.721E−2 | 3.911 | −19.5 | 8.996E−4 | 140 | −19.5 |
| $\delta\theta_{ELA3}$ (arcsec) | | | | | | | | | |
| +10 | 3.906E−3 | 3.593E−4 | 8.707E−4 | 5.358E−4 | 3.906E−3 | −19.5 | 7.446E−6 | 140 | −19.5 |
| −10 | 3.904E−3 | 3.413E−4 | 8.703E−4 | 5.084E−4 | 3.904E−3 | −19.5 | 7.116E−6 | 140 | −19.5 |
| +100 | 3.918E−2 | 4.441E−3 | 8.727E−3 | 6.592E−3 | 3.918E−2 | −19.5 | 8.930E−5 | 140 | −19.5 |
| −100 | 3.892E−2 | 2.600E−3 | 8.684E−3 | 3.851E−3 | 3.892E−2 | −19.5 | 5.632E−5 | 140 | −19.5 |

Table 6.4.2: Maximum errors in the knowledge of the absolute LOS and change in LOS caused by errors in knowledge of the direction of the scanner elevation axis. For a nominal direction of **ELA** obtained by rotating the $\mathbf{R_2}$ axis 0.05 degrees about the $\mathbf{R_3}$ axes.

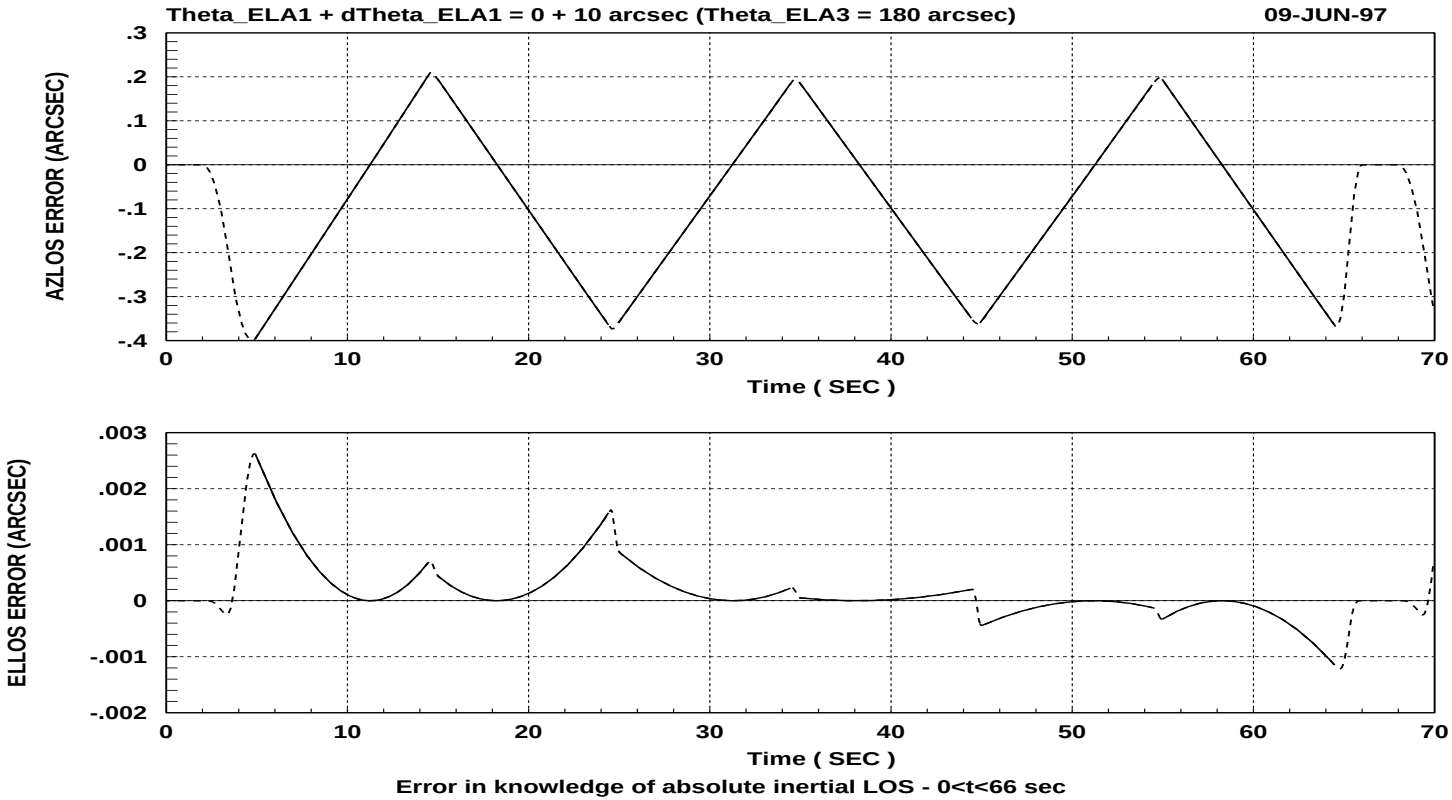


Figure 6.4.3: Errors in the knowledge of the inertial LOS caused by errors in knowledge of the direction of the scanner elevation axis ($\theta_{ELA1}$). For a nominal direction of **ELA** obtained by rotating the $\mathbf{R}_2$ axis 0.05 degrees about the $\mathbf{R}_3$ axes.

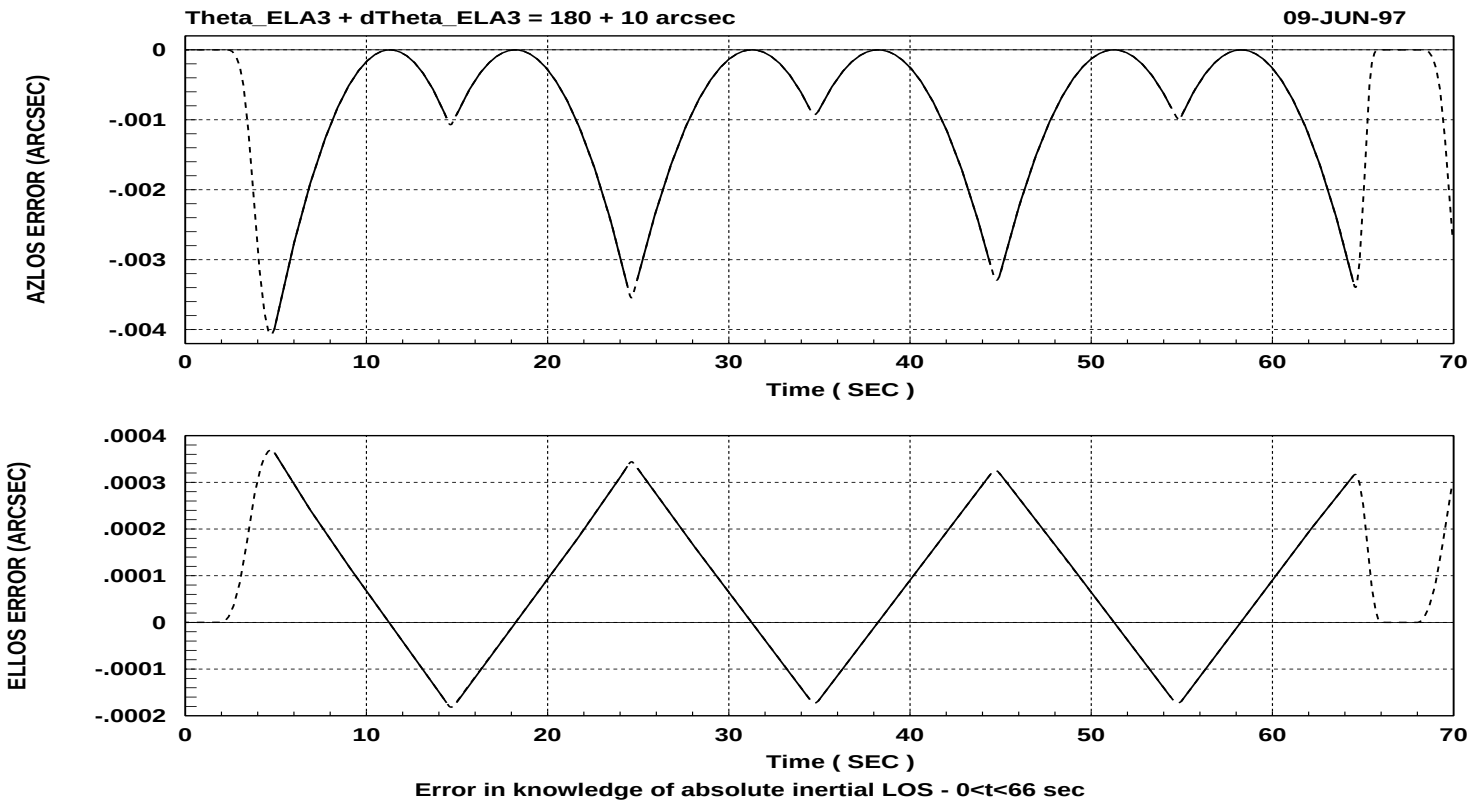


Figure 6.4.4: Errors in the knowledge of the inertial LOS caused by errors in knowledge of the direction of the scanner elevation axis ($\theta_{ELA3}$). For a nominal direction of **ELA** obtained by rotating the $\mathbf{R}_2$ axis 0.05 degrees about the $\mathbf{R}_3$ axes.

## 6.5 KNOWLEDGE OF THE DIRECTION OF THE WOBBLE SENSORS SENSITIVE AXIS

In the simulations the direction of the i[th] wobble sensor sensitive axis is defined by a unit vector, **UWi**, expressed in the reference frame, O, fixed to the optical bench. Errors in the knowledge of the LOS and change of LOS are calculated for two baseline configurations:

The first baseline configuration has all the wobble sensors with their sensitive axis parallel to the Z-axis of the optical bench, i.e. **UWi** = $\mathbf{O_3}$. In this case knowledge errors in the direction of the sensors sensitive axis are introduced in the simulation by rotating the sensitive axis from its baseline configuration about axis $\mathbf{O_1}$ and $\mathbf{O_2}$. Note that one rotation is considered at a time:

$$\mathbf{UWi} = -\sin\theta_{UWi1}\,\mathbf{O_2} + \cos\theta_{UWi1}\,\mathbf{O_3} \qquad \text{or} \tag{6.5.1}$$

$$\mathbf{UWi} = \sin\theta_{UWi2}\,\mathbf{O_1} + \cos\theta_{UWi2}\,\mathbf{O_3} \tag{6.5.2}$$

In the second baseline configuration the direction of the sensitive axis of wobble sensors 1 and 2 is obtained by a first rotation of $\mathbf{O_3}$ about the optical bench X-axis, and a second rotation about the intermediate Y-axis, resulting in a combined rotation angle of 0.25 degrees with respect to $\mathbf{O_3}$. Errors in the direction of wobble sensors 1 and 2 from this baseline configuration are obtained by varying the two rotations just described from their baseline values:

$$\begin{aligned}\mathbf{UWi} = {} & \sin(\theta_{UWi1o} + \delta\theta_{UWi1})\,\mathbf{O_1} - \cos(\theta_{UWi2o} + \delta\theta_{UWi2})\sin(\theta_{UWi1o} + \delta\theta_{UWi1})\,\mathbf{O_2} + \\ & \cos(\theta_{UWi2o} + \delta\theta_{UWi2})\cos(\theta_{UWi1o} + \delta\theta_{UWi1})\,\mathbf{O_3}\end{aligned} \tag{6.5.3}$$

The errors in knowledge of the absolute LOS and change in LOS, for 0 < t < 66 sec and 0 < t < 10 sec, caused by errors in the knowledge of the direction of the wobble sensors sensitive axis are presented in Tables 6.5.1 and 6.5.2, for wobble sensors 1 and 2 (i = 1, 2)[1] and for the two baseline configurations described. Note that wobble sensors 3 and 4 have their sensitive axis parallel to the $\mathbf{O_3}$ axis in all cases.

The fact that the errors caused by $\theta_{UWi1}$ and $\theta_{UWi2}$ are the same is expected because the baseline configuration has zero wobble[2], and suggests that a single parameter $\theta_{UWi}$ (angle between $\mathbf{O_3}$ and **UWi**) should be used in specifying the alignment of the wobble sensors sensitive axis. A similar argument applies to $\delta\theta_{UWi1o}$ and $\delta\theta_{UWi2o}$.

Figures 6.5.1 through 6.5.8 show the errors in the direction of the line-of-sight in inertial space due to errors in the knowledge of the direction of the wobble sensors sensitive axis.

---

[1] The wobble sensors are used in pairs (1,3) and (2,4). The line connecting sensors 1 and 3 is parallel to $\mathbf{O_1}$ and the line connecting sensors 2 and 4 is parallel to $\mathbf{O_2}$. Misalignment of sensors 1 and 3 cause similar to errors, and the same argument is valid with respect to sensors 2 and 4.

[2] The errors would differ if a non-zero wobble was used for the nominal case, but this is a second order effect and should not significantly impact the results.

| Parameter | | | 0 < t < 66 sec | | 0 < t < 10 sec | | | | |
|---|---|---|---|---|---|---|---|---|---|
| | $\delta A$ (arcsec) | $\delta E$ (arcsec) | $\delta \Delta A_m$ (arcsec) | $\delta \Delta E$ (arcsec) | $\delta A$ (arcsec), | $a$ (deg) | $\delta \Delta E$ (arcsec), | θ (arcsec), | $a$ (deg) |
| $\theta_{UW11}$ (arcsec) | | | | | | | | | |
| +10 | 1.232E−4 | 7.638E−4 | 7.964E−5 | 8.534E−5 | 1.232E−4 | −19.5 | 3.024E−8 | 140 | −19.5 |
| −10 | 1.232E−4 | 7.638E−4 | 7.964E−5 | 8.534E−5 | 1.232E−4 | −19.5 | 3.024E−8 | 140 | −19.5 |
| +100 | 1.232E−2 | 7.638E−2 | 7.964E−3 | 8.534E−3 | 1.232E−2 | −19.5 | 3.026E−6 | 140 | −19.5 |
| −100 | 1.232E−2 | 7.638E−2 | 7.964E−3 | 8.534E−3 | 1.232E−2 | −19.5 | 3.026E−6 | 140 | −19.5 |
| $\theta_{UW12}$ (arcsec) | | | | | | | | | |
| +10 | 1.232E−4 | 7.639E−4 | 7.965E−5 | 8.535E−5 | 1.232E−4 | −19.5 | 3.027E−8 | 140 | −19.5 |
| −10 | 1.232E−4 | 7.637E−4 | 7.964E−5 | 8.533E−5 | 1.232E−4 | −19.5 | 3.024E−8 | 140 | −19.5 |
| +100 | 1.233E−2 | 7.644E−2 | 7.971E−3 | 8.541E−3 | 1.233E−2 | −19.5 | 3.028E−6 | 140 | −19.5 |
| −100 | 1.231E−2 | 7.632E−2 | 7.958E−3 | 8.528E−3 | 1.231E−2 | −19.5 | 3.023E−6 | 140 | −19.5 |
| $\theta_{UW21}$ (arcsec) | | | | | | | | | |
| +10 | 4.998E−5 | 2.413E−4 | 2.275E−5 | 3.726E−4 | 4.998E−5 | −19.5 | 1.257E−8 | 140 | −19.5 |
| −10 | 4.997E−5 | 2.412E−4 | 2.275E−5 | 3.726E−4 | 4.997E−5 | −19.5 | 1.256E−8 | 140 | −19.5 |
| +100 | 5.001E−3 | 2.414E−2 | 2.277E−3 | 3.729E−2 | 5.001E−3 | −19.5 | 1.258E−6 | 140 | −19.5 |
| −100 | 4.993E−3 | 2.411E−2 | 2.274E−3 | 3.723E−2 | 4.993E−3 | −19.5 | 1.256E−6 | 140 | −19.5 |
| $\theta_{UW22}$ (arcsec) | | | | | | | | | |
| +10 | 4.997E−5 | 2.412E−4 | 2.275E−5 | 3.726E−4 | 4.997E−5 | −19.5 | 1.255E−8 | 140 | −19.5 |
| −10 | 4.997E−5 | 2.412E−4 | 2.275E−5 | 3.726E−4 | 4.997E−5 | −19.5 | 1.255E−8 | 140 | −19.5 |
| +100 | 4.997E−3 | 2.412E−2 | 2.275E−3 | 3.726E−2 | 4.997E−3 | −19.5 | 1.257E−6 | 140 | −19.5 |
| −100 | 4.997E−3 | 2.412E−2 | 2.275E−3 | 3.726E−2 | 4.997E−3 | −19.5 | 1.257E−6 | 140 | −19.5 |

Table 6.5.1: Maximum errors in the knowledge of the absolute LOS and change in LOS caused by errors in knowledge of the direction of the wobble sensors sensitive axis. Nominal direction of the wobble sensors is with the sensitive axis parallel to the optical bench Z-axis, $\mathbf{O}_3$.

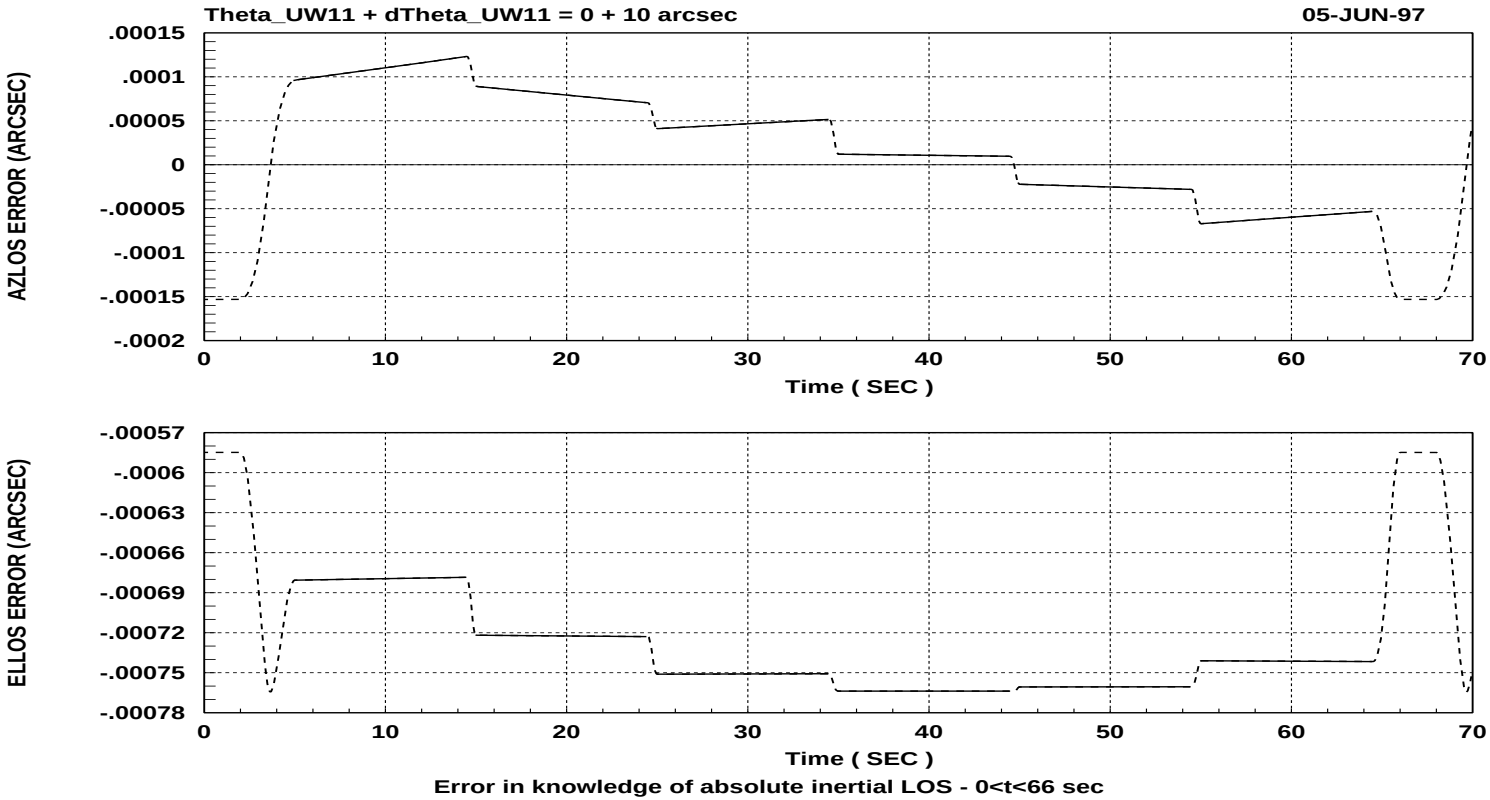


Figure 6.5.1: Errors in the knowledge of the inertial LOS caused by errors in knowledge of the direction of the wobble sensors sensitive axis ($\theta_{UW11}$) . Nominal direction of the wobble sensors is with the sensitive axis parallel to the optical bench Z-axis, $\mathbf{O}_3$.

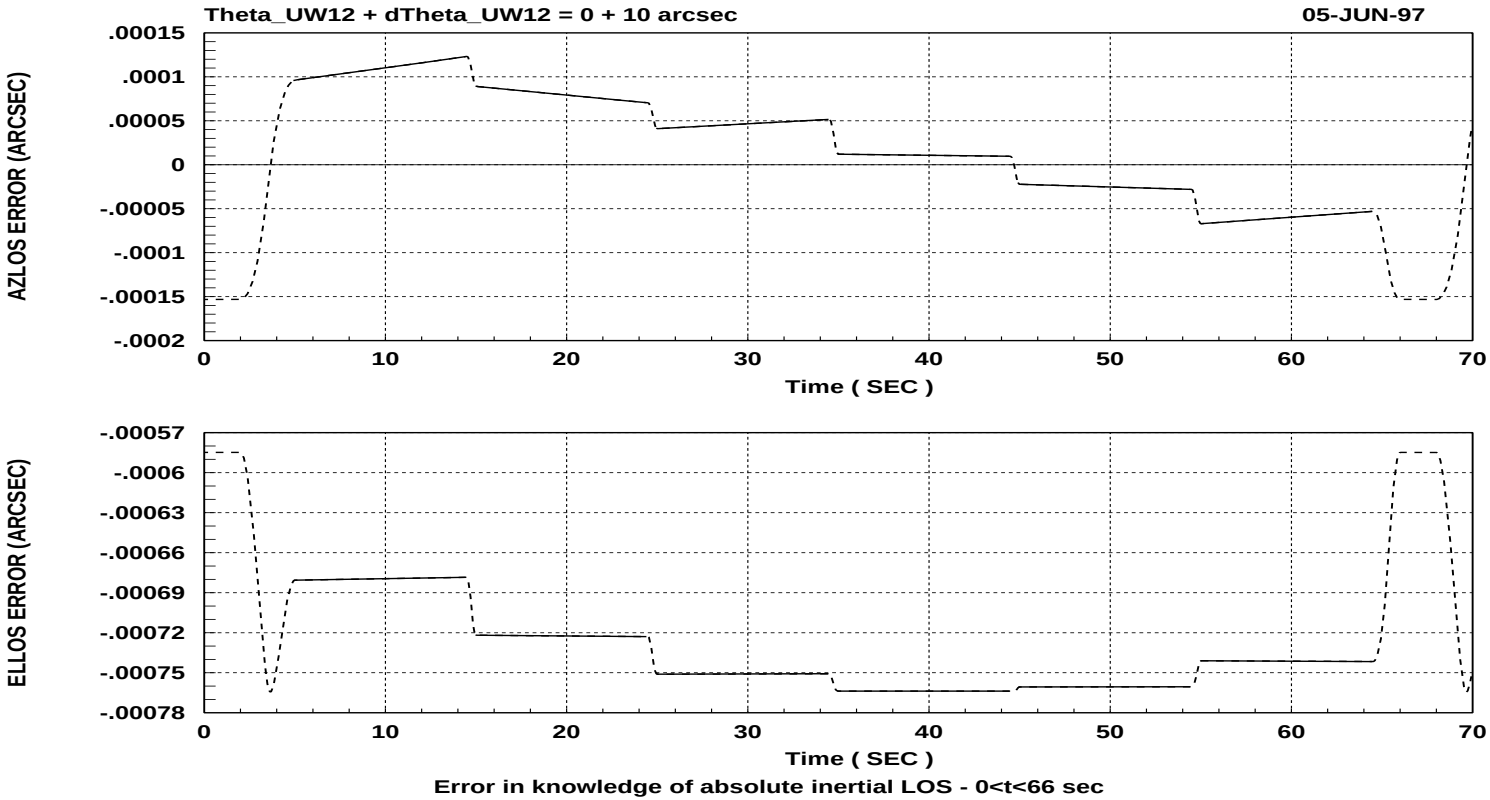


Figure 6.5.2: Errors in the knowledge of the inertial LOS caused by errors in knowledge of the direction of the wobble sensors sensitive axis ($\theta_{UW12}$) . Nominal direction of the wobble sensors is with the sensitive axis parallel to the optical bench Z-axis, $\mathbf{O}_3$.

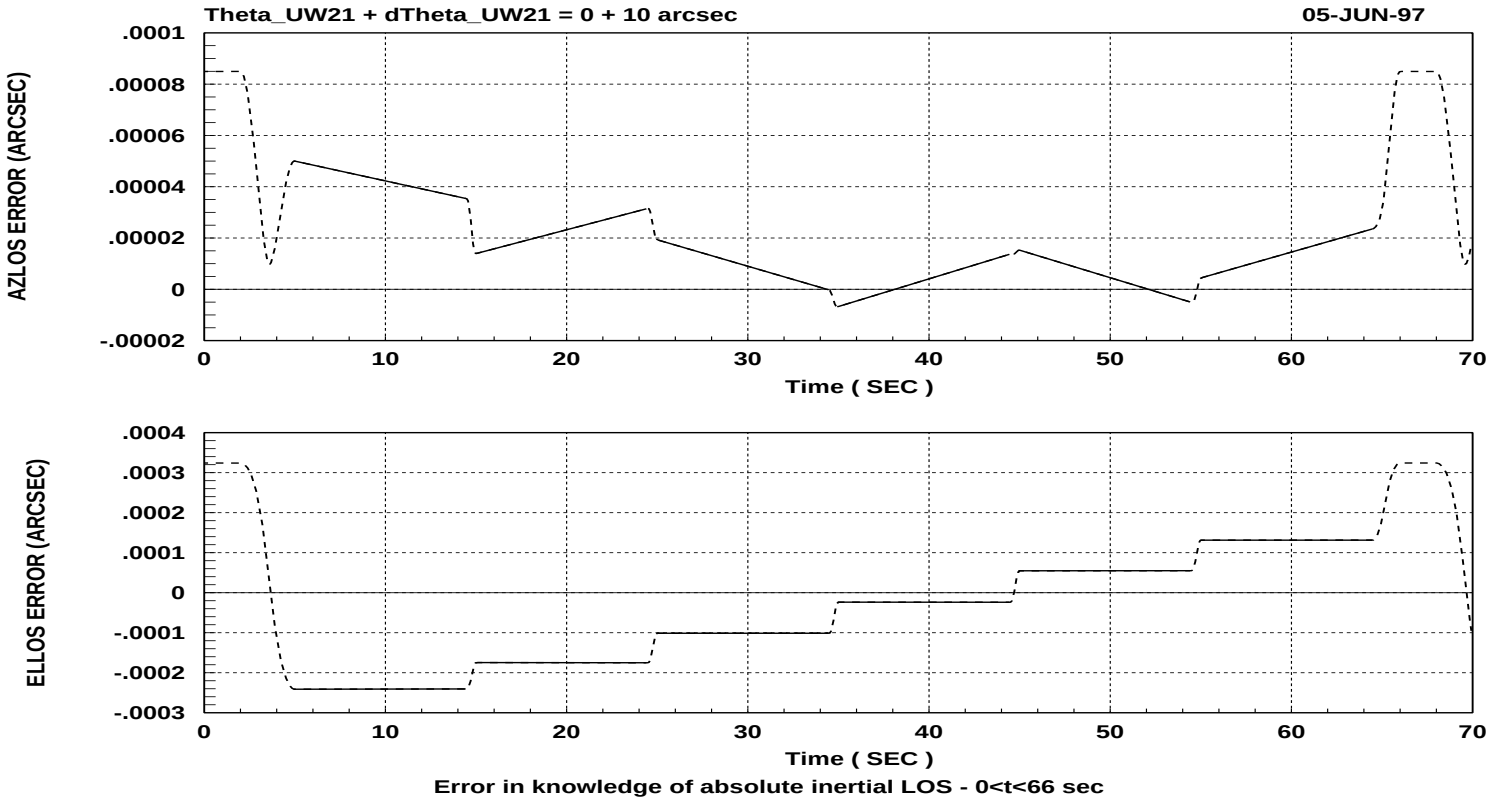


Figure 6.5.3: Errors in the knowledge of the inertial LOS caused by errors in knowledge of the direction of the wobble sensors sensitive axis ($\theta_{UW21}$) . Nominal direction of the wobble sensors is with the sensitive axis parallel to the optical bench Z-axis, $\mathbf{O}_3$.

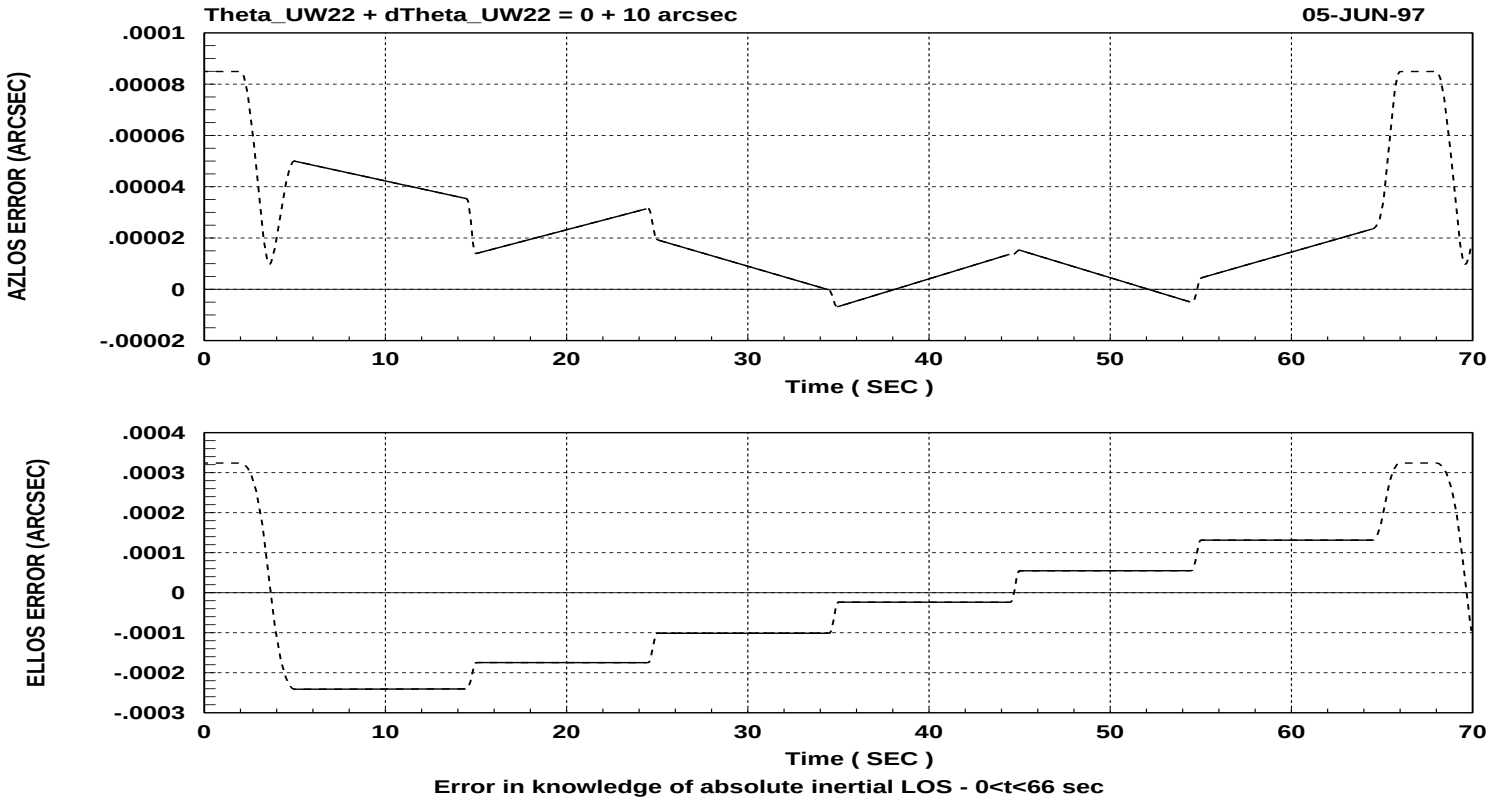


Figure 6.5.4: Errors in the knowledge of the inertial LOS caused by errors in knowledge of the direction of the wobble sensors sensitive axis ($\theta_{UW22}$) . Nominal direction of the wobble sensors is with the sensitive axis parallel to the optical bench Z-axis, $\mathbf{O}_3$.

| Parameter | | | 0 < t < 66 sec | | 0 < t < 10 sec | | | | |
|---|---|---|---|---|---|---|---|---|---|
| | $\delta A$ (arcsec) | $\delta E$ (arcsec) | $\delta \Delta A_m$ (arcsec) | $\delta \Delta E$ (arcsec) | $\delta A$ (arcsec), | $a$ (deg) | $\delta \Delta E$ (arcsec), | θ (arcsec), | $a$ (deg) |
| $\delta\theta_{UW11}$ (arcsec) | | | | | | | | | |
| +10 | 1.598E−2 | 9.896E−2 | 1.033E−2 | 1.092E−2 | 1.598E−2 | −19.5 | 3.924E−6 | 140 | −19.5 |
| −10 | 1.574E−2 | 9.742E−2 | 1.017E−2 | 1.075E−2 | 1.574E−2 | −19.5 | 3.863E−6 | 140 | −19.5 |
| +100 | 1.710E−1 | 1.059 | 1.105E−1 | 1.168E−1 | 1.710E−1 | −19.5 | 4.198E−5 | 140 | −19.5 |
| −100 | 1.462E−1 | 9.051E−1 | 9.450E−2 | 9.986E−2 | 1.462E−1 | −19.5 | 3.590E−5 | 140 | −19.5 |
| $\delta\theta_{UW12}$ (arcsec) | | | | | | | | | |
| +10 | 1.599E−2 | 9.896E−2 | 1.033E−2 | 1.092E−2 | 1.599E−2 | −19.5 | 3.925E−6 | 140 | −19.5 |
| −10 | 1.574E−2 | 9.741E−2 | 1.017E−2 | 1.075E−2 | 1.574E−2 | −19.5 | 3.863E−6 | 140 | −19.5 |
| +100 | 1.711E−1 | 1.059 | 1.106E−1 | 1.169E−1 | 1.711E−1 | −19.5 | 4.202E−5 | 140 | −19.5 |
| −100 | 1.461E−1 | 9.044E−1 | 9.443E−2 | 9.978E−2 | 1.461E−1 | −19.5 | 3.587E−5 | 140 | −19.5 |
| $\delta\theta_{UW21}$ (arcsec) | | | | | | | | | |
| +10 | 6.536E−3 | 3.168E−2 | 2.999E−3 | 4.823E−2 | 6.536E−3 | −19.5 | 1.643E−6 | 140 | −19.5 |
| −10 | 6.434E−3 | 3.119E−2 | 2.952E−3 | 4.748E−2 | 6.434E−3 | −19.5 | 1.617E−6 | 140 | −19.5 |
| +100 | 6.997E−2 | 3.392E−1 | 3.211E−2 | 5.164E−1 | 6.997E−2 | −19.5 | 1.759E−5 | 140 | −19.5 |
| −100 | 5.973E−2 | 2.896E−1 | 2.741E−2 | 4.408E−1 | 5.973E−2 | −19.5 | 1.501E−5 | 140 | −19.5 |
| $\delta\theta_{UW22}$ (arcsec) | | | | | | | | | |
| +10 | 6.536E−3 | 3.168E−2 | 2.999E−3 | 4.823E−2 | 6.536E−3 | −19.5 | 1.643E−6 | 140 | −19.5 |
| −10 | 6.434E−3 | 3.119E−2 | 2.953E−3 | 4.748E−2 | 6.434E−3 | −19.5 | 1.617E−6 | 140 | −19.5 |
| +100 | 6.992E−2 | 3.389E−1 | 3.209E−2 | 5.160E−1 | 6.992E−2 | −19.5 | 1.757E−5 | 140 | −19.5 |
| −100 | 5.978E−2 | 2.898E−1 | 2.743E−2 | 4.411E−1 | 5.978E−2 | −19.5 | 1.502E−5 | 140 | −19.5 |

Table 6.5.2: Maximum errors in the knowledge of the absolute LOS and change in LOS caused by errors in knowledge of the direction of the wobble sensors sensitive axis. Nominal direction of the sensitive axis of wobble sensors 1 and 2 is obtained by rotation the optical bench Z-axis, $\mathbf{O}_3$ , about the X-axis, $\mathbf{O}_1$ , and a second rotation about the intermediate Y-axis, for a combined rotation angle of 0.25 degrees with respect to $\mathbf{O}_3$ .

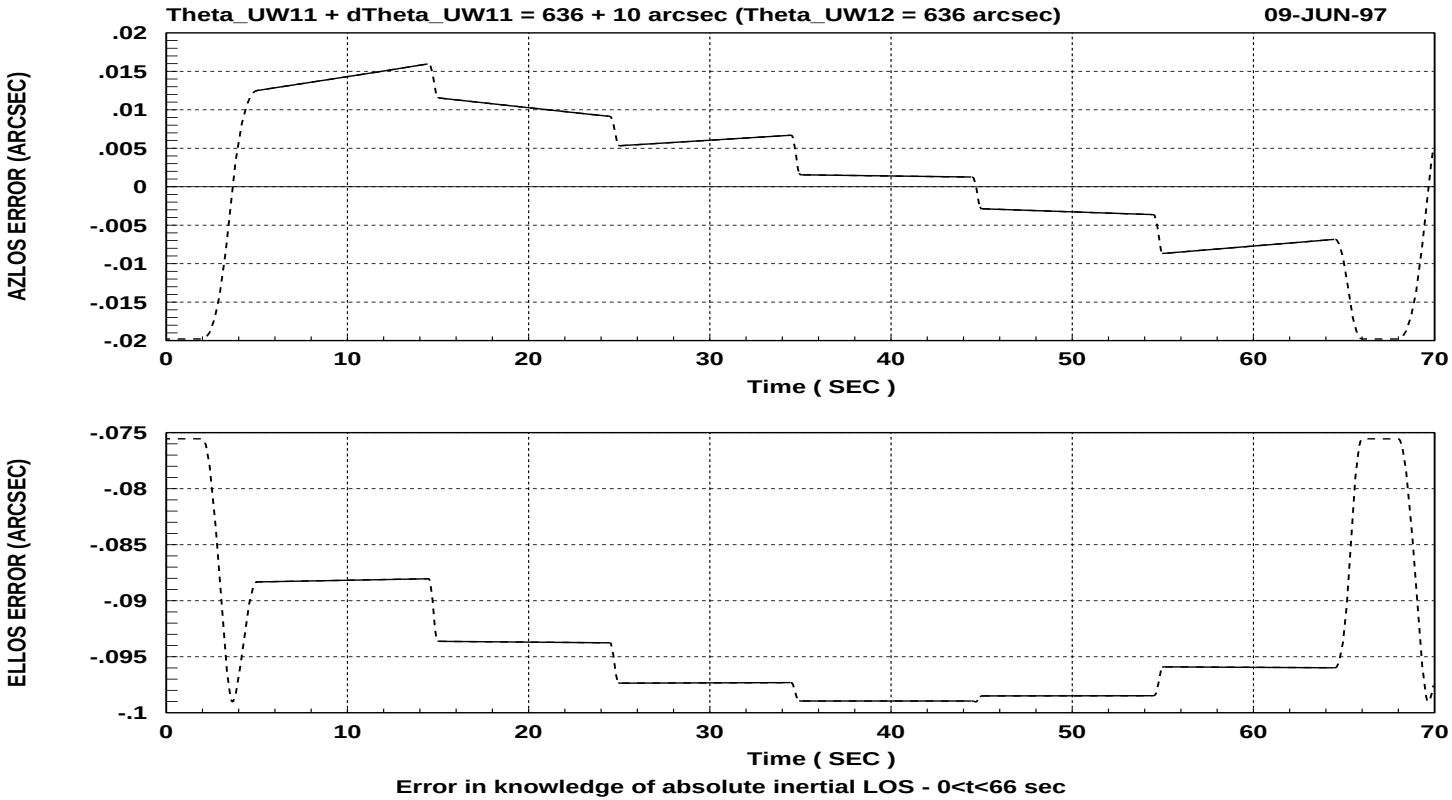


Figure 6.5.5: Errors in the knowledge of the inertial LOS caused by errors in knowledge of the direction of the wobble sensors sensitive axis ($\theta_{UW11}$). Nominal direction of the sensitive axis of wobble sensors 1 and 2 is obtained by rotation the optical bench Z-axis, $\mathbf{O}_3$ , about the X-axis, $\mathbf{O}_1$ , and a second rotation about the intermediate Y-axis, for a combined rotation angle of 0.25 degrees with respect to $\mathbf{O}_3$ .

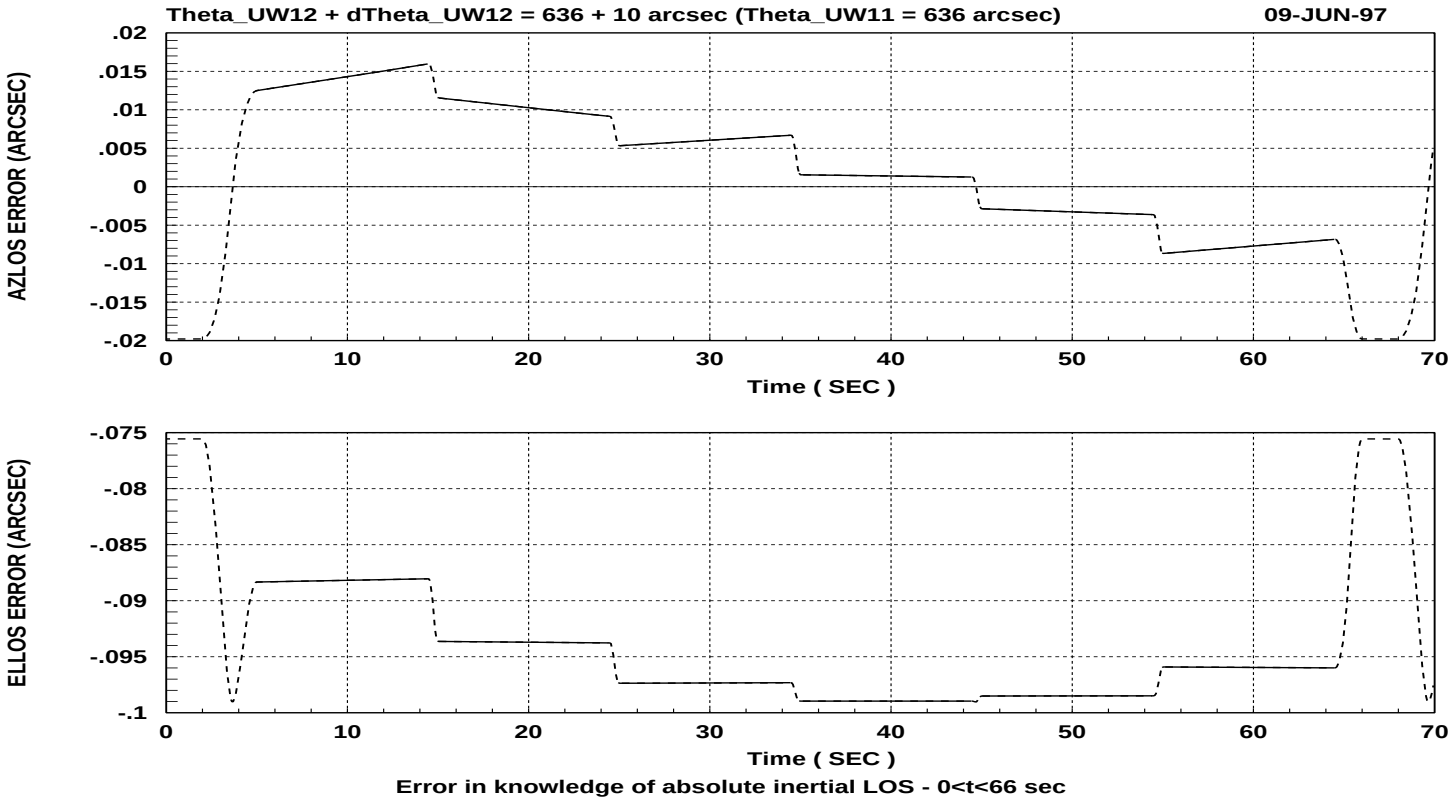


Figure 6.5.6: Errors in the knowledge of the inertial LOS caused by errors in knowledge of the direction of the wobble sensors sensitive axis ($\theta_{UW12}$). Nominal direction of the sensitive axis of wobble sensors 1 and 2 is obtained by rotation the optical bench Z-axis, $\mathbf{O}_3$ , about the X-axis, $\mathbf{O}_1$ , and a second rotation about the intermediate Y-axis, for a combined rotation angle of 0.25 degrees with respect to $\mathbf{O}_3$ .

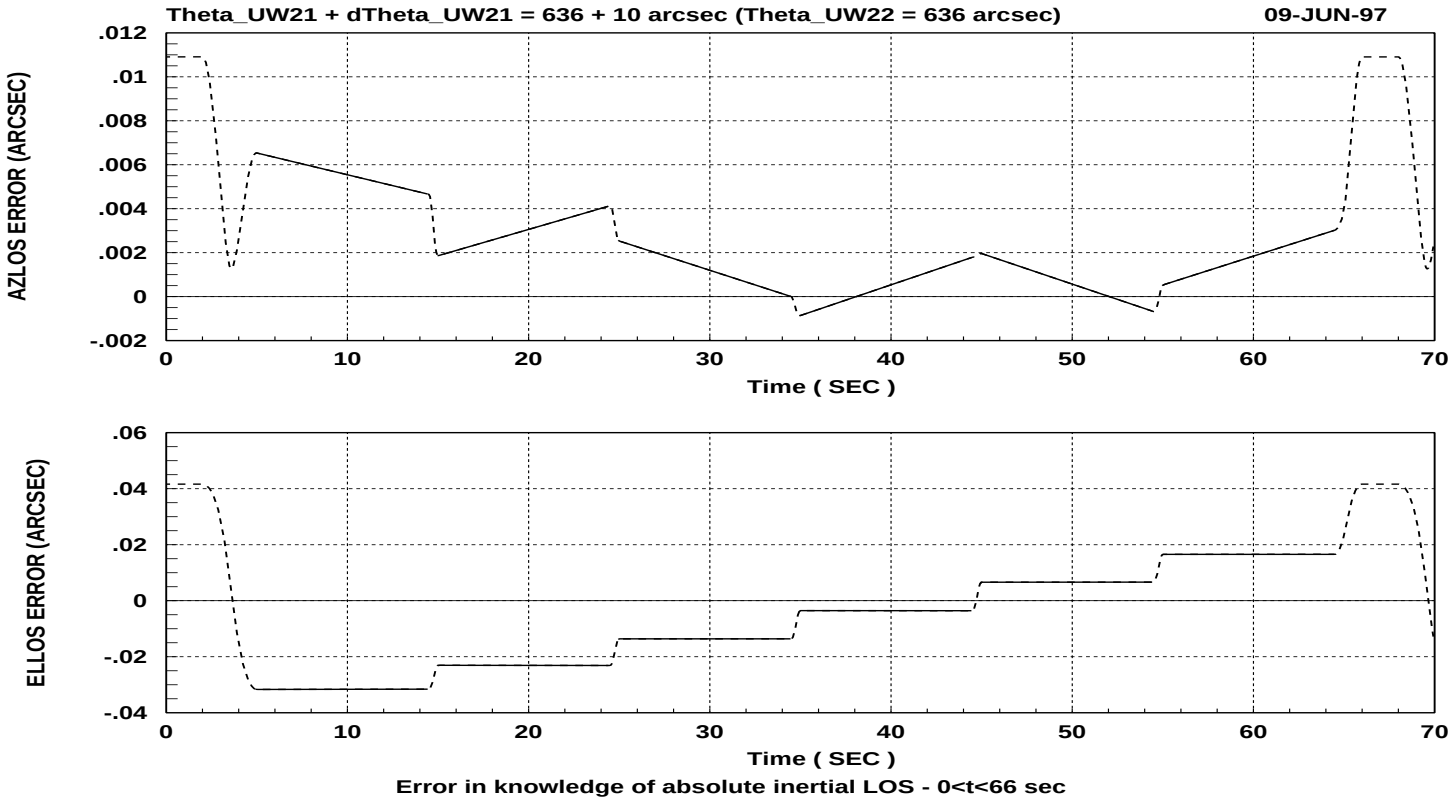


Figure 6.5.7: Errors in the knowledge of the inertial LOS caused by errors in knowledge of the direction of the wobble sensors sensitive axis ($\theta_{UW21}$). Nominal direction of the sensitive axis of wobble sensors 1 and 2 is obtained by rotation the optical bench Z-axis, $\mathbf{O}_3$ , about the X-axis, $\mathbf{O}_1$ , and a second rotation about the intermediate Y-axis, for a combined rotation angle of 0.25 degrees with respect to $\mathbf{O}_3$ .

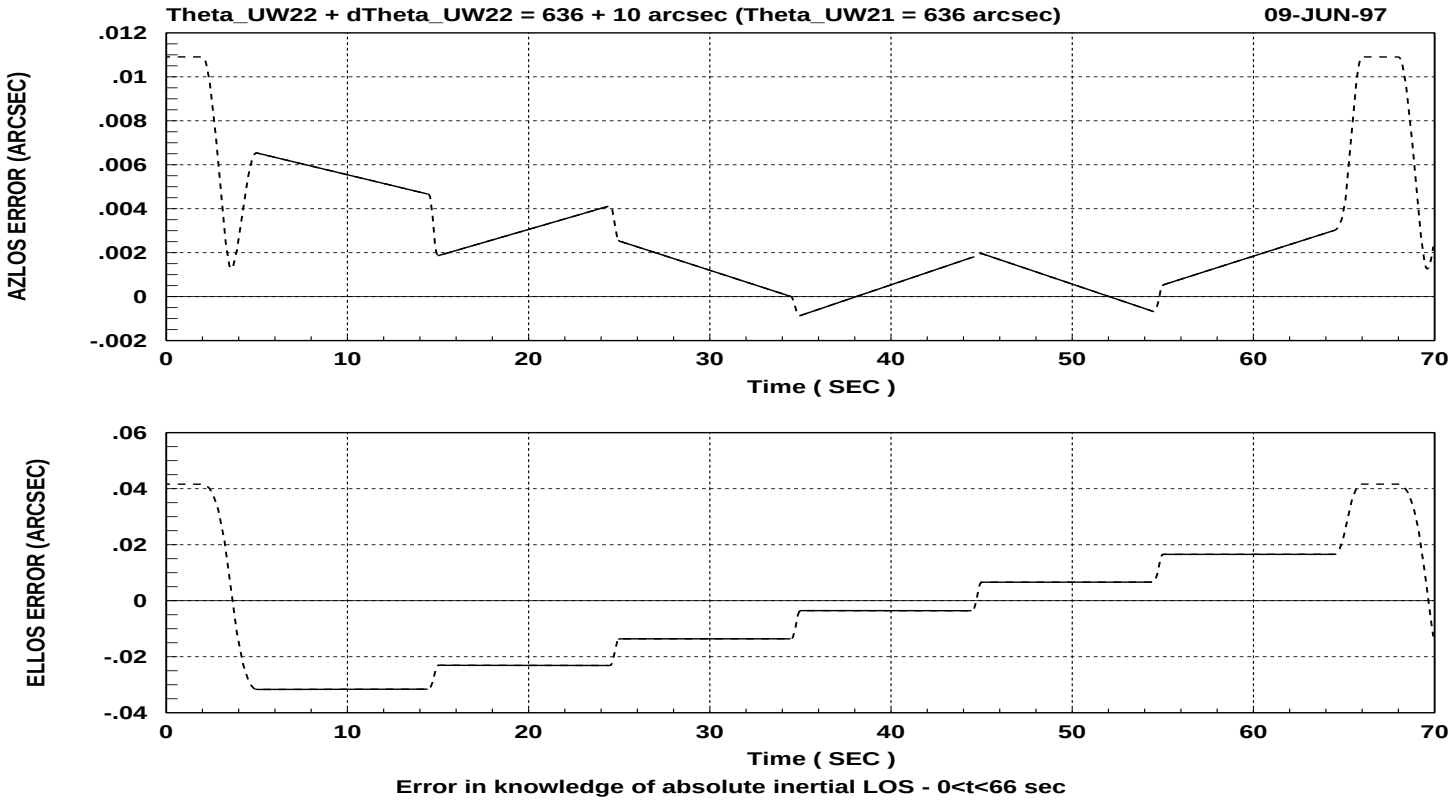


Figure 6.5.8: Errors in the knowledge of the inertial LOS caused by errors in knowledge of the direction of the wobble sensors sensitive axis ($\theta_{UW22}$). Nominal direction of the sensitive axis of wobble sensors 1 and 2 is obtained by rotation the optical bench Z-axis, $\mathbf{O}_3$ , about the X-axis, $\mathbf{O}_1$ , and a second rotation about the intermediate Y-axis, for a combined rotation angle of 0.25 degrees with respect to $\mathbf{O}_3$ .

## 6.6 KNOWLEDGE OF THE POSITION OF THE WOBBLE SENSORS

In the simulations the position of the $i^{th}$ wobble sensor, with respect to point OR fixed in the azimuth gimbal and in the optical bench, is defined by a unit vector, **LWi**, expressed in reference frame, O, fixed to the optical bench. Knowledge errors in the position of the sensors are introduced in the simulation by changing the location of the sensors from their nominal configuration. Changes, $\delta X$, $\delta Y$, and $\delta Z$, are introduced as displacements in the $\mathbf{O_1}$, $\mathbf{O_2}$, and $\mathbf{O_3}$ directions, one at a time.

$$\mathbf{LWi} = LW_{i1}\,\mathbf{O}_1 + LW_{i2}\,\mathbf{O_2} + LW_{i3}\,\mathbf{O_3} \tag{6.6.1}$$

The errors in knowledge of the absolute LOS and change in LOS, for 0 < t < 66 sec and 0 < t < 10 sec, caused by errors in the knowledge of the position of wobble sensors 1 and 2[1] are presented in Table 6.6.1. To obtain these results the various metrics were linerized with respect to the disturbance in the parameters, *i.e.* position of wobble sensor, and with respect to the wobble and maximum errors were computed numerically for each linearized metric. This was required because for a baseline configuration in which the wobble is zero the line-of-sight does not depend on the in-plane ($\mathbf{O_1O_2}$ -plane) position of the wobble sensors, *i.e.* errors due to these parameters depend on the wobble. The results reported in Table 6.6.1 are maximum errors in LOS knowledge for any allowable wobble within the expected wobble range.

The range and nominal position of the wobble sensors allow the measurement of a maximum tilt of the azimuth axis of ±0.025 degrees (±90 arcsec). These values are used to determine the maximum wobble used to compute the maximum LOS errors due to errors in the position of the wobble sensors.

[1] The wobble sensors are used in pairs (1,3) and (2,4). The line connecting sensors 1 and 3 is parallel to $\mathbf{O_1}$ and the line connecting sensors 2 and 4 is parallel to $\mathbf{O_2}$. Error in position knowledge of sensors 1 and 3 cause similar to errors, and the same argument is valid with respect to sensors 2 and 4.

| Parameter | | | 0 < t < 66 sec | | 0 < t < 10 sec | | | | |
|---|---|---|---|---|---|---|---|---|---|
| | $\delta A$ (arcsec) | $\delta E$ (arcsec) | $\delta \Delta A_m$ (arcsec) | $\delta \Delta E$ (arcsec) | $\delta A$ (arcsec), | $a$ (deg) | $\delta \Delta E$ (arcsec), | θ (arcsec), | $a$ (deg) |
| $\delta LW_{11}$ (μm) | | | | | | | | | |
| +10 | 2.468E−3 | 1.529E−2 | 3.789E−3 | 3.051E−2 | 2.468E−3 | −19.5 | 2.114E−5 | 5832 | −13.6 |
| −10 | 2.468E−3 | 1.529E−2 | 3.790E−3 | 3.052E−2 | 2.468E−3 | −19.5 | 2.114E−5 | 5832 | −13.6 |
| +100 | 2.466E−2 | 1.528E−1 | 3.786E−2 | 3.049E−1 | 2.466E−2 | −19.5 | 2.112E−4 | 5832 | −13.6 |
| −100 | 2.470E−2 | 1.530E−1 | 3.793E−2 | 3.054E−1 | 2.470E−2 | −19.5 | 2.116E−4 | 5832 | −13.6 |
| $\delta LW_{12}$ (μm) | | | | | | | | | |
| +10 | 2.466E−3 | 1.529E−2 | 3.785E−3 | 3.051E−2 | 2.466E−3 | −19.5 | 2.110E−5 | 5832 | −13.6 |
| −10 | 2.466E−3 | 1.529E−2 | 3.785E−3 | 3.051E−2 | 2.466E−3 | −19.5 | 2.110E−5 | 5832 | −13.6 |
| +100 | 2.466E−2 | 1.529E−1 | 3.785E−2 | 3.051E−1 | 2.466E−2 | −19.5 | 2.110E−4 | 5832 | −13.6 |
| −100 | 2.466E−2 | 1.529E−1 | 3.785E−2 | 3.051E−1 | 2.466E−2 | −19.5 | 2.110E−4 | 5832 | −13.6 |
| $\delta LW_{13}$ (μm) | | | | | | | | | |
| +10 | 5.678 | 3.504E+1 | 9.038E+1 | 3.909E+1 | 5.678 | −19.5 | 1.004E−1 | 6181 | −19.5 |
| −10 | 5.682 | 3.504E+1 | 9.044E+1 | 3.909E+1 | 5.682 | −19.5 | 1.004E−1 | 6181 | −19.5 |
| +100 | 5.663E+1 | 3.5040E+2 | 9.011E+2 | 3.907E+2 | 5.663E+1 | −19.5 | 9.995E−1 | 6181 | −19.5 |
| −100 | 5.697E+1 | 3.5040E+2 | 9.071E+2 | 3.910E+2 | 5.697E+1 | −19.5 | 1.009 | 6181 | −19.5 |
| $\delta LW_{21}$ (μm) | | | | | | | | | |
| +10 | 9.993E−4 | 4.828E−3 | 1.307E−3 | 8.329E−3 | 9.993E−4 | −19.5 | 8.590E−6 | 2885 | −19.5 |
| −10 | 9.993E−4 | 4.828E−3 | 1.307E−3 | 8.329E−3 | 9.993E−4 | −19.5 | 8.590E−6 | 2885 | −19.5 |
| +100 | 9.993E−3 | 4.828E−2 | 1.307E−2 | 8.329E−2 | 9.993E−3 | −19.5 | 8.590E−5 | 2885 | −19.5 |
| −100 | 9.993E−3 | 4.828E−2 | 1.307E−2 | 8.329E−2 | 9.993E−3 | −19.5 | 8.590E−5 | 2885 | −19.5 |
| $\delta LW_{22}$ (μm) | | | | | | | | | |
| +10 | 9.999E−4 | 4.829E−3 | 1.308E−3 | 8.330E−3 | 9.999E−4 | −19.5 | 8.613E−6 | 2885 | −19.5 |
| −10 | 9.997E−4 | 4.828E−3 | 1.308E−3 | 8.328E−3 | 9.997E−4 | −19.5 | 8.612E−6 | 2885 | −19.5 |
| +100 | 1.000E−2 | 4.832E−2 | 1.309E−2 | 8.336E−2 | 1.000E−2 | −19.5 | 8.620E−5 | 2885 | −19.5 |
| −100 | 9.990E−3 | 4.824E−2 | 1.307E−2 | 8.322E−2 | 9.990E−3 | −19.5 | 8.605E−5 | 2885 | −19.5 |
| $\delta LW_{23}$ (μm) | | | | | | | | | |
| +10 | 2.305 | 1.107E+1 | 3.171E+1 | 1.710E+1 | 2.305 | −19.5 | 3.889E−2 | 6181 | −19.5 |
| −10 | 2.304 | 1.107E+1 | 3.170E+1 | 1.710E+1 | 2.304 | −19.5 | 3.894E−2 | 6181 | −19.5 |
| +100 | 2.308E+1 | 1.166E+2 | 3.177E+2 | 1.7103E+2 | 2.308E+1 | −19.5 | 3.864E−1 | 6181 | −19.5 |
| −100 | 2.301E+1 | 1.166E+2 | 3.165E+2 | 1.7103E+2 | 2.301E+1 | −19.5 | 3.919E−1 | 6181 | −19.5 |

Table 6.6.1: Max. errors in the knowledge of the LOS and change in LOS caused by errors in knowledge of the position of the wobble sensors.

## 6.7 AZIMUTH AND ELEVATION SENSOR BIAS

The errors in knowledge of the LOS and change in LOS due to biases in the signals from the azimuth and elevation sensors are obtained by adding a bias or offset to the azimuth and elevation shaft angles and to the signals from the wobble sensors which are used as inputs for the retrieval algorithm. Note that biases in signals from the azimuth and elevation encoders are equivalent to the misalignment of the mirror datum position as described in Section 6.2 of this document. Adding a bias to the signals from the wobble sensors is similar to displacing the wobble sensors as described in Section 6.6 of this document.

The errors in knowledge of the absolute LOS and change in LOS for $0 < t < 66$ sec and $0 < t < 10$ sec caused by biases in the signals from the azimuth and elevation encoders ($e_{bias}$ and $a_{bias}$) are listed in Table 6.7.1, and errors due to biases in the signals from the wobble sensors[1] are listed in Table 6.7.2.

Figures 6.7.1 through 6.7.4 show the errors in the direction of the line-of-sight in inertial space due to errors in the knowledge of bias of the azimuth and elevation sensors.

[1] Signals from the wobble sensors are *SWik* defined as the differential measure from sensors *i* and *k*.

| Parameter | | | 0 < t < 66 sec | | 0 < t < 10 sec | | | | |
|---|---|---|---|---|---|---|---|---|---|
| | $\delta A$ (arcsec) | $\delta E$ (arcsec) | $\delta \Delta A_m$ (arcsec) | $\delta \Delta E$ (arcsec) | $\delta A$ (arcsec), $a$ (deg) | | $\delta \Delta E$ (arcsec), θ (arcsec), $a$ (deg) | | |
| $e_{\text{bias}}$ (arcsec) | | | | | | | | | |
| +10 | 3.348 | 1.999E+1 | 2.165 | 1.161 | 3.348 | −19.5 | 8.175E−4 | 140 | −19.5 |
| −10 | 3.347 | 1.999E+1 | 2.165 | 1.161 | 3.347 | −19.5 | 8.173E−4 | 140 | −19.5 |
| +100 | 3.352E+1 | 1.999E+2 | 2.168E+1 | 1.162E+1 | 3.352E+1 | −19.5 | 8.188E−3 | 140 | −19.5 |
| −100 | 3.343E+1 | 1.999E+2 | 2.162E+1 | 1.161E+1 | 3.343E+1 | −19.5 | 8.161E−3 | 140 | −19.5 |
| $a_{\text{bias}}$ (arcsec) | | | | | | | | | |
| +10 | 2.009E+1 | 1.295E−1 | 1.996E+1 | 1.985E−1 | 2.009E+1 | −19.5 | 2.452E−3 | 140 | −19.5 |
| −10 | 2.009E+1 | 1.295E−1 | 1.996E+1 | 1.985E−1 | 2.009E+1 | −19.5 | 2.452E−3 | 140 | −19.5 |
| +100 | 2.0094E+2 | 1.294 | 1.9962E+2 | 1.984 | 2.0094E+2 | −19.5 | 2.450E−2 | 140 | −19.5 |
| −100 | 2.0094E+2 | 1.296 | 1.9962E+2 | 1.986 | 2.0094E+2 | −19.5 | 2.454E−2 | 140 | −19.5 |

Table 6.7.1: Maximum errors in the knowledge of the absolute LOS and change in LOS caused by bias in the azimuth and elevation encoders.

| Parameter | | | 0 < t < 66 sec | | 0 < t < 10 sec | | | | |
|---|---|---|---|---|---|---|---|---|---|
| | $\delta A$ (arcsec) | $\delta E$ (arcsec) | $\delta \Delta A_m$ (arcsec) | $\delta \Delta E$ (arcsec) | $\delta A$ (arcsec), $a$ (deg) | | $\delta \Delta E$ (arcsec), θ (arcsec), $a$ (deg) | | |
| $SW31_{bias}$ (μm) | | | | | | | | | |
| +10 | 5.655 | 3.504E+1 | 3.655 | 3.915 | 5.655 | −19.5 | 1.389E−3 | 140 | −19.5 |
| −10 | 5.652 | 3.504E+1 | 3.653 | 3.915 | 5.652 | −19.5 | 1.387E−3 | 140 | −19.5 |
| +100 | 5.671E+1 | 3.5040E+2 | 3.666E+1 | 3.917E+1 | 5.671E+1 | −19.5 | 1.394E−2 | 140 | −19.5 |
| −100 | 5.636E+1 | 3.5040E+2 | 3.641E+1 | 3.914E+1 | 5.636E+1 | −19.5 | 1.382E−2 | 140 | −19.5 |
| $SW42_{bias}$ (μm) | | | | | | | | | |
| +10 | 2.292 | 1.107E+1 | 1.044 | 1.709E+1 | 2.292 | −19.5 | 5.771E−4 | 140 | −19.5 |
| −10 | 2.293 | 1.107E+1 | 1.044 | 1.709E+1 | 2.293 | −19.5 | 5.764E−4 | 140 | −19.5 |
| +100 | 2.289E+1 | 1.1067E+2 | 1.041E+1 | 1.7094E+2 | 2.289E+1 | −19.5 | 5.800E−3 | 140 | −19.5 |
| −100 | 2.296E+1 | 1.1067E+2 | 1.047E+1 | 1.7094E+2 | 2.296E+1 | −19.5 | 5.734E−3 | 140 | −19.5 |

Table 6.7.2: Maximum errors in the knowledge of the absolute LOS and change in LOS caused by bias in the signals from the wobble sensors.

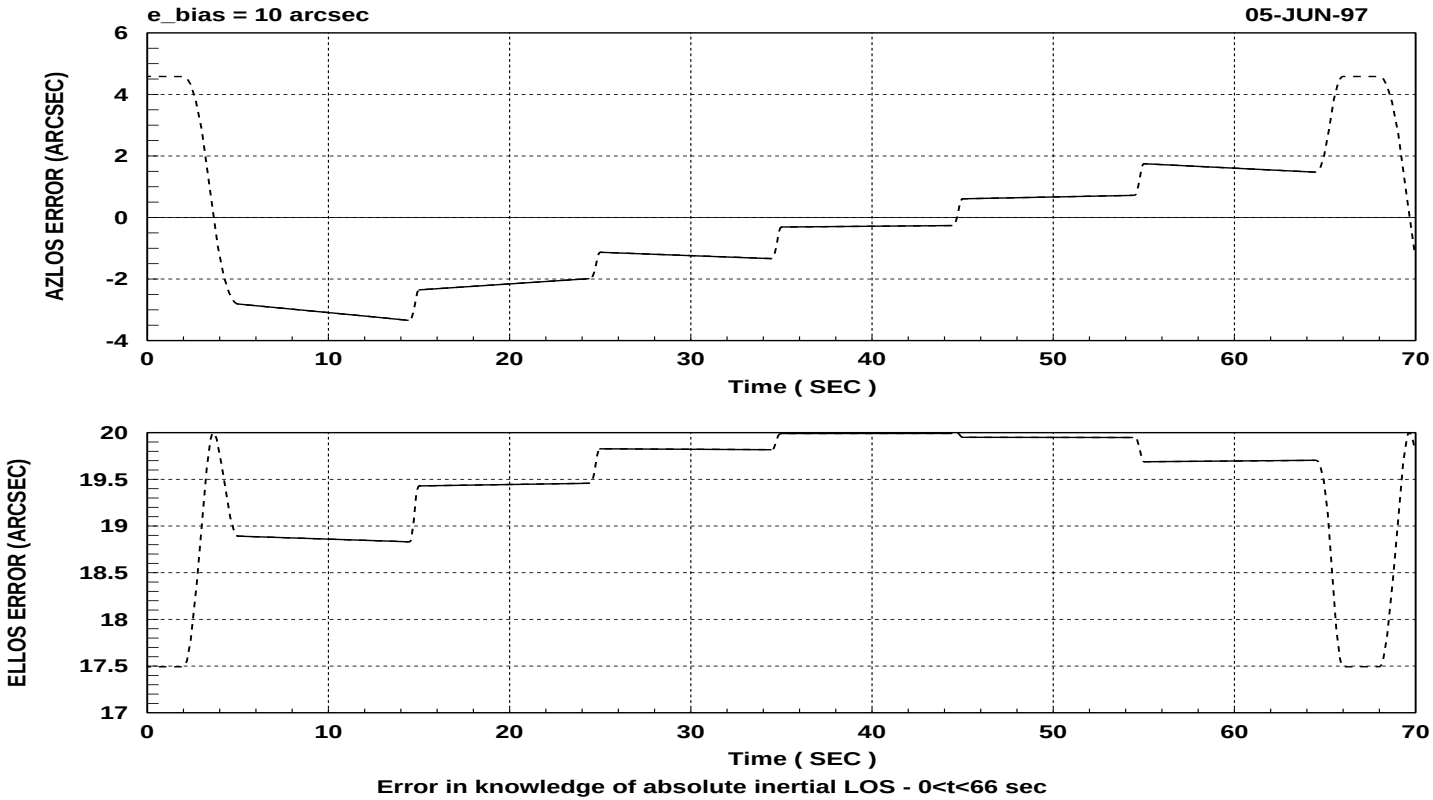


Figure 6.7.1: Errors in the knowledge of the inertial LOS caused by bias in the elevation encoder.

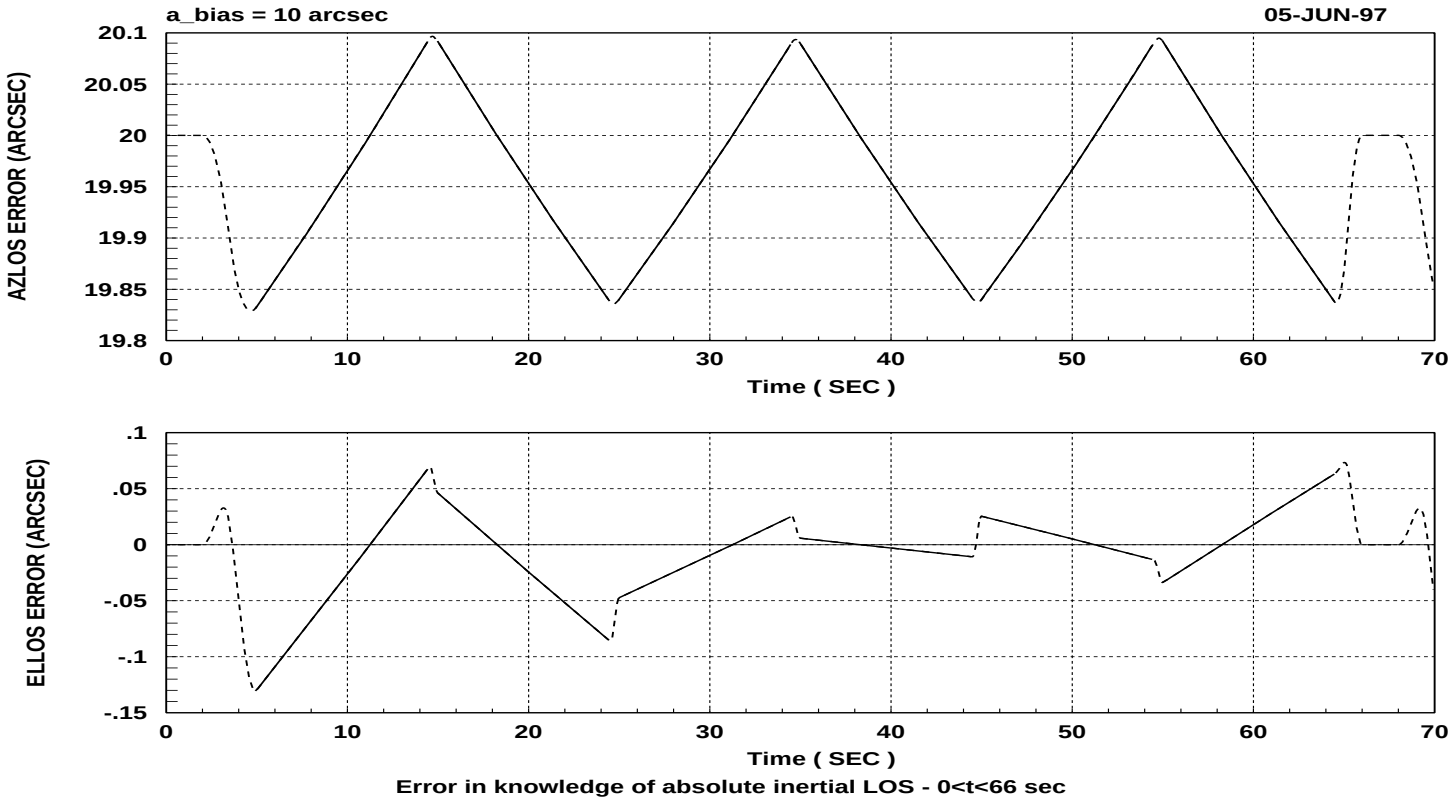


Figure 6.7.2: Errors in the knowledge of the inertial LOS caused by bias in the azimuth encoder.

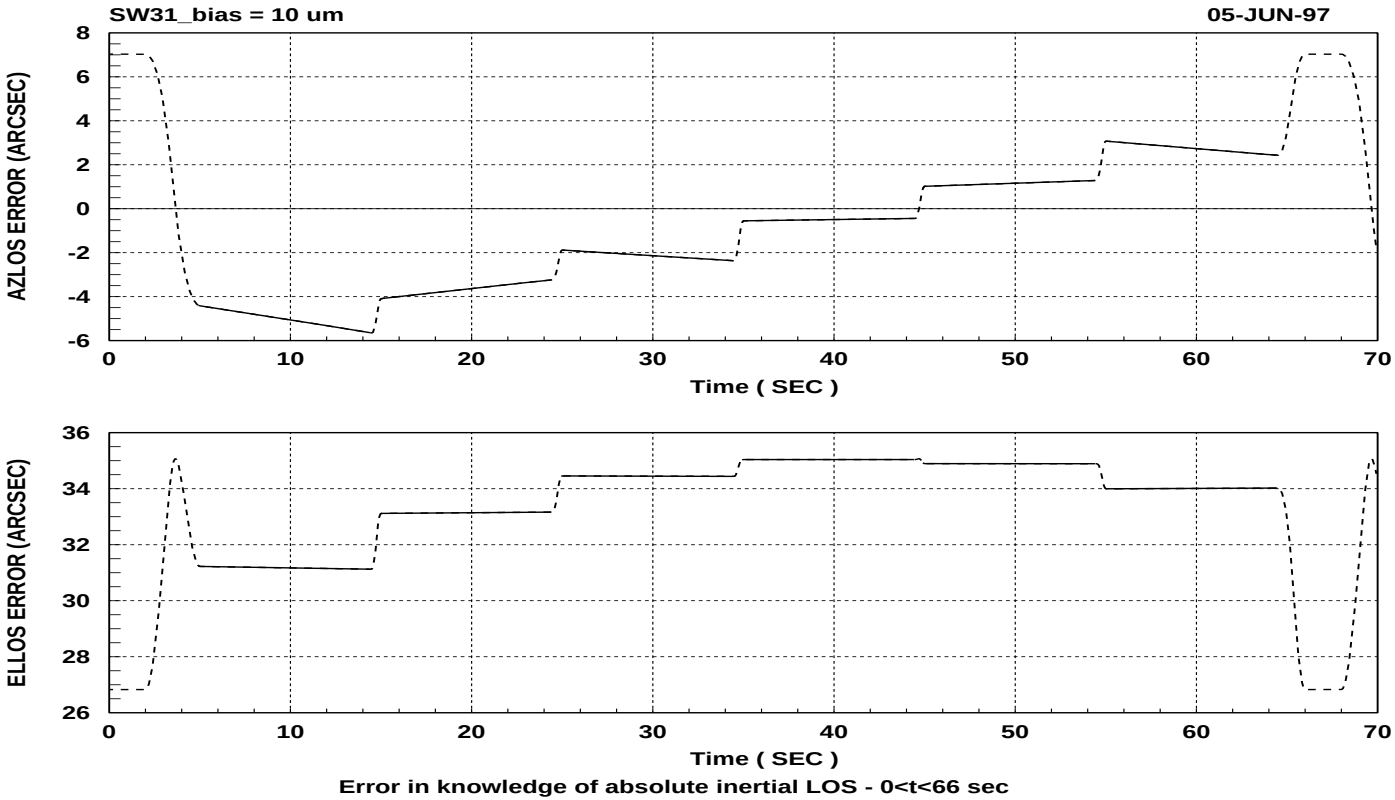


Figure 6.7.3: Errors in the knowledge of the inertial LOS caused by bias in the signals from the wobble sensors (*SW31*).

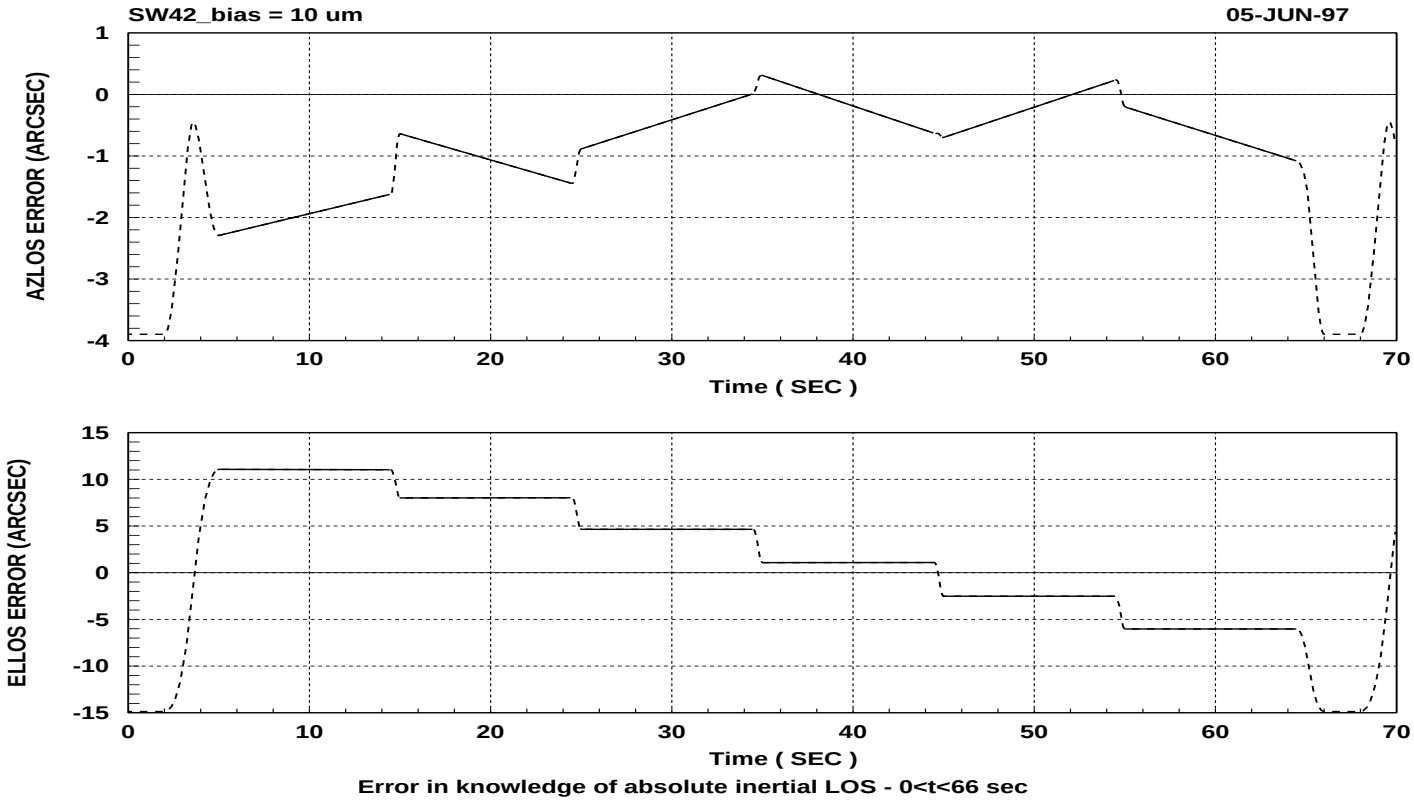


Figure 6.7.4: Errors in the knowledge of the inertial LOS caused by bias in the signals from the wobble sensors (*SW42*).

## 6.8 AZIMUTH AND ELEVATION SENSOR DRIFT

The errors in knowledge of the LOS and change in LOS due to drift in the signals from the azimuth and elevation sensors are obtained by adding a linear drift (constant*time) to the azimuth and elevation shaft angles and to the signal from the wobble sensors which are used as inputs for the retrieval algorithm, i.e.:

sensor signal = nominal sensor signal + drift rate * time (6.8.1)

The errors in knowledge of the absolute LOS and change in LOS for $0 < t < 66$ sec and $0 < t < 10$ sec caused by drift in the signals from the azimuth and elevation encoders ($e_{drift}$ and $a_{drift}$) are listed in Table 6.8.1, and errors due to drift in the signals from the wobble sensors[1] are listed in Table 6.8.2.

Note: As a guideline to choosing the drift rates on Tables 8.1 and 8.2 the following information was used:
Maximum rate of change of average temperature[2] = 0.2°C/minute
Wobble sensors thermal stability = 0.05%FSO[3]/°C
Azimuth and Elevation encoders thermal stability = 0.01%FSO/°C

Figures 6.8.1 through 6.8.4 show the errors in the direction of the line-of-sight in inertial space due to drift in the signals from the azimuth and elevation sensors.

[1] Signals from the wobble sensors are *SWik* defined as the differential measure from sensors *i* and *k*.
[2] Data obtained from the temperature of the Encoder Electronics Assembly (EEA) box and Wobble Sensor Electronics Assembly (WSEA) box during a complete orbit.
[3] Full Scale Output. For the wobble sensors: 25µm. For the azimuth and elevation encoders: 54.5 degrees and 3.89 degrees respectively.

| Parameter | | | 0 < t < 66 sec | | 0 < t < 10 sec | | | | |
|---|---|---|---|---|---|---|---|---|---|
| | $\delta A$ (arcsec) | $\delta E$ (arcsec) | $\delta \Delta A_m$ (arcsec) | $\delta \Delta E$ (arcsec) | $\delta A$ (arcsec), $a$ (deg) | | $\delta \Delta E$ (arcsec), θ (arcsec), $a$ (deg) | | |
| $e_{\text{drift}}$ (arcsec/minute) | | | | | | | | | |
| +0.1 | 1.602E−2 | 2.118E−1 | 1.596E−2 | 1.961E−1 | 1.602E−2 | +10.05 | 3.981E−4 | 140 | −1.78 |
| −0.1 | 1.602E−2 | 2.118E−1 | 1.596E−2 | 1.961E−1 | 1.602E−2 | +10.05 | 3.981E−4 | 140 | −1.78 |
| +1 | 1.602E−1 | 2.118 | 1.596E−1 | 1.961 | 1.602E−1 | +10.05 | 3.981E−3 | 140 | −1.78 |
| −1 | 1.602E−1 | 2.118 | 1.596E−1 | 1.961 | 1.602E−1 | +10.05 | 3.981E−3 | 140 | −1.78 |
| $a_{\text{drift}}$ (arcsec/minute) | | | | | | | | | |
| +0.1 | 2.132E−1 | 6.807E−4 | 1.987E−1 | 1.032E−3 | 2.132E−1 | +10.05 | 1.370E−5 | 140 | +10.05 |
| −0.1 | 2.132E−1 | 6.807E−4 | 1.987E−1 | 1.032E−3 | 2.132E−1 | +10.05 | 1.370E−5 | 140 | +10.05 |
| +1 | 2.132 | 6.807E−3 | 1.987 | 1.032E−2 | 2.132 | +10.05 | 1.370E−4 | 140 | +10.05 |
| −1 | 2.132 | 6.807E−3 | 1.987 | 1.032E−2 | 2.132 | +10.05 | 1.370E−4 | 140 | +10.05 |

Table 6.8.1: Maximum errors in the knowledge of the absolute LOS and change in LOS caused by drift in the azimuth and elevation encoders.

| Parameter | | | 0 < t < 66 sec | | 0 < t < 10 sec | | | | |
|---|---|---|---|---|---|---|---|---|---|
| | $\delta A$ (arcsec) | $\delta E$ (arcsec) | $\delta \Delta A_m$ (arcsec) | $\delta \Delta E$ (arcsec) | $\delta A$ (arcsec), $a$ (deg) | | $\delta \Delta E$ (arcsec), θ (arcsec), $a$ (deg) | | |
| $SW31_{drift}$ (μm/minute) | | | | | | | | | |
| +1E−3 | 2.819E−4 | 3.657E−3 | 2.727E−4 | 3.397E−3 | 2.819E−4 | +10.05 | 6.978E−6 | 140 | −1.78 |
| −1E−3 | 2.819E−4 | 3.657E−3 | 2.727E−4 | 3.397E−3 | 2.819E−4 | +10.05 | 6.978E−6 | 140 | −1.78 |
| +1E−2 | 2.819E−3 | 3.657E−2 | 2.727E−3 | 3.397E−2 | 2.819E−3 | +10.05 | 6.978E−5 | 140 | −1.78 |
| −1E−2 | 2.819E−3 | 3.657E−2 | 2.727E−3 | 3.397E−2 | 2.819E−3 | +10.05 | 6.978E−5 | 140 | −1.78 |
| $SW42_{drift}$ (μm/minute) | | | | | | | | | |
| +1E−3 | 1.164E−4 | 6.479E−4 | 6.528E−5 | 9.755E−4 | 1.164E−4 | +10.05 | 2.096E−6 | 140 | −19.5 |
| −1E−3 | 1.164E−4 | 6.479E−4 | 6.528E−5 | 9.755E−4 | 1.164E−4 | +10.05 | 2.096E−6 | 140 | −19.5 |
| +1E−2 | 1.164E−3 | 6.479E−3 | 6.528E−4 | 9.755E−3 | 1.164E−3 | +10.05 | 2.096E−5 | 140 | −19.5 |
| −1E−2 | 1.164E−3 | 6.479E−3 | 6.528E−4 | 9.755E−3 | 1.164E−3 | +10.05 | 2.096E−5 | 140 | −19.5 |

Table 6.8.2: Maximum errors in the knowledge of the absolute LOS and change in LOS caused by drift in the signals from the wobble sensors.

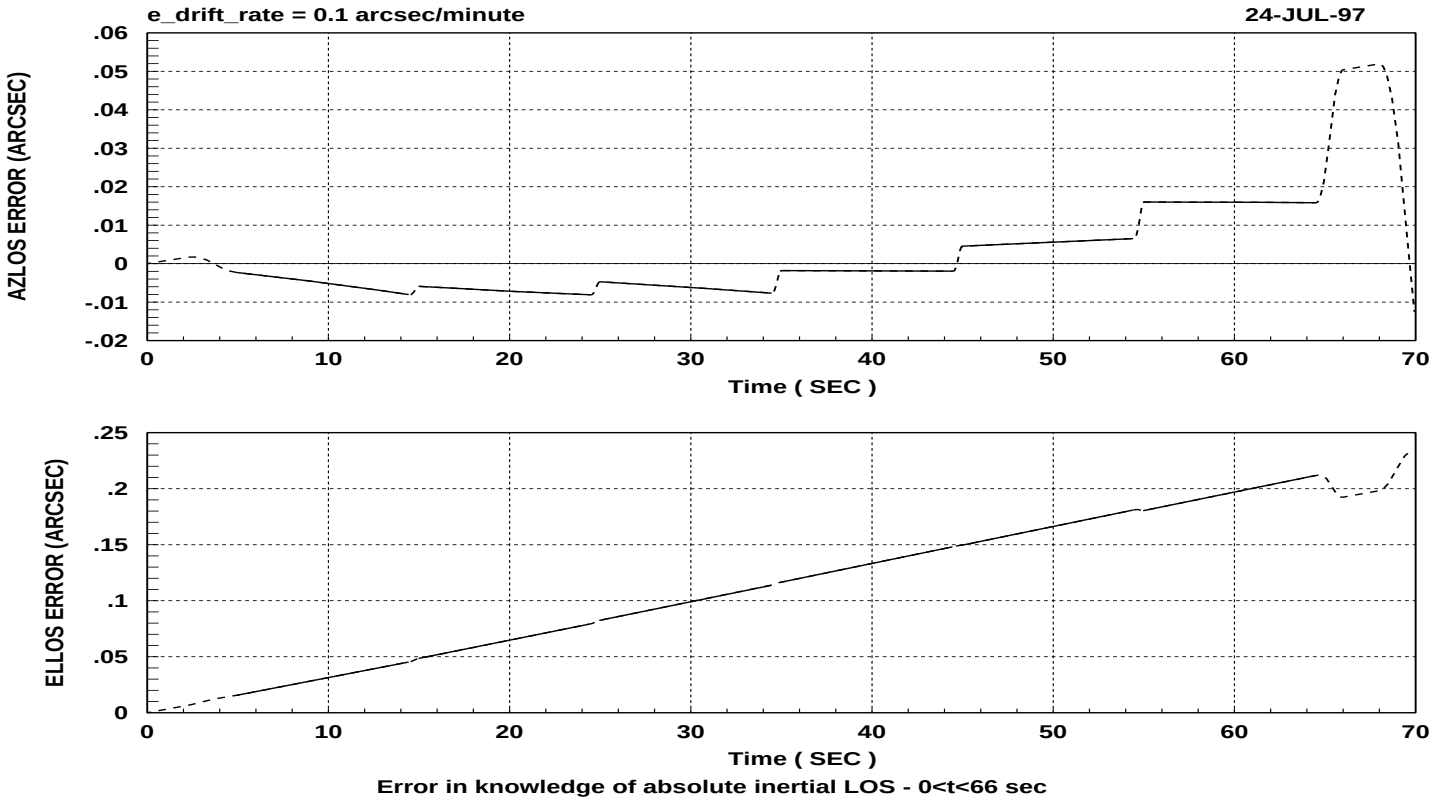


Figure 6.8.1: Errors in the knowledge of the inertial LOS caused by drift in the signal from the elevation encoder.

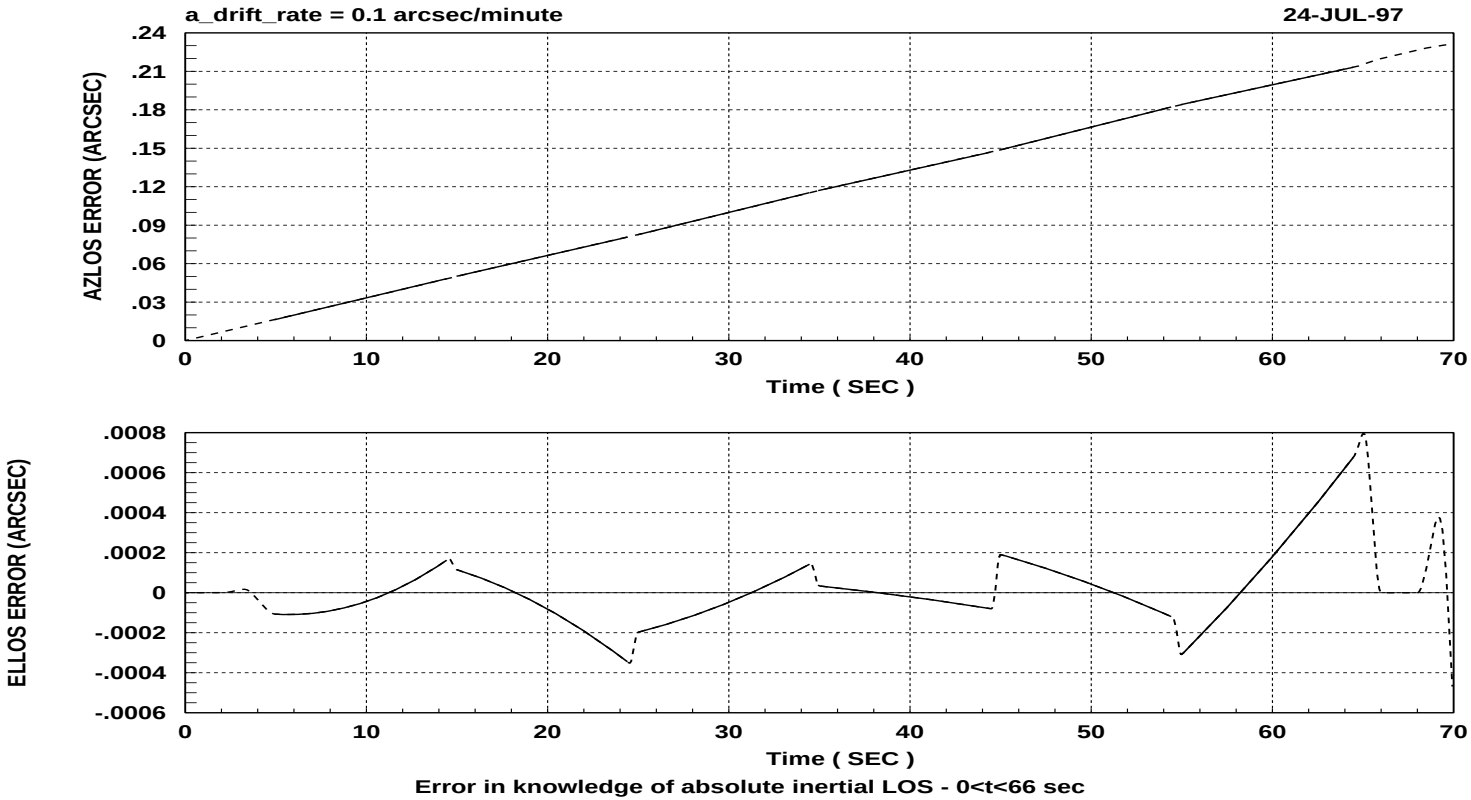


Figure 6.8.2: Errors in the knowledge of the inertial LOS caused by drift in the signal from the azimuth encoder.

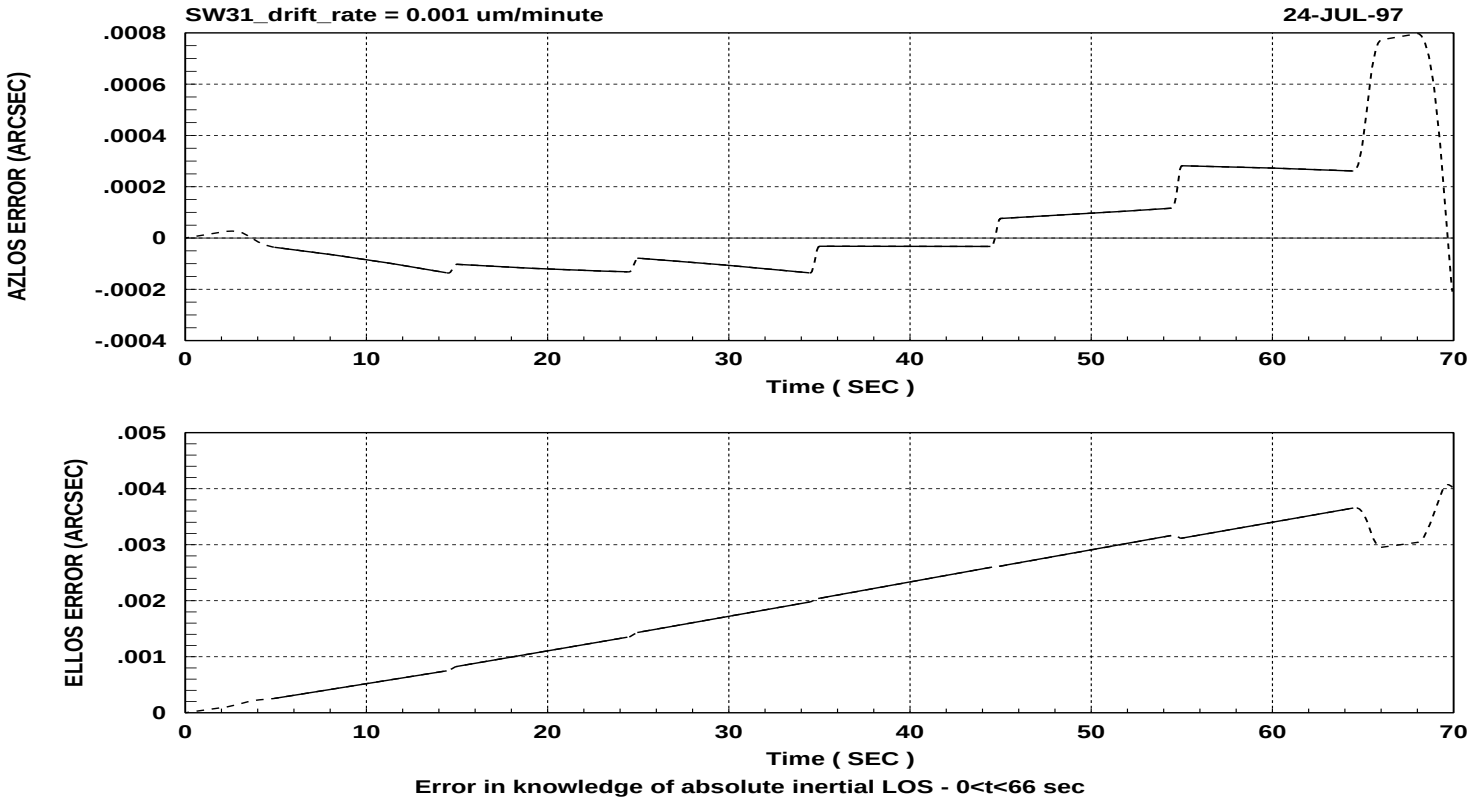


Figure 6.8.3: Errors in the knowledge of the inertial LOS caused by drift in the signal from the wobble sensors (*SW31*).

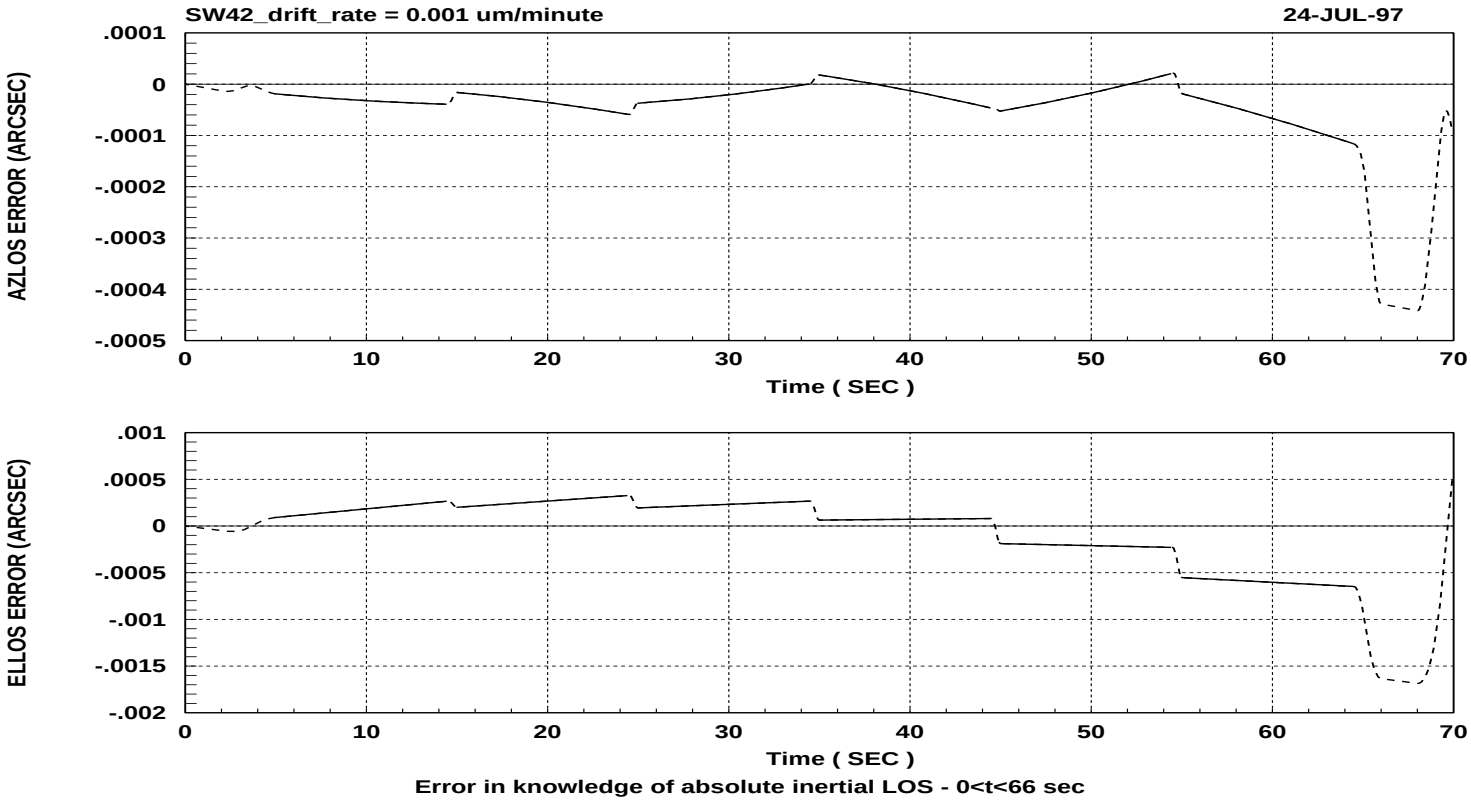


Figure 6.8.4: Errors in the knowledge of the inertial LOS caused by drift in the signal from the wobble sensors (*SW42*).

## 6.9 AZIMUTH AND ELEVATION SENSOR SCALE FACTOR

Errors in the knowledge of the azimuth sensors and elevation encoder scale factor result in errors in the knowledge of the LOS and change in LOS. To quantify these errors an estimate for the LOS is obtained by multiplying the signals from the sensors by a factor different from unit and comparing the resulting estimate of the LOS and change in LOS with the case where the correct measurement values from the sensors are used in the retrieval of the LOS. Only one of the signals is scaled at a given time to access the effect of each error separately. Variables $\delta k_a$ , $\delta k_e$ , $\delta k_{SW31}$ , and $\delta k_{SW42}$ are the errors in the scale factor of the signals from the azimuth encoder, elevation encoder and wobble sensors[1] respectively.

Note that to access the effect of error in knowledge of the wobble sensors scale factor a baseline configuration for which the signal from the wobble sensors is different from zero is required. This is necessary because for a baseline configuration in which the wobble is zero the output from the differential signal for the wobble sensors is also zero and a change in scale factor will not have any effect in the retrieval of the line-of-sight. The results reported in Table 6.9.3 refer to wobble functions which produce maximum error in LOS knowledge due to errors in scale factor of the wobble sensors.

<u>Construction of wobble for maximum LOS error due to errors in wobble sensor scale factor:</u>

During each elevation scan there is no change in azimuth shaft angle, consequently there is no change in the readings from the wobble sensors. Therefore, within each elevation scan, an error in the position of the wobble sensors is equivalent to a bias in the signals from the wobble sensors. The maximum errors can be obtained by constructing a wobble which has maximum value, $M_{WOB}$, at the elevation scan for which the errors due to wobble sensor bias are maximum, and has value $-M_{WOB}$ at the elevation scan for which the errors due to wobble sensor bias are the second largest. Table 6.9.1 lists the elevation scans for which the errors in LOS elevation and azimuth angles due to bias in the signal from the wobble sensors are the largest and second largest. This information is used to construct the wobble functions used to determine the maximum LOS errors due to errors in the position of the wobble sensors. Data on the table was obtained from the results for error in knowledge of the LOS due to bias in the signals from the wobble sensors (Section 6.7 of this report).

[1] Signals from the wobble sensors are *SWik* defined as the differential measure from sensors *i* and *k*.

| PARAMETER | ELEVATION SCAN |
|---|---|
| Largest error in ELLOS due to bias in the differential signal from wobble sensors 1 and 3 | 4th |
| Second largest error in ELLOS due to bias in the differential signal from wobble sensors 1 and 3 | 5th |
| Largest error in ELLOS due to bias in the differential signal from wobble sensors 2 and 4 | 1st |
| Second largest error in ELLOS due to bias in the differential signal from wobble sensors 2 and 4 | 2nd |
| Largest error in AZLOS due to bias in the differential signal from wobble sensors 1 and 3 | 1st |
| Second largest error in AZLOS due to bias in the differential signal from wobble sensors 1 and 3 | 2nd |
| Largest error in AZLOS due to bias in the differential signal from wobble sensors 2 and 4 | 1st |
| Second largest error in AZLOS due to bias in the differential signal from wobble sensors 2 and 4 | 2nd |

Table 6.9.1: Information used to construct wobble for worst case LOS knowledge error due to error in the knowledge of wobble sensors scale factor.

The range and nominal position of the wobble sensors allow the measurement of a maximum tilt of the azimuth axis of ±0.025 degrees (±90 arcsec). These values were used in constructing the wobble functions which generate maximum LOS errors due to errors the knowledge of wobble sensors scale factor.

The errors in knowledge of the absolute LOS and change in LOS for $0 < t < 66$ sec and $0 < t < 10$ sec caused by errors in the knowledge of the scale factors of the azimuth and elevation encoders are listed in Table 6.9.2. Results for the errors in the knowledge of the wobble sensors scale factors are presented in Table 6.9.3.

Figures 6.9.1 through 6.9.5 show the errors in the direction of the line-of-sight in inertial space due to errors in knowledge of the scale factor of the azimuth and elevation sensors.

| Parameter | | | 0 < t < 66 sec | | 0 < t < 10 sec | | | | |
|---|---|---|---|---|---|---|---|---|---|
| | $\delta A$ (arcsec) | $\delta E$ (arcsec) | $\delta \Delta A_m$ (arcsec) | $\delta \Delta E$ (arcsec) | $\delta A$ (arcsec), | $a$ (deg) | $\delta \Delta E$ (arcsec), | θ (arcsec), | $a$ (deg) |
| $\delta k_a/k_a$ (%) | | | | | | | | | |
| +0.01 | 1.4111E+1 | 9.094E−2 | 9.769 | 1.394E−1 | 1.4111E+1 | −19.5 | 1.722E−3 | 140 | −19.5 |
| −0.01 | 1.4111E+1 | 9.093E−2 | 9.769 | 1.394E−1 | 1.4111E+1 | −19.5 | 1.722E−3 | 140 | −19.5 |
| +0.1 | 1.411E+2 | 9.098E−1 | 9.769E+1 | 1.395 | 1.411E+2 | −19.5 | 1.723E−2 | 140 | −19.5 |
| −0.1 | 1.411E+2 | 9.089E−1 | 9.769E+1 | 1.393 | 1.411E+2 | −19.5 | 1.721E−2 | 140 | −19.5 |
| $\delta k_e/k_e$ (%) | | | | | | | | | |
| +0.01 | 1.143E−1 | 7.684E−1 | 1.824E−2 | 1.166 | 1.143E−1 | −19.5 | 1.403E−2 | 140 | −19.5 |
| −0.01 | 1.143E−1 | 7.684E−1 | 1.824E−2 | 1.166 | 1.143E−1 | −19.5 | 1.403E−2 | 140 | −19.5 |
| +0.1 | 1.143 | 7.684 | 1.824E−1 | 1.1664E+1 | 1.143 | −19.5 | 1.401E−1 | 140 | −19.5 |
| −0.1 | 1.143 | 7.684 | 1.825E−1 | 1.1664E+1 | 1.143 | −19.5 | 1.404E−1 | 140 | −19.5 |

Table 6.9.2: Maximum errors in the knowledge of the absolute LOS and change in LOS caused by errors in the knowledge of the azimuth and elevation encoder scale factor.

| Parameter | | | 0 < t < 66 sec | | 0 < t < 10 sec | | | | |
|---|---|---|---|---|---|---|---|---|---|
| | $\delta A$ (arcsec) | $\delta E$ (arcsec) | $\delta \Delta A_m$ (arcsec) | $\delta \Delta E$ (arcsec) | $\delta A$ (arcsec), | $a$ (deg) | $\delta \Delta E$ (arcsec), | θ (arcsec), | $a$ (deg) |
| $\delta k_{SW31}/k_{SW31}$ (%) | | | | | | | | | |
| +0.01 | 2.910E−3 | 1.798E−2 | 1.882E−3 | 3.589E−2 | 2.910E−3 | −19.5 | 7.069E−7 | 140 | −19.5 |
| −0.01 | 2.910E−3 | 1.798E−2 | 1.882E−3 | 3.589E−2 | 2.910E−3 | −19.5 | 7.069E−7 | 140 | −19.5 |
| +0.1 | 2.910E−2 | 1.798E−1 | 1.882E−2 | 3.589E−1 | 2.910E−2 | −19.5 | 7.069E−6 | 140 | −19.5 |
| −0.1 | 2.910E−2 | 1.798E−1 | 1.882E−2 | 3.589E−1 | 2.910E−2 | −19.5 | 7.069E−6 | 140 | −19.5 |
| $\delta k_{SW42}/k_{SW42}$ (%) | | | | | | | | | |
| +0.01 | 1.175E−3 | 5.679E−3 | 5.373E−4 | 9.797E−3 | 1.175E−3 | −19.5 | 2.788E−7 | 140 | −19.5 |
| −0.01 | 1.175E−3 | 5.679E−3 | 5.373E−4 | 9.797E−3 | 1.175E−3 | −19.5 | 2.788E−7 | 140 | −19.5 |
| +0.1 | 1.175E−2 | 5.679E−2 | 5.373E−3 | 9.797E−2 | 1.175E−2 | −19.5 | 2.788E−6 | 140 | −19.5 |
| −0.1 | 1.175E−2 | 5.679E−2 | 5.373E−3 | 9.797E−2 | 1.175E−2 | −19.5 | 2.788E−6 | 140 | −19.5 |

Table 6.9.3: Maximum errors in the knowledge of the absolute LOS and change in LOS caused by errors in the knowledge of the scale factor of the wobble sensors.

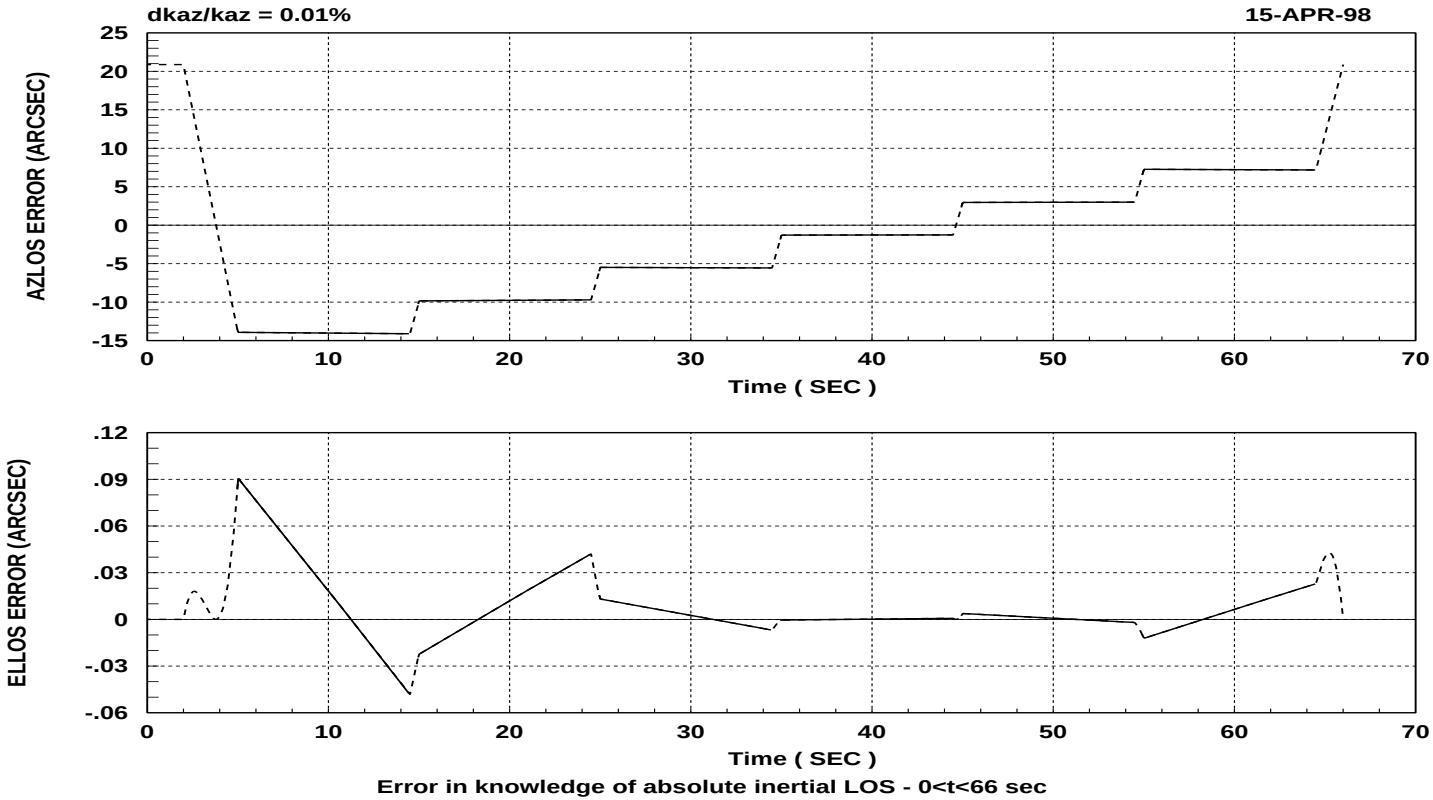


Figure 6.9.1: Errors in the knowledge of the inertial LOS caused by error in the knowledge of the scale factor of the azimuth encoder.

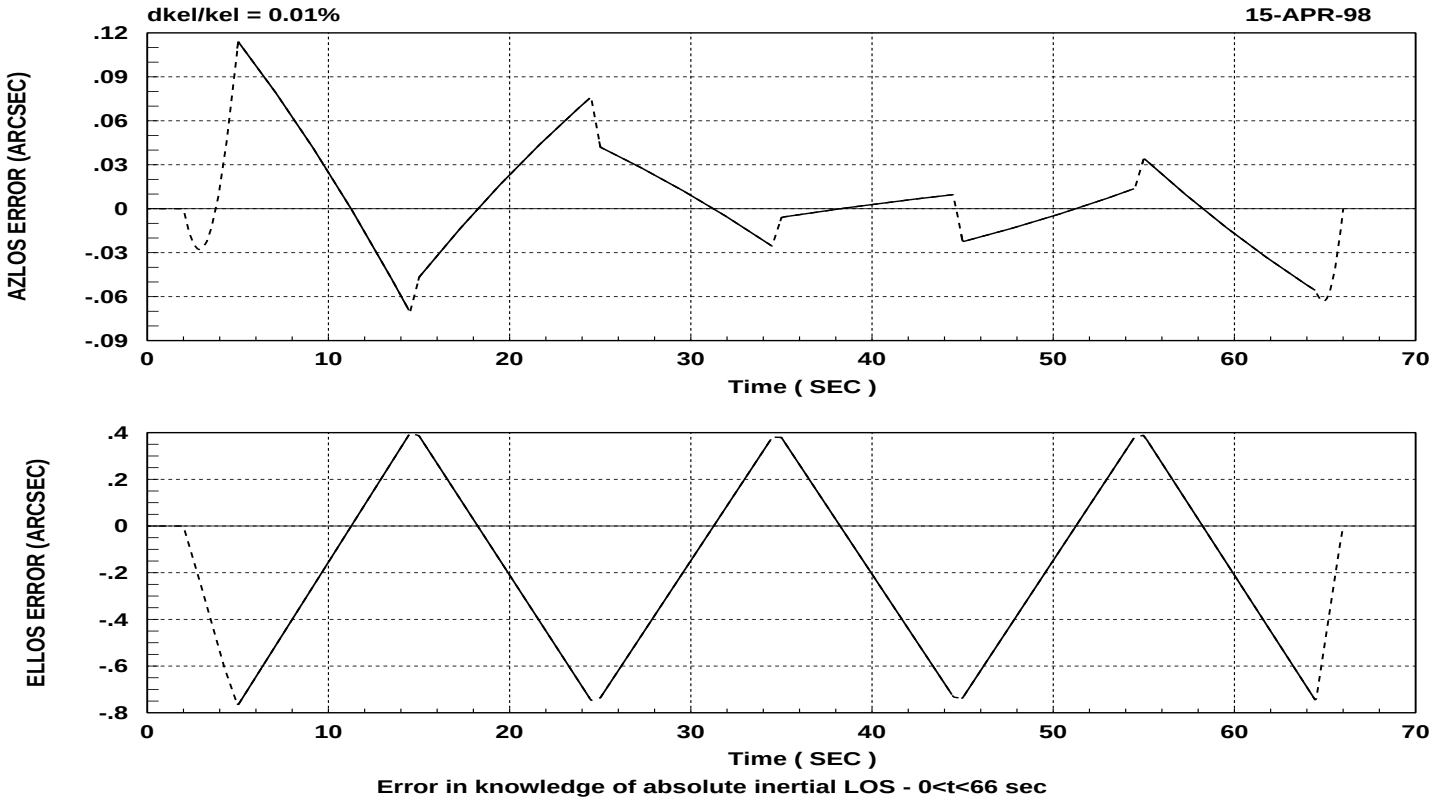


Figure 6.9.2: Errors in the knowledge of the inertial LOS caused by error in the knowledge of the scale factor of the elevation encoder.

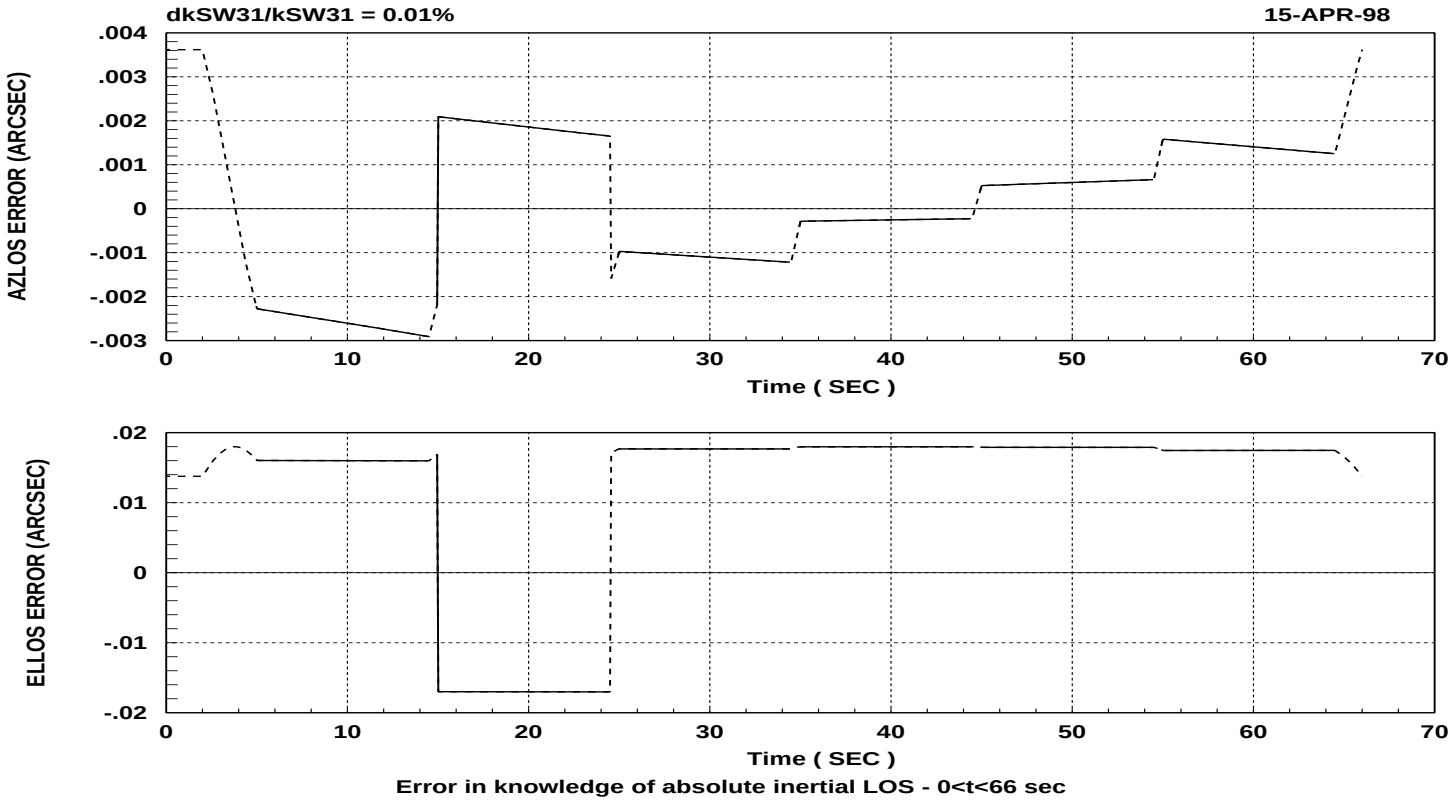


Figure 6.9.3: Errors in the knowledge of the inertial LOS caused by error in the knowledge of the scale factor of the wobble sensors (*SW31*). Wobble of the azimuth axis selected for maximum error in AZLOS due to scale factor effect.

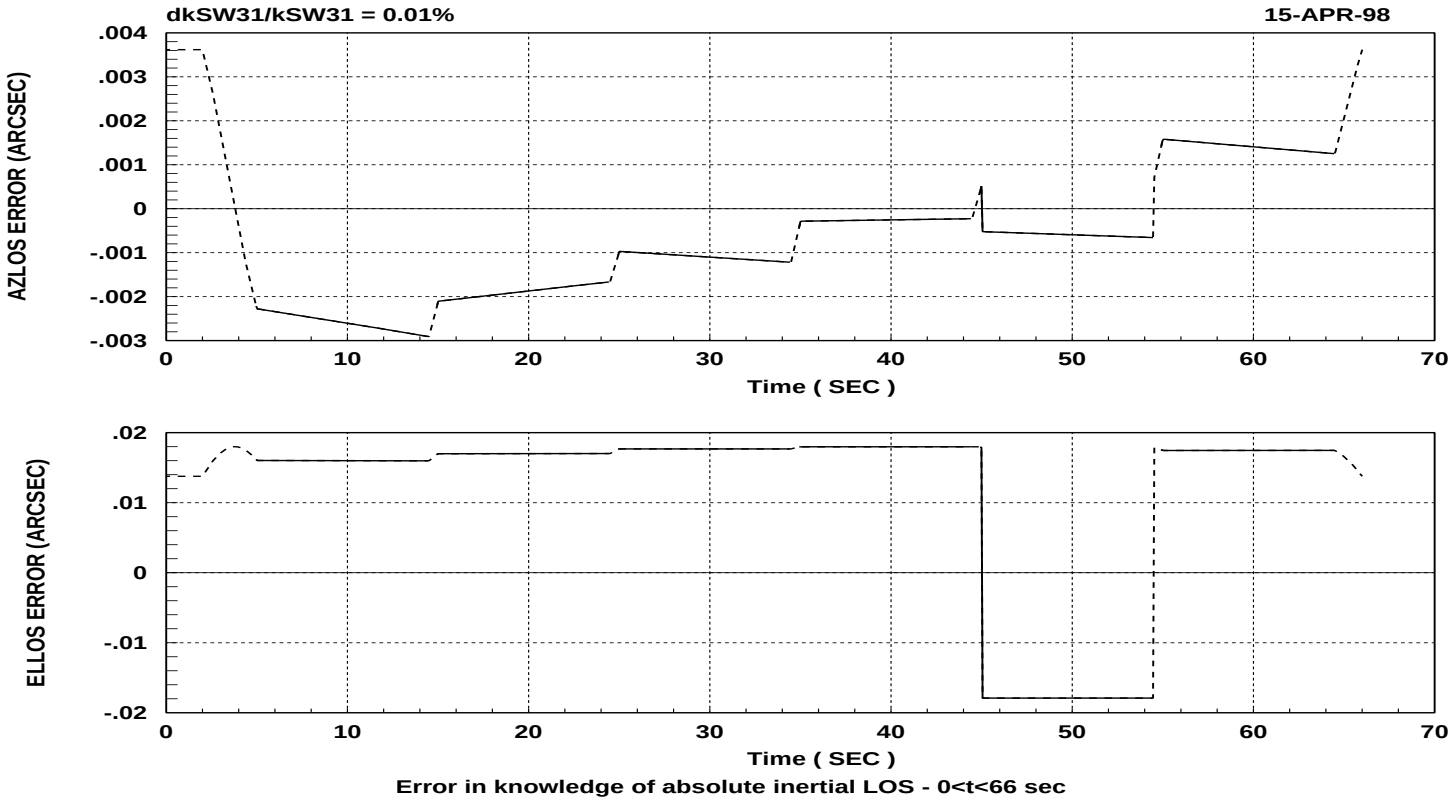


Figure 6.9.4: Errors in the knowledge of the inertial LOS caused by error in the knowledge of the scale factor of the wobble sensors (*SW31*). Wobble of the azimuth axis selected for maximum error in ELLOS due to scale factor effect.

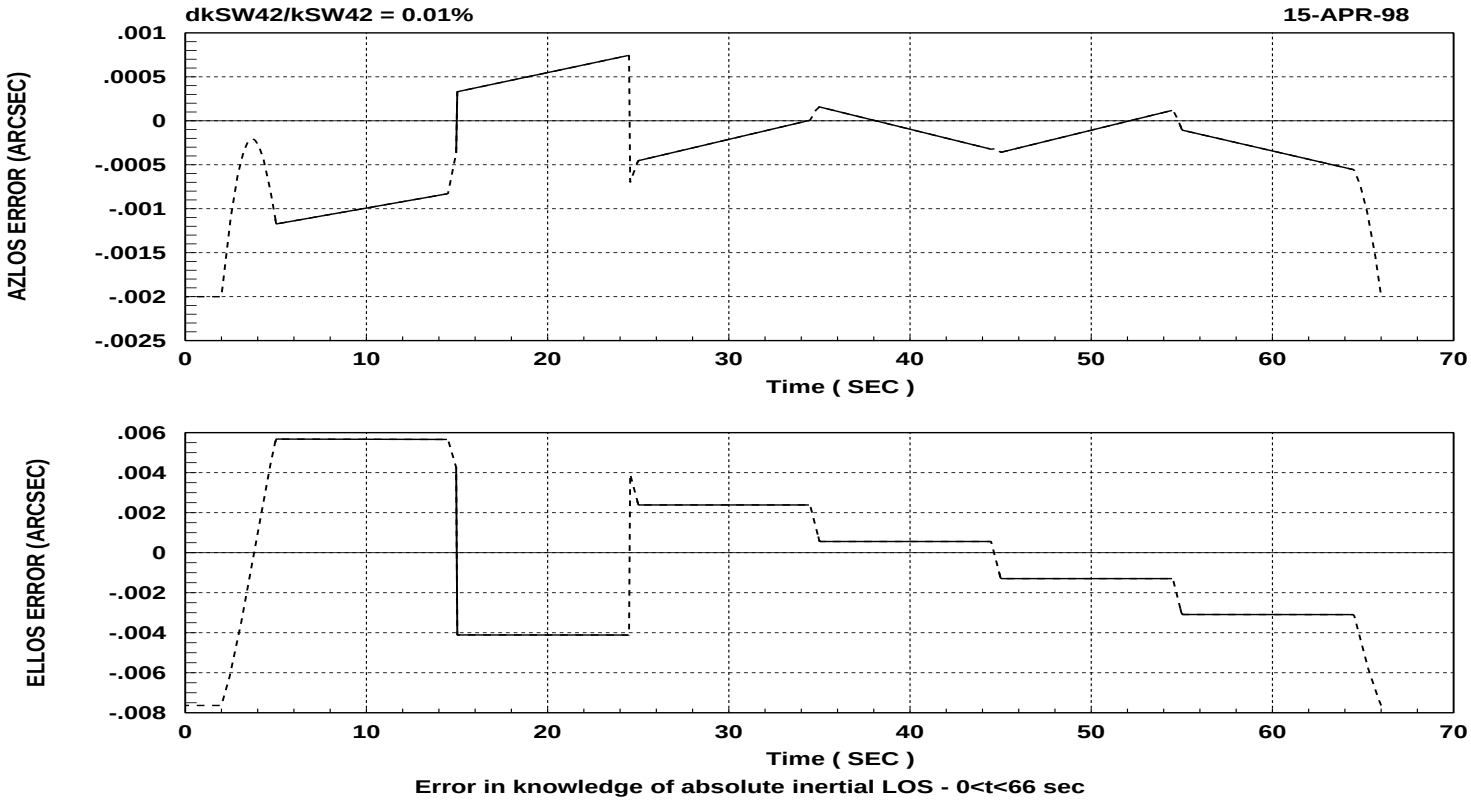


Figure 6.9.5: Errors in the knowledge of the inertial LOS caused by error in the knowledge of the scale factor of the wobble sensors (*SW42*). Wobble of the azimuth axis selected for maximum errors in AZLOS and ELLOS due to scale factor effect.

## 6.10 RADIANCE /LOS SENSORS NON-SIMULTANEOUS SAMPLING

The detectors are not sampled at the same time as the LOS sensors[1]. From a radiometric point of view, there is an optimum time for sampling each detector. Variables $\tau_a$ ,$\tau_e$ , $\tau_{SW31}$ , and $\tau_{SW42}$ are used to represent the time delays between the time at which the LOS sensors are sampled and the ideal time for sampling a given detector. Errors in the knowledge of these time delays, $\delta\tau$ , cause errors in the knowledge of the LOS and change in LOS. To quantify these errors the estimate for the LOS is obtained by delaying the signal from one of the sensors and comparing the resulting estimate of the LOS and change in LOS with the case where there is no time delay, *i.e.* it is assumed that the baseline value of $\tau_a$ ,$\tau_e$ , $\tau_{SW31}$ , and $\tau_{SW42}$ are zero in which case $\tau=\delta\tau$.

In accessing the LOS errors caused by the error sources just described it is important to consider the proper environment, *e.g.* motion of the spacecraft/optical bench. The reason is: The LOS elevation angle is stabilized with respect to inertial space and motion of the bench will show-up in the signals from the elevation encoder. Since during an elevation scan the azimuth axis does not move this effect will not show-up in the signals from the azimuth encoder nor in the signals from the wobble sensors.

The errors in knowledge of the absolute LOS and change in LOS for $0 < t < 66$ sec and $0 < t < 10$ sec caused by errors in the knowledge of the time delays are listed in Table 6.10.1.

Figure 6.10.1 show the errors in the direction of the line-of-sight in inertial space due to a 10 micro-second radiance/elevation encoder sample synchronization error.

[1] Because of the particular way the scanner operates, *i.e.* no motion of the azimuth axes is expected during an elevation scan, the non-simultaneous sampling of the radiance and azimuth sensors do not contribute to errors in the knowledge of the line-of-sight.

| Parameter | | | 0 < t < 66 sec | | 0 < t < 10 sec | | | | |
|---|---|---|---|---|---|---|---|---|---|
| | $\delta A$ (arcsec) | $\delta E$ (arcsec) | $\delta \Delta A_m$ (arcsec) | $\delta \Delta E$ (arcsec) | $\delta A$ (arcsec), $a$ (deg) | | $\delta \Delta E$ (arcsec), $\theta$ (arcsec), $a$ (deg) | | |
| $\tau_e$ (μsec) | | | | | | | | | |
| 1 | 2.179E−4 | 1.229E−3 | 1.330E−4 | 2.429E−3 | 2.179E−4 | −19.5 | 2.629E−6 | 140 | +10.05 |
| 10 | 2.179E−3 | 1.229E−2 | 1.330E−3 | 2.429E−2 | 2.179E−3 | −19.5 | 2.629E−5 | 140 | +10.05 |
| 100 | 2.179E−2 | 1.229E−1 | 1.330E−2 | 2.429E−1 | 2.179E−2 | −19.5 | 2.629E−4 | 140 | +10.05 |
| $\tau_a$ (μsec)<br>$\tau_{SW31}$ (μsec)<br>$\tau_{SW42}$ (μsec) | Not applicable. See footnote on previous page. | | | | | | | | |

Table 6.10.1: Maximum errors in the knowledge of the absolute LOS and change in LOS caused by errors in knowledge of the time delay between the radiometric sampling and the sampling of the LOS sensors. Results obtained using a nominal case with on-orbit random vibration environment as defined in the ITS SP-HIR-013P (page 39).

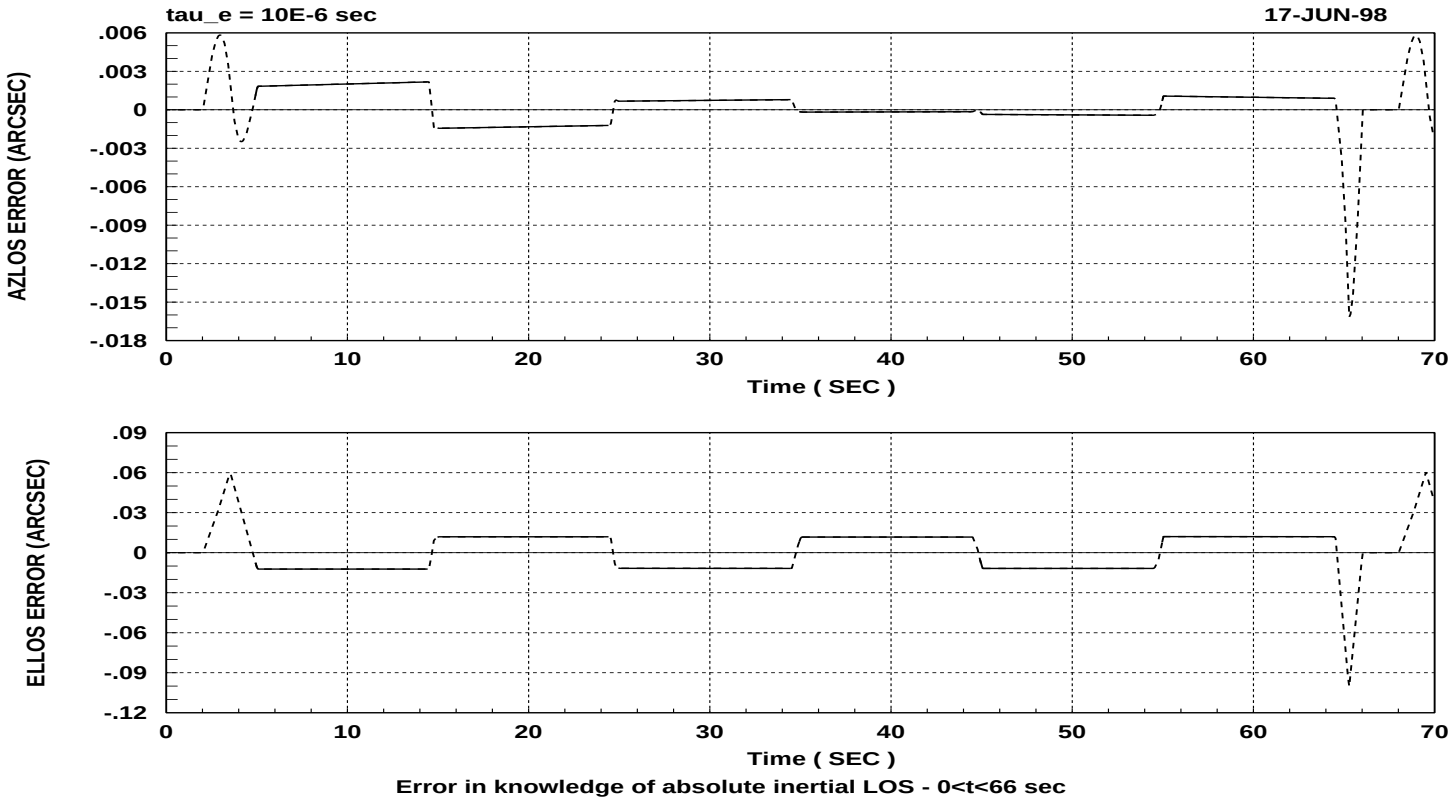


Figure 6.10.1: Errors in the knowledge of the inertial LOS caused by a 10-micro-second radiance/elevation encoder sample synchronization error.

## 6.11 ERRORS DUE TO NOISE, NON-LINEARITIES AND QUANTIZATION

Noise, unknown non-linearities and quantization in the signals from the azimuth and elevation encoders and wobble sensors result in errors in the knowledge of the LOS and change in LOS. To quantify the errors due to these sources, the absolute errors in the line-of-sight inertial azimuth and elevation angles, $\delta A$ and $\delta E$, due to errors in the signals from the sensors, $\delta$signal, are used. These absolute errors are given in Section 6.7, where errors due to bias in the signals from the various sensors are determined. LOS errors due to errors in the signals from the sensors can also be computed as

$$\delta E \cong \frac{f\,E}{f\,signal}\delta signal \qquad \delta A \cong \frac{f\,A}{f\,signal}\delta signal \tag{6.11.1}$$

Where the sum is conducted on the signals from all sensors.

For the system in the baseline configuration the line-of-sight angles relate to the shaft angles as follows[1]:

$$\sin E = \sin E_0 \cos(2e) + \cos(E_0)\cos a \sin(2e) \tag{6.11.2}$$

$$\tan A = \frac{-\cos E_0 \sin(2a)\cos^2 e + \sin E_0 \sin a \sin(2e)}{\cos E_0(1 - 2\cos^2 a \cos^2 e) + \sin E_0 \cos a \sin(2e)} \tag{6.11.3}$$

In this case the partial derivatives with respect to the signals of the elevation and azimuth encoders are:

$$\frac{f\,E}{f\,a} = \frac{-\cos E_0 \sin a \sin(2e)}{\sqrt{1-(\sin E_0 \cos(2e) + \cos E_0 \cos a \sin(2e))^2}} \tag{6.11.4}$$

$$\frac{f\,E}{f\,e} = \frac{2(\cos E_0 \cos a \cos(2e) - \sin E_0 \sin(2e))}{\sqrt{1-(\sin E_0 \cos(2e) + \cos E_0 \cos a \sin(2e))^2}} \tag{6.11.5}$$

$$\begin{aligned}\frac{f\,A}{f\,a} = \frac{1}{D}&(2\cos(2a)\cos^2 e(-1 + 2\cos^2 a \cos^2 e)\cos^2 E_0 + 2\cos^4 e \sin^2(2a)\cos^2 E_0 + \\ &+ \sin(2e)\sin E_0(\cos a \cos E_0 + \cos^2 a \sin(2e)\sin E_0 + \sin^2 a \sin(2e)\sin E_0)) + \\ &- 4\cos a \cos^3 e \sin e \sin(2E_0)\end{aligned} \tag{6.11.6}$$

$$\begin{aligned}\frac{f\,A}{f\,e} = \frac{\cos E_0 \sin a}{2D}&(-\sin(a - 2e - E_0) - 2\sin(2e - E_0) + \sin(a + 2e - E_0) + \\ &- \sin(a - 2e + E_0) + 2\sin(2e + E_0) + \sin(a + 2e + E_0))\end{aligned} \tag{6.11.7}$$

$$\begin{aligned}D \ldots &\cos^2 E_0(1 - 4\cos^2 a \cos^2 e + 4\cos^4 a \cos^4 e + \cos^4 e \sin^2(2a)) + \\ &- \frac{\sin(2e)\sin E_0}{2}(\cos(a - 2e - E_0) - \cos(2e - E_0) + \cos(a + 2e - E_0) +\end{aligned}$$

[1] Derivation of Scanner Control Algorithms - TC-LOC-142, by Dr. Alain Carrier, December 1995.

$$+\cos(a-2e+E_0)+\cos(2e+E_0)+\cos(a+2e+E_0)) \qquad (6.11.8)$$

Plots with the results of the partial derivatives as a function of time for the Alternate Global Scan Mode are presented in Figures 6.11.1 and 6.11.2. It should be noted that these plots are in agreement with the errors in LOS due to a unit error (unit bias) in azimuth and elevation shaft angles, Figures 6.11.3 and 6.11.4. Figures 6.11.5 and 6.11.6 show the errors in inertial LOS due to a unit error (unit bias) in the signals from the wobble sensors. The maximum absolute values of the LOS errors due to unit errors in the signals from the various sensors (sensitivities) are given in Table 6.11.1.

| Error in Sensor Signal | Maximum Absolute Error in LOS Inertial Angles | |
|---|---|---|
| | *δA (arcsec)* | *δE (arcsec)* |
| *δe = 1 arcsec* | 3.347E−1 (= *∂A/∂e*) | 1.999 (= *∂E/∂e*) |
| *δa = 1 arcsec* | 2.009 (= *∂A/∂a*) | 1.295E−2 (= *∂E/∂a*) |
| *δSW31 = 1 μm* | 5.653E−1 | 3.504 |
| *δSW42 = 1 1 μm* | 2.292E−1 | 1.107 |

Table 6.11.1: Maximum absolute values of LOS errors due to unit errors in the signals from the sensors.

Following the errors in LOS due to noise, non-linearities and quantization on the signals from the sensors are computed using the information contained in Figures 6.11.1 through 6.11.6 and in Table 6.11.1.

### 6.11.1 NOISE

For errors in the signals from the encoders due to noise, which is assumed uncorrelated for any two samples, the errors in change of LOS, $\delta\Delta A$ and $\delta\Delta E$, are obtained from the absolute errors as follows:

$$\delta\Delta A\big|_{NOISE} = \sqrt{2}\delta A \qquad \delta\Delta E\big|_{NOISE} = \sqrt{2}\delta E \qquad (6.11.9)$$

Maximum errors in the LOS and change of LOS due to noise in the signals from the sensors are listed in Table 6.11.2. It is assumed that the noise does not have a low frequency content, and when averaged over a single elevation scan (approximately 10 seconds) its effect on the measurement should be negligible. Therefore, no significant error in the average value of the LOS inertial azimuth angle is expected.

### 6.11.2 NON-LINEARITIES AND QUANTIZATION

For errors in the signals from the encoders due to non-linearities and quantization, the errors for change of LOS, $\delta\Delta A$ and $\delta\Delta E$ are obtained from the absolute errors as follows:

**<u>Elevation Encoder</u>**

Within a single elevation scan the maximum errors in change of LOS due to unknown non-linearities and quantization of the signal from the elevation encoder are equal to two times the maximum absolute errors.

$$\delta\Delta A\big|_{\substack{NONLINEARITIES\\ \&\ QUANTIZATION}} = 2\delta A \qquad \delta\Delta E\big|_{\substack{NONLINEARITIES\\ \&\ QUANTIZATION}} = 2\delta E \qquad (6.11.10)$$

Among any two elevation scans the maximum errors in change of LOS due to unknown non-linearities and quantization of the signal from the elevation encoder are equal to the sum of the maximum absolute error among all elevation scans, $\delta LOS_{MAX1}$ , plus the maximum absolute

error among all elevation scans except the scan in which $\delta LOS_{MAX1}$ occurs, called $\delta LOS_{MAX2}$. Where $\delta LOS$ means $\delta A$ or $\delta E$.

**Azimuth Sensors**

The term azimuth sensors includes both the azimuth encoder and wobble sensors.

Within a single elevation scan, because the azimuth angle does not change, maximum errors in change of LOS due to unknown non-linearities and quantization of the signals form azimuth sensors are obtained from the absolute LOS errors by: computing the maximum among all scans of the quantities obtained by subtracting the minimum value of the absolute error within a given elevation scan from the maximum value of the absolute error within the same elevation scan.

Among any two elevation scans the maximum errors in change of LOS due to unknown non-linearities and quantization of the signals from the azimuth sensors are equal to the sum of the maximum absolute error among all elevation scans, $\delta LOS_{MAX1}$ , plus the maximum absolute error among all elevation scans except the scan in which $\delta LOS_{MAX1}$ occurs, called $\delta LOS_{MAX2}$. Where $\delta LOS$ means $\delta A$ or $\delta E$.

It should be noted that this approach computes an upper-bound for the errors due to quantization. The actual expected errors should be smaller because of the presence of noise which spans several quantization steps has the effect of averaging out the quantization errors.

Maximum errors in the LOS and change of LOS due to unknown non-linearities noise in the signals from the sensors are listed in Table 6.11.3. It is assumed that the noise does not have a low frequency content, and

| Parameter | | | 0 < t < 66 sec | | 0 < t < 10 sec | | | | |
|---|---|---|---|---|---|---|---|---|---|
| | $\delta A$ (arcsec) | $\delta E$ (arcsec) | $\delta \Delta A_m$ (arcsec) | $\delta \Delta E$ (arcsec) | $\delta A$ (arcsec), $a$ (deg) | | $\delta \Delta E$ (arcsec), θ (arcsec), $a$ (deg) | | |
| *Noise Amplitude* | | | | | | | | | |
| $\lvert e_{NOISE} \rvert$ = 1 arcsec | 3.347E−1 | 1.999 | ≈ 0 | 2.827 | 3.347E−1 | −19.5 | 2.827 | not applicable | −19.5 |
| $\lvert a_{NOISE} \rvert$ = 1 arcsec | 2.009 | 1.295E−2 | ≈ 0 | 1.831E−2 | 2.009 | −19.5 | 1.831E−2 | not applicable | −19.5 |
| $\lvert SW31_{NOISE} \rvert$ = 1 μm | 5.653E−1 | 3.504 | ≈ 0 | 4.955 | 5.653E−1 | −19.5 | 4.955 | not applicable | −19.5 |
| $\lvert SW42_{NOISE} \rvert$ = 1 μm | 2.292E−1 | 1.107 | ≈ 0 | 1.566 | 2.292E−1 | −19.5 | 1.566 | not applicable | −19.5 |

Table 6.11.2: Maximum errors in the knowledge of the absolute LOS and change in LOS caused by noise in the signals from the azimuth and elevation sensors.

| Parameter | | | 0 < t < 66 sec | | 0 < t < 10 sec | | | | |
|---|---|---|---|---|---|---|---|---|---|
| *Magnitude of* | $\delta A$ (arcsec) | $\delta E$ (arcsec) | $\delta \Delta A_m$ (arcsec) | $\delta \Delta E$ (arcsec) | $\delta A$ (arcsec), $a$ (deg) | | $\delta \Delta E$ (arcsec), θ (arcsec), $a$ (deg) | | |
| *Non-linearity or Quantization* | | | | | | | | | |
| $\lvert e_{NL\&Q} \rvert$ = 1 arcsec | 3.347E−1 | 1.999 | 4.680E−1 | 3.994 | 3.347E−1 | −19.5 | 3.998 | not applicable | −19.5 |
| $\lvert a_{NL\&Q} \rvert$ = 1 arcsec | 2.009 | 1.295E−2 | 1.824E−4 | 2.156E−2 | 2.009 | −19.5 | 1.985E−2 | 6181 | −0.34 |
| $\lvert SW31_{NL\&Q} \rvert$ = 1 μm | 5.653E−1 | 3.504 | 7.773E−1 | 6.993 | 5.653E−1 | −19.5 | 1.002E−2 | 6181 | −0.34 |
| $\lvert SW42_{NL\&Q} \rvert$ = 1 μm | 2.292E−1 | 1.107 | 1.790E−1 | 1.909 | 2.292E−1 | −19.5 | 3.894E−3 | 6181 | −0.34 |

Table 6.11.3: Maximum errors in the knowledge of the absolute LOS and change in LOS caused by unknown non-linearities and quantization in the signals from the azimuth and elevation sensors.

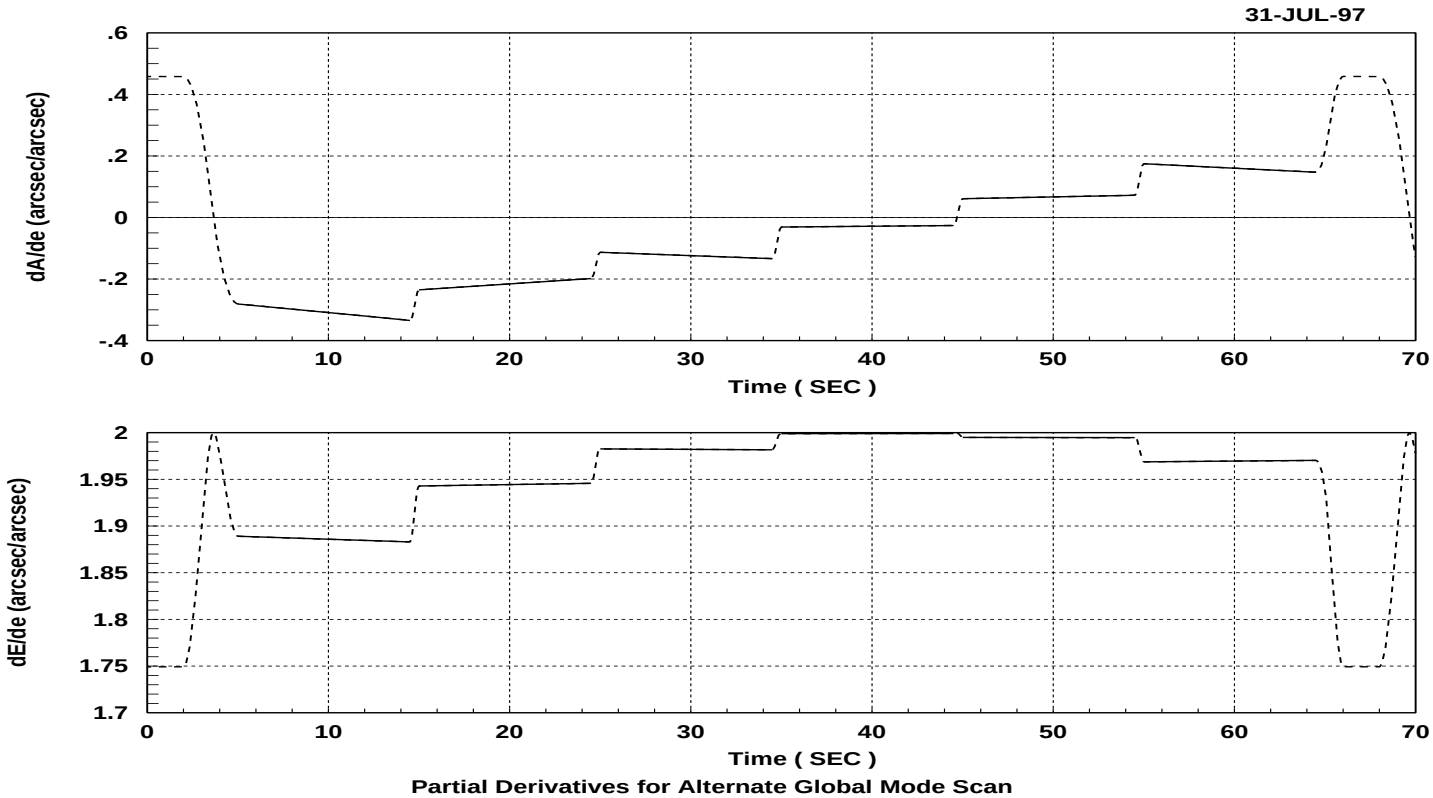


Figure 6.11.1: Partial derivatives of LOS inertial azimuth and elevation, $A$ and $E$, angles with respect to elevation shaft angle, $e$, for the Alternate Global Mode Scan Pattern. Obtained using Equations 6.11.5 and 6.11.7.

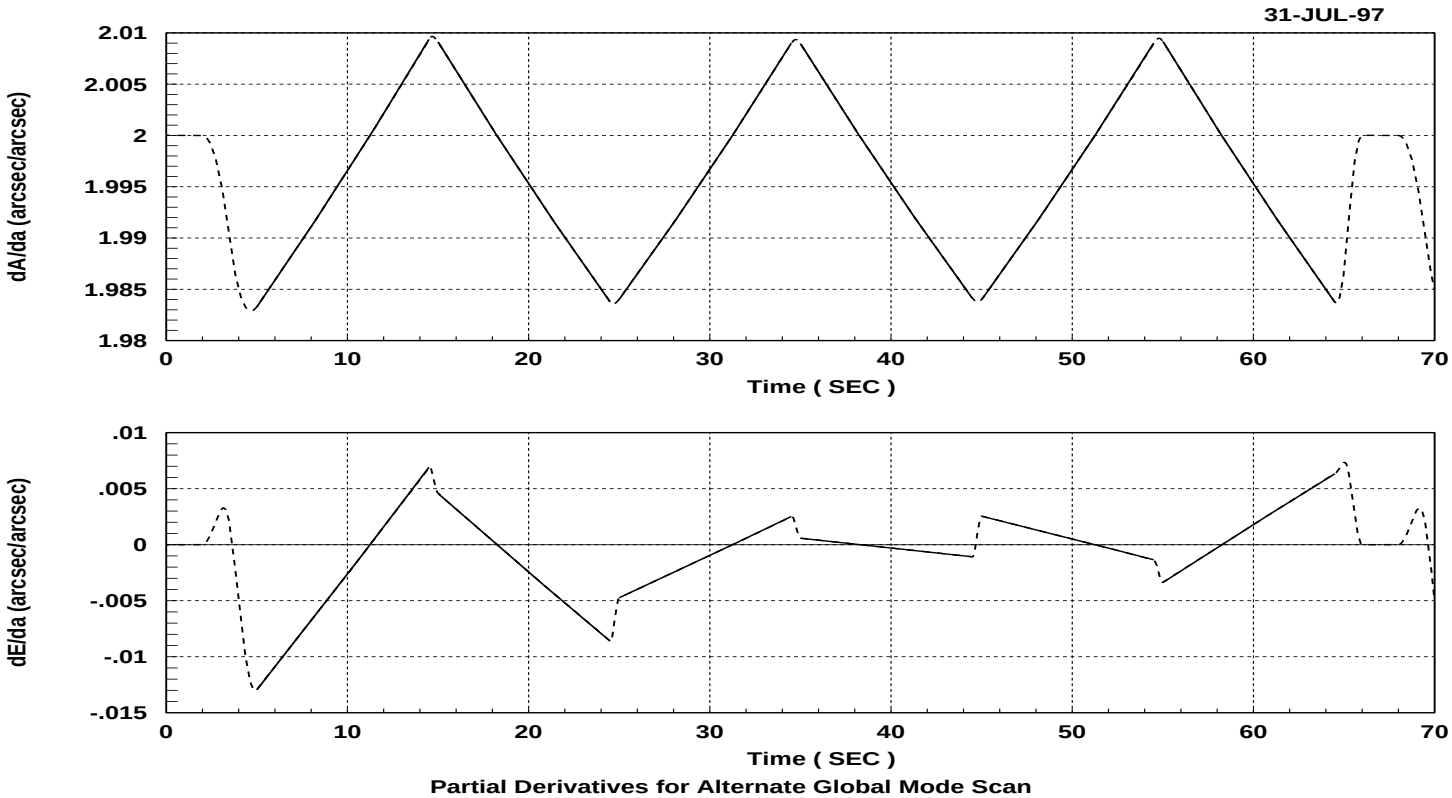


Figure 6.11.2: Partial derivatives of LOS inertial azimuth and elevation, *A* and *E*, angles with respect to azimuth shaft angle, *a*, for the Alternate Global Mode Scan Pattern. Obtained using Equations 6.11.4 and 6.11.6.

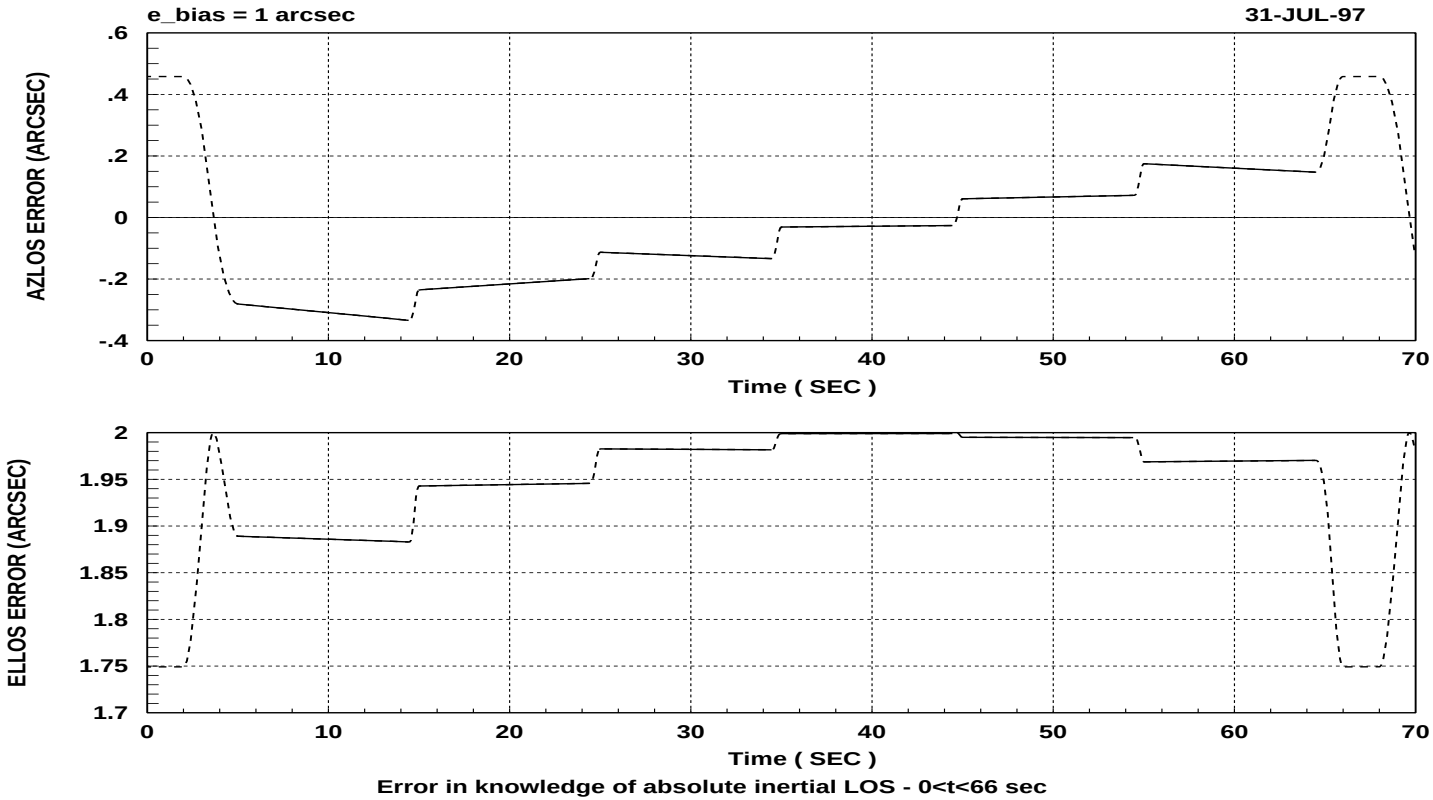


Figure 6.11.3: Errors in inertial LOS caused by 1 arcsec error in the signal from the elevation encoder.

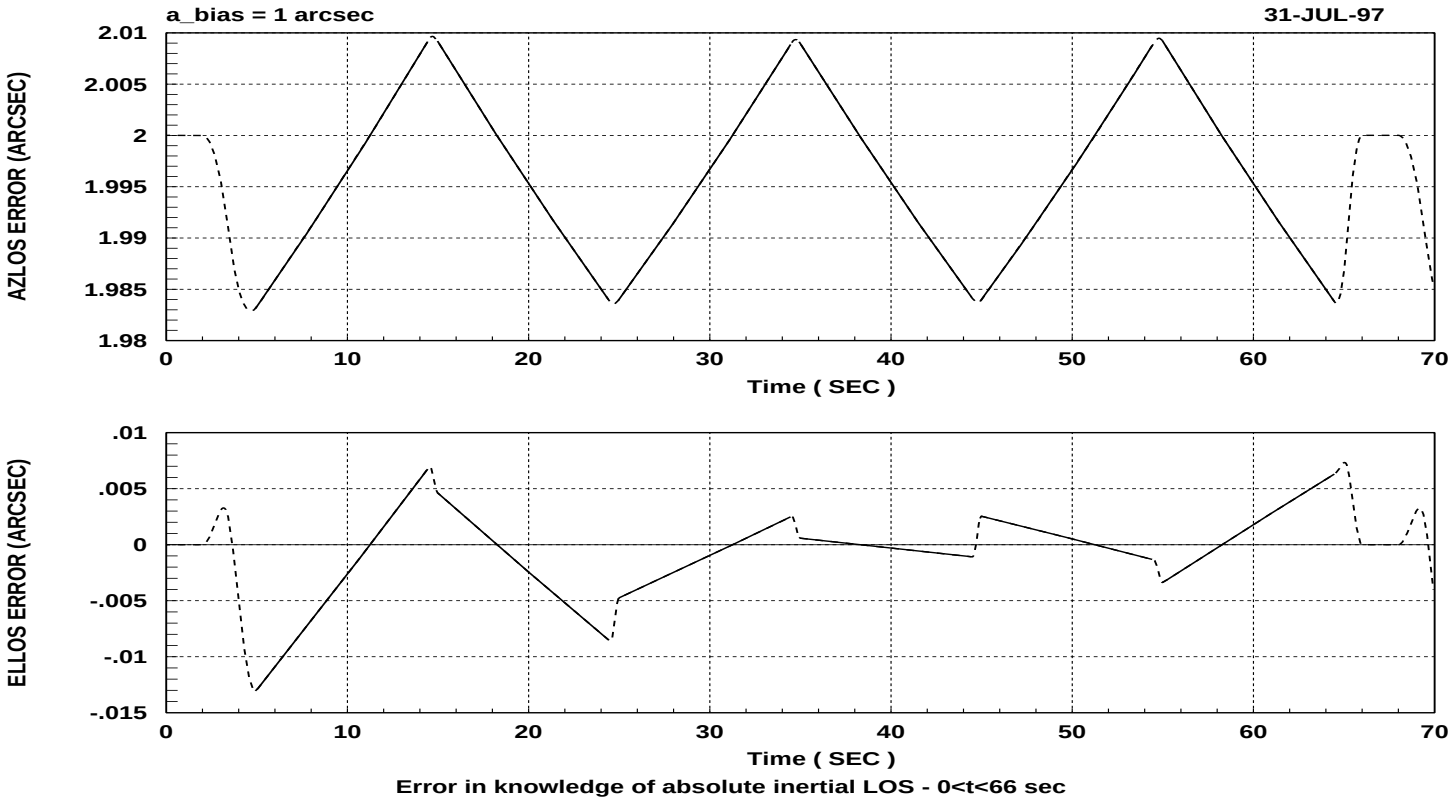


Figure 6.11.4: Errors in inertial LOS caused by 1 arcsec error in the signal from the azimuth encoder.

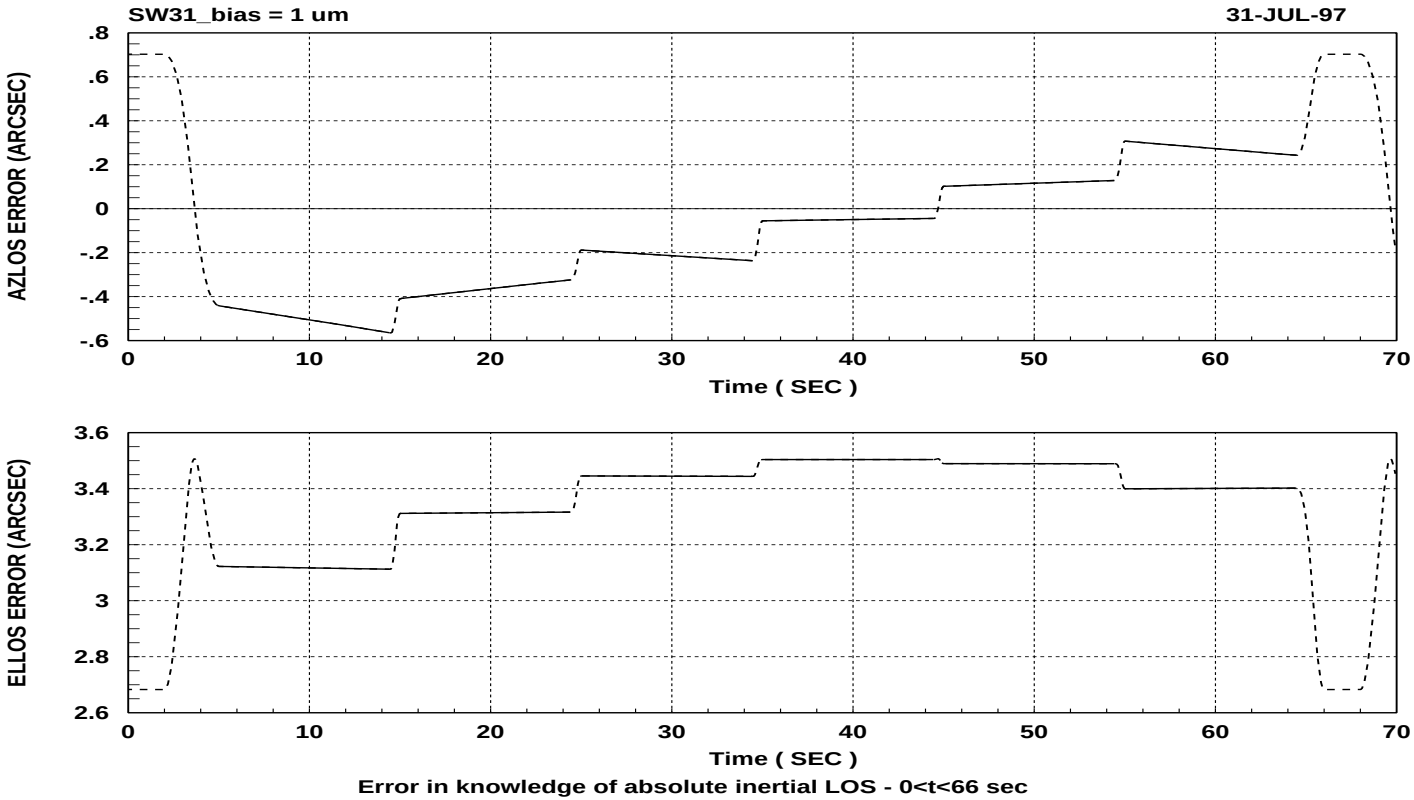


Figure 6.11.5: Errors in inertial LOS caused by 1 μm error in the signal from the wobble sensors (*SW31*).

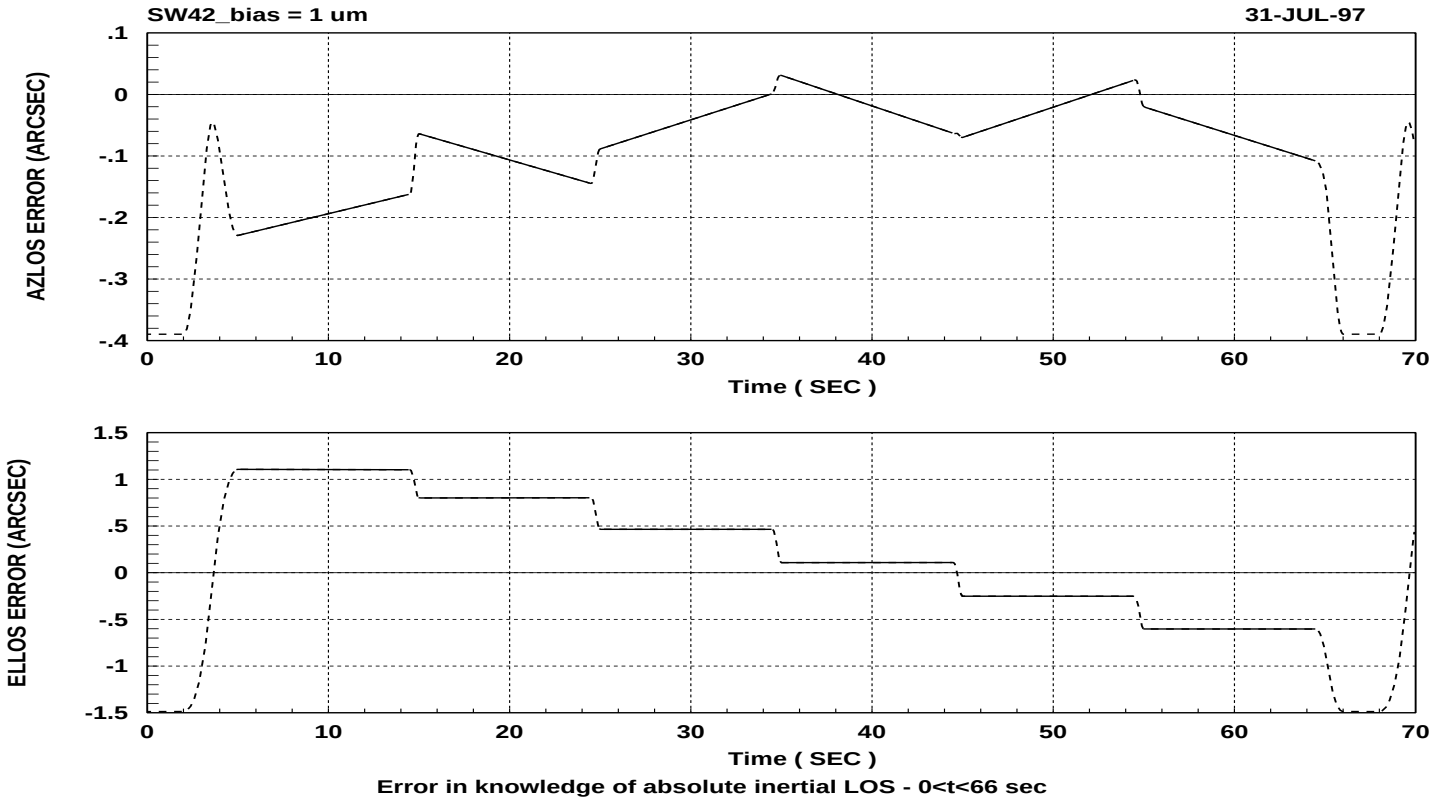


Figure 6.11.6: Errors in inertial LOS caused by 1 μm error in the signal from the wobble sensors (*SW42*).

# 7 NOTES

**LOS Error due to z-component of Wobble Sensor Position Versus Error due to Misalignment of the Azimuth Axis of Rotation**

An error in the z-component of the wobble sensor position causes a large error in the knowledge of the change of the line-of-sight azimuth and elevation angles ($\delta\Delta A$ *and* $\delta\Delta E$) as seen in Section 6.6. In contrast relatively small errors occur due to a misalignment of the azimuth axis. This is because an error in the z-component of the position of the wobble sensor 1, *i.e.* error in $LW_{13}$ , is equivalent to: a misalignment of the azimuth axes plus an offset in the elevation shaft angle. The results in the following table confirm that this is in fact the case. On the first row results are presented for the case where there is a misalignment of the azimuth axes (**AZA**) obtained by rotating the axes by 10 arcsec about the $\mathbf{O_2}$ direction. The second row shows similar results for the case where $\delta LW_{13}$ = 5.7 μm and an offset equal to 10 arcsec is added to the elevation shaft angle. As seem the results are in good agreement which confirms the explanation given above.

| Parameter | 0 < t < 66 sec | | | 0 < t < 10 sec | | | | |
|---|---|---|---|---|---|---|---|---|
| | $\delta A$ (arcsec) | $\delta\Delta A_m$ (arcsec) | $\delta\Delta E$ (arcsec) | $\delta A$ , a (arcsec, deg) | | $\delta\Delta E$ , θ , a (arcsec, arcsec, deg) | | |
| $\theta_{AZA2}$ = 10 arcsec | 5.751E−1 | 8.165E−2 | 1.076 | 2.921E−1 | −19.5 | 7.660E−5 | 140 | −19.5 |
| $\delta LW_{13}$ = 5.7 μm and $e_{offset}$ = 10 arcsec | 5.762E−1 | 8.229E−2 | 1.075 | 2.929E−1 | −19.5 | 7.683E−5 | 140 | −19.5 |

Table 7.1: Maximum LOS errors due to z-component of wobble sensor position and errors due to to misalignment of the azimuth axis of rotation and offset in elevation shaft angle

**LOS Error due to Misalignment of the Projected Optical Axis Versus Error due to an Offset in Elevation Shaft Angle**

In comparing the errors in the knowledge of the change in the LOS elevation angle due to a misalignment of the **POA** (defined as a change in $E_0$) and due to an offset in the elevation shaft angle ($\delta e$ or $\delta ROT_2$) there is a three order of magnitude difference in $\delta\Delta E$ for 0<t<66 sec and an order of magnitude difference in $\delta\Delta E$ for 0<t<10 sec. These large differences are counter intuitive and require further investigation to assure that the retrieval code is not in error. To address this issue the following equation relating the LOS elevation angle, *E*, to the shaft angles *a* and *e* is used to compute the sensitivities to error in $E_0$ and to an offset in the elevation shaft angle, *e*.

$$\sin E = \sin E_0 \cos(2e) + \cos(E_0)\cos a \sin(2e) \tag{7.1}$$

$$\frac{\delta E}{\delta e} = \frac{2(\cos E_0 \cos a \cos(2e) - \sin E_0 \sin(2e))}{\sqrt{1-(\sin E_0 \cos(2e) + \cos E_0 \cos a \sin(2e))^2}} \tag{7.2}$$

$$\frac{\delta E}{\delta E_0} = \frac{\cos E_0 \cos(2e) - \sin E_0 \cos a \sin(2e)}{\sqrt{1-(\sin E_0 \cos(2e) + \cos E_0 \cos a \sin(2e))^2}} \tag{7.3}$$

Absolute errors in the inertial LOS elevation angle, $E$, computed using the equations above are in agreement with the results obtained using the retrieval algorithm. Therefore, although counter-intuitive, the large differences in sensitivities due to errors in $E_0$ and $e$ are believed to be correct.